NASA CR 114630
AVAILABLE TO THE PUBLIC
AIRESEARCH 73-210148

A STUDY OF SMALL TURBOFAN ENGINES APPLICABLE TO GENERAL-AVIATION AIRCRAFT

FINAL REPORT

SEPTEMBER 1973

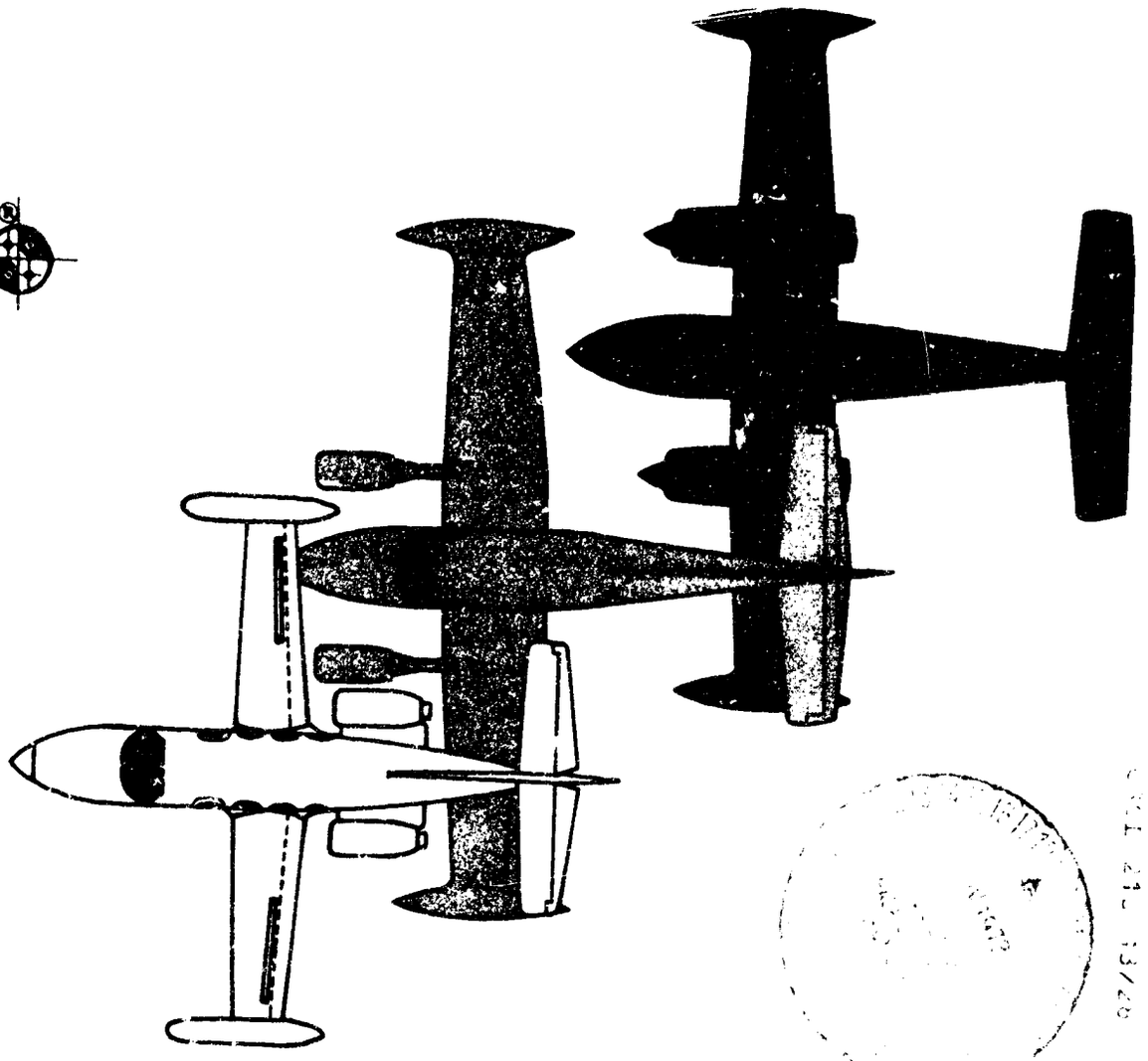

AIRESEARCH MANUFACTURING COMPANY OF ARIZONA
A DIVISION OF THE GARRETT CORPORATION

NASA CR 114630
AVAILABLE TO THE PUBLIC
AIRESEARCH 73-210148

A STUDY OF SMALL TURBOFAN ENGINES APPLICABLE TO GENERAL-AVIATION AIRCRAFT

FINAL REPORT

by G. L. Merrill, G. A. Burnett, C. C. Alsworth, et al.

SEPTEMBER 1973

Prepared under Contract No. NAS2-6799 by

AIRESEARCH MANUFACTURING COMPANY OF ARIZONA
A DIVISION OF THE GARRETT CORPORATION
Sky Harbor Airport, 402 South 36th Street
PHOENIX, ARIZONA 85034

for

Ames Research Center

NATIONAL AERONAUTICS AND SPACE ADMINISTRATION

Systems Study Division

CONTENTS

CONTENTS (CONTD)

CONTENTS (CONTD)

A STUDY OF SMALL TURBOFAN ENGINES APPLICABLE TO GENERAL-AVIATION AIRCRAFT

by C. L. Merrill, G. A. Burnett, C. C. Alsworth, et al.

SUMMARY

This report presents the results of a study sponsored by the NASA Ames Systems Study Division (Contract NAS2-6799) concerning the applicability of small turbofan engines to general-aviation airplanes.

Because of its high overall propulsion-system efficiency, the turbofan engine is now being chosen for most military and commercial airplanes. It is therefore desirable to evaluate the further applicability of turbofan engines to smaller general-aviation airplanes. This initial study by NASA Ames and AiResearch establishes engine and engine/airplane performance, weight, size, and cost interrelationships and evaluates the effects of specific engine noise constraints. The methods whereby these interrelationships and effects were determined and the results of synthesis and sensitivity analyses are described. In addition to engine price, engine performance quality was found to be a very important determinant of airplane size, the resultant price, and operating cost.

INTRODUCTION

A recent FAA census (presented in Reference 1) of the general-aviation airplane fleet indicates that, of about 141,000 registered airplanes counted, only 2,535 were turbine-powered. Only a small portion of these turbine-powered airplanes have turbofan propulsion systems. There are only three turbofan-powered general-aviation airplanes available in the world today for purchase by a potential customer, and these range in price from $750,000 to $3 million. This is a remarkable contrast to commercial and military aviation, where the turbofan engine has become the standard propulsion system for transport, bomber, and fighter airplanes. The reason for this dominance of turbofans is clear; the turbofan engine, in an appropriate design and cycle, and because of its light weight and small size, has the highest overall propulsion-system efficiency of all alternatives. It has proven to provide the most cost-effective airplane for any mission or role for which it is designed.

The fact that only one turbofan-powered airplane model having a gross weight less than 5443 kg (12,000 lb) is available for sale today, and that no others are in development, indicates that inhibiting factors exist. These factors have stifled the availability of turbofans in a market where they should be welcomed. The inhibiting factors have been identified as:

- Lack of military requirements for small turbofan engines and, consequently, no military sponsorship of small turbofan development
- A consensus that turbomachinery is too expensive for smaller, general-aviation airplanes
- A similar consensus that turbofans are inefficient below flight speeds of about 644 km/hr (400 mph)
- A general satisfaction with the existing propulsion systems that fall below the power level of today's smallest available turbofan.

These considerations have provided sufficient reason to slow the downward penetration of turbofans into the smaller aircraft end of the general-aviation market spectrum.

The study reported in this document is the first thorough investigation into the applicability of turbofan propulsion, seeking to identify advantages and overcome disadvantages of turbofans for smaller general-aviation airplanes. It was formulated to complement the small turbofan design and development

activities of the NASA Lewis Research Center. As such, the overall purpose of the study was to establish the performance, weight, size, and cost interrelationships of small turbofan engines so that their potential applicability could be effectively evaluated. A further purpose of the study was the evaluation of the effects of specific engine noise requirements on turbofan engine design and the resultant engine cost. Specific objectives of the study were:

- To establish, to the extent possible, the "best" engine cycles that minimize airplane purchase price and hourly operating costs
- To evaluate engine component configurations, and to establish combinations of components for these cycles

In order to evaluate the engine and engine/airplane interrelationships, an airplane and mission model was postulated. The basic tool used in the evaluation of engine and airplane design, analysis, and cost variables was a comprehensive aircraft synthesis computer program, prepared for this study by personnel of the NASA Ames Systems Study Division. This computer program permitted an extensive examination of many variables to be carried out quickly and accurately. The program based on an extensive and comprehensive set of preliminary design procedures, was designed to compute engine and airplane size, purchase price, and operating costs. When examining any one variable or listing of variables affecting these outputs, the program computes a new-solution airplane.

At the beginning of the study, it was considered vital to acquire insight into the power requirements of the current spectrum of general-aviation airplanes and to identify the efficiency attainments of contemporary propulsion systems. Several propulsion-system types are represented in the current airplanes. Therefore, a basis was sought for making efficiency comparisons between the types, in order that efficiency elements most pertinent to turbofans could be sought in the course of the study.

A large number of correlations of propulsion-system characteristics were derived from Reference 2, which gives size, power, price, and performance data for general-aviation airplanes. The airplanes that were examined ranged in gross weight from 544 to over 27215 kg (1200 to over 60,000 lb), in cruise speed from 137 to nearly 966 km/hr (85 to nearly 600 mph), in installed power from 45 kw to over 14914 kw (60 shaft horsepower to over 20,000 gas horsepower), and in basic price from about $5,000 to over $3 million. The most notable correlation was found in the plot of airplane basic price versus installed power. Figure 1 shows the near-linear relationship in this log-log plot, over about 2.5

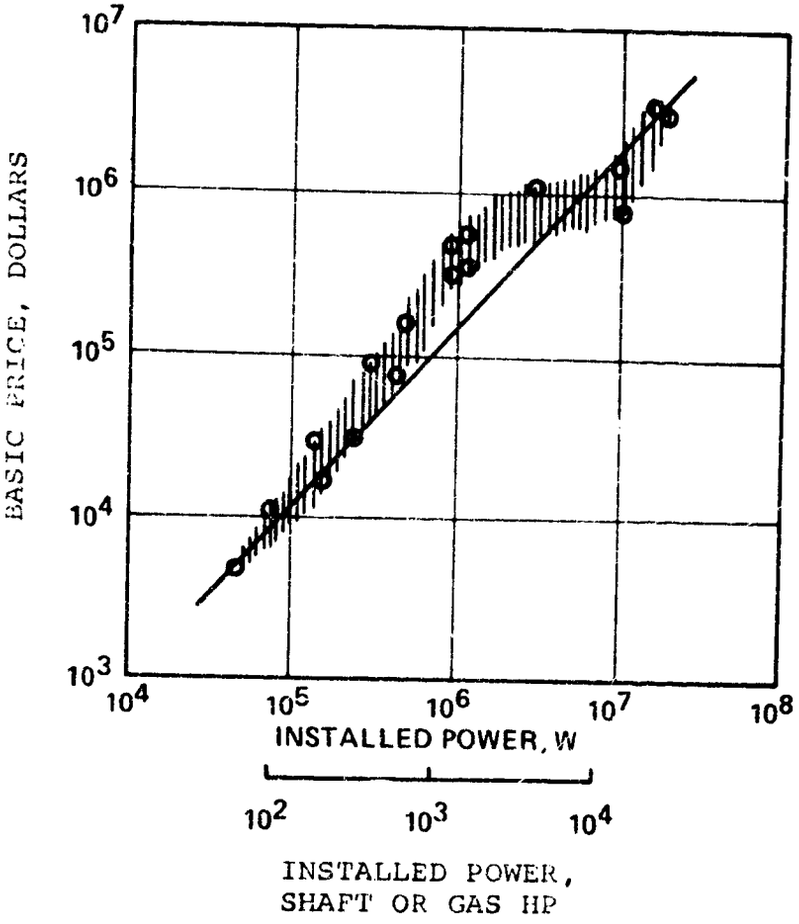

Figure 1. Basic Price Versus Installed Power of General-Aviation Airplanes.

orders of magnitude in each parameter. Overall propulsion-system efficiency is a significant determinant of airplane size and the resultant price. Therefore, the near-linear relationship in this plot implies near equality in the efficiency of the various propulsion-system types represented.

The elements of overall efficiency listed below are common to all aircraft engines:

- Thermodynamic efficiency (converting fuel to gas or shaft power)
- Propulsive efficiency (converting power to propulsive thrust)
- Installed-to-uninstalled thrust ratio (drag penalty charged to engine installation)
- Thrust-to-weight ratio (weight penalty charged to engine installation)

Each of these elements can be identified and quantified in the reciprocating engine/propeller system, in turboprops, turbofans, and in turbojets. Although the values of these elements vary greatly between engine types, their overall efficiency products have been determined to be nearly equal. This is explained by the fact that propulsion systems using propellers have high propulsive efficiency but suffer large, offsetting weight and drag penalties, when compared with turbojets and turbofans having lower propulsive efficiency.

It was learned from the foregoing efficiency comparisons that the propulsive efficiency element was most significant in defining efficient turbofans for smaller and slower airplanes. It was found that the light-weight and low-drag advantages of turbine engines can be substantially eroded, if engine cycle and configuration selection is made without separate quantitative assessment and optimization of the engine characteristics that determine propulsive efficiency. Because of these findings, analytical procedures were devised early in the investigation that would permit separate calculation of the thermal and propulsive efficiencies of turbofan cycles. By this procedure, the fan pressure ratio and core jet velocity, which gave maximum propulsive efficiency are first calculated for a design cruise speed and altitude. The engine thrust per unit-airflow and thrust per unit-frontal area are then calculated. With these parameters determined, nacelle drag versus engine specific thrust can be optimized by trade-off analysis to obtain maximum net propulsive efficiency. With net propulsive efficiency maximized, cycle analysis efforts are then centered on thermal efficiency considerations and the attendant tradeoffs between internal cycle quality, engine weight, and engine cost.

This procedure accomplishes a large portion of the definition of optimized turbofan engines, without recourse to parametric cycle analysis. By these methods, optimum engines can be quickly defined for any airplane cruise speed and altitude. During the course of this investigation, the methods described here were used to define turbofans having overall propulsion system efficiencies that were competitive with those of other engine types used in contemporary smaller and slower general-aviation airplanes. These methods are described further, and an example engine/airplane conceptual design derived with the use of these methods is outlined in Appendix A.

SYMBOLS

A	Effective nozzle area, sq ft
AR	Aspect ratio
B_i	Number of blades on the i stage rotor
BPR	Bypass ratio
°C	Degrees centigrade
C_D	Drag coefficient
C_{Di}	Induced drag coefficient
$C_{D\ wet}$	Drag coefficient referenced to the wetted area
C_L	Lift coefficient
CU	Customary units
D_e	Effective diameter of the combustor, ft
EPNdB	Effective perceived noise level
e	Oswald efficiency factor
°F	Degrees Fahrenheit
F	Engine thrust, N (lbf)
f	Function of
f_a	Fuel-air ratio
F_i	Fundamental blade passage frequency of the i stage rotor
F_N	Net thrust, N (lbf)
F_{cruise}	Cruise thrust, N (lbf)
fpm	Feet per minute
ft	Feet
F_{SLS}	Sea level static thrust, N (lbf)
F/W_a	Engine specific thrust, or thrust per unit airflow N-s/kg [lbf/(lbm/sec)]
gal	Gallon
HP	Horsepower
HR	Hour
In.	Inch(es)

SYMBOLS (CONTD)

ISA	International Standard Atmosphere
°K	Degrees Kelvin
K	Thousand
kg	Kilogram
kt	Knot
L	Length
l	Liter
lb	Pound(s)
ln	Logarithm
m	Meter
mm	Millimeter
mph	Miles per hour
N	Newton
N_G	Gas generator speed, rpm
N_G	Speed governor
n_i	Rotational speed of the i stage rotor, revolutions per second
n. mi.	Nautical miles
$OASPL_A$	Space-average sound pressure level
$OASPL_M$	Peak overall sound pressure level
P	Acoustical power output, lb-ft per sec
p	Pressure, lb per sq ft
P_3	Compressor discharge pressure, N/cm^2 (psia)
P_4	Turbine inlet pressure, lb per sq ft
P_{cd}	Compressor discharge pressure, N/cm^2 (psia)
P_{CV}	Pressure control valve
PNdB	Perceived noise level
psf	Pounds per square foot
psi	Pounds per square inch
PWL	Power level
q	Dynamic pressure
°R	Degrees Rankine
r	Distance to sideline, ft

SYMBOLS (CONTD)

S	Wing area, sq m (sq ft)
SI	Systeme International
SLS	Sea level static
sec	Second
S_{wet}	Wetted area, sq m (sq ft)
T	Temperature, °R
TAS	True airspeed, knots
T_{avg}	Average temperature, °K (°R)
$T_{max.}$	Maximum temperature, °K (°R)
TSFC	Thrust specific fuel consumption, kg/N-hr [(lbm/hr)/lbf]
T_{t2}	Inlet total temperature, °K (°R)
T_2	Inlet temperature, °K (°R)
T_4	Turbine inlet temperature, °K (°R)
U	Jet velocity, ft per sec
V_d	Combustor discharge velocity, ft per sec
V_s	Airplane stall speed, km/hr (mph)
W	Weight, kg (lbm)
W	Combustion energy release, lb-ft per sec
$\dot{W}_a$	Airflow rate, lb per sec
$\dot{W}_f$	Fuel flow rate, lb per sec
W_{cruise}	Average weight at cruise, kg (lbm)
W_e	Empty weight, kg (lbm)
W_{eng}	Engine weight, kg (lbm)
W_1	Weight at end of cruise, kg (lbm)
W_f	Fuel flow, kg/hr (lbm/hr)
W_{fuel}	Fuel weight, kg (lbm)

SYMBOLS (CONTD)

W_g	Aircraft gross weight, kg (lbm)
W_p	Propulsion weight, kg (lbm)
W/S	Wing loading, kg/m^2 (lbm/ft^2)
W_s	Structure weight, kg (lbm)
α	Angle of attack, degrees
γ	Angle between flight path and horizon, degrees
ρ	Jet density, lb per cubic ft
θ	Cruise flight time, hr

PHASE I - PRELIMINARY ENGINE AND AIRPLANE STUDIES

Preliminary Aircraft and Engine Analyses

Airplane modeling and sizing studies.- In order to evaluate the performance, weight, size, and cost interrelationships of small turbofan engines, fixed airplane and mission models were established. General characteristics of the airplane and mission models are listed in Table I. These characteristics were chosen as representative of high-performance, light, twin-engine business airplanes. By assessing their effects on the airplane model size, purchase price, and operating costs, the engine interrelationships could be determined and a cost-effective engine defined.

TABLE I. SELECTED AIRPLANE CHARACTERISTICS FOR TURBOFAN EVALUATION

Configuration	Twin-engine/6 seats
Cruise speed (design)	648 km/hr (350 kts) TAS
Cruise altitude (design)	7315 m (24,000 ft)
Takeoff and landing distance (maximum)	914 m (3000 ft)
Range	1000 n. mi.
Maximum allowable noise at takeoff 152 m (500 ft) sideline	85 and 95 PNdB
Maximum allowable noise at approach 113 m (370 ft) altitude	85 and 95 PNdB

In order to establish baseline size, weight, drag, and performance characteristics for the airplane model, 15 existing light twin airplanes were compared with respect to 9 performance and configuration parameters. The airplanes and rating categories used in the comparison are shown in Table II.

The Cessna Model 340 was selected from this group as the best example of airframe size and design for use in the modeling exercise.

The Model 340 is a pressurized, six-seat, light twin airplane base-priced at $127,500 (1972). A list of specification and performance data derived from the Cessna Model 340 brochure is

TABLE II. CANDIDATE AIRCRAFT EVALUATED FOR USE IN SMALL TURBOFAN ENGINE STUDY PROGRAM.

AIRPLANE (+ = within, criteria; - = outside criteria)	CRITERIA SPEED 648 KM HR (350 KTS) CRUISE	CRUISE ALTITUDE 7315M (24K FT)	RANGE (1000 N.MI.) ①	PAYLOAD 544 KG (1200 LBS)	FIELD LENGTH 914 M (3000 FT)	PRESSURIZATION 3.8 N/CM² (5.5 PSI)	JET STANDARD AVIONICS AVAIL	CAPACITY (6 SEATS MAX)	GROSS WT. 3175 KG (≤ 7000 LBS) ②	SCORE ③
TWIN COMANCHE	-	-	-	+	+	-	+	+	+	5
APACHE	-	-	-	+	+	-	+	+	+	5
NAVAJO	-	+	+	+	+	+	+	-	-	6
BARON	-	-	+	+	+	-	+	+	+	6
DUKE	-	+	+	+	+	④	+	-	-	5+
QUEEN AIR 80	-	-	+	+	+	-	+	-	-	4
KING AIR	-	+	+	+	+	④	+	-	-	5+
SKYMASTER	-	-	-	+	+	-	-	+	+	4
310	-	-	-	+	+	-	+	+	+	5
340	-	+	-	+	+	④	+	+	+	6+
421	-	+	+	+	+	④	+	-	-	5+
CITATION	+	+	+	+	+	+	+	-	-	7
SHRIKE	-	-	-	+	+	-	+	+	+	5
TURBOCOMMANDER	-	+	+	+	+	④	+	-	-	5+
MU-2	-	+	+	+	+	④	+	-	-	5+

① - FULL PAYLOAD RANGE
② - CENTER AISLE NOT REQUIRED
③ - THRUST LIMIT 6672 N (≤ 1500 LB)
④ - PRESSURIZATION EXISTS AT 2.9 TO 3.45 N/CM² (4.2 TO 5.0 PSI)

presented in Table III. Included in the airplane base price are sufficient avionics to maintain visual flight rules operation; however, the more sophisticated avionics are listed as optional. When typically equipped for instrument flight rules operation (de-icing and anti-icing systems, dual avionics, three-axis autopilot) and air conditioning, the list price increases to approximately $200,000. The weight of the added equipment would be about 263 kg (580 lb) resulting in substantially less payload/range capability than listed in the brochure. This optional equipment would be standard "equipment fit" in a 648 km/hr (350-knot), turbofan-powered airplane.

Prior to receipt of Model 340 engineering data from Cessna, a preliminary sizing exercise was performed for a Model-340-derived, turbofan-powered, base-line airplane. This derivative was defined with use of published data of the Model 340 Airplane equipped with Teledyne CMC TSI0520-K reciprocating engines. The methods used in this sizing exercise permit quick, brief definitions of candidate airplanes, based on similarities to existing designs. The methods described below produced results that were very close to the sizing results achieved after several months of additional work.

Step 1.- Determine new airplane structural weight plus equipment weight: Estimate the propulsion system weight, including engines, propellers, and nacelles. Subtract the propulsion weight from the airplane-empty weight. Add an estimated amount for increased "q" (dynamic pressure) capability, increased cabin pressure differential, and additional avionics. Estimated new structure and equipment weight is 1160 kg (2557 lb) at 2710 kg (5975 lb) gross weight.

Step 2.- Determine the wetted area from a published three-view drawing of the reference airplane: Estimated wetted area is 107 m^2 (1153 sq ft).

Step 3.- Determine the wetted-area drag coefficient of the reference airplane: From the published gross weight, wing area, and maximum speed at altitude, calculate the lift coefficient. With the aspect ratio and an estimated span efficiency factor, calculate the induced drag at maximum speed. Assuming maximum advertised horsepower and an estimated propeller efficiency (debased to account for slipstream drag and engine cooling--67 percent in this case), calculate the thrust horsepower and total drag. Subtract the induced drag and divide by the wetted area and "q". Estimated wetted-area drag coefficient is 0.00405.

TABLE III. CESSNA MODEL 340 BROCHURE DATA.

1972 PRESSURIZED 340 SPECIFICATIONS & PERFORMANCE

USEFUL LOAD	2278 lbs	1033 kg
GROSS WEIGHT	[illegible]	2710 kg
SPEED (Best Power Mixture)		
Maximum (at sea level)	[illegible]	[illegible]
Maximum (16,000 ft)	[illegible]	[illegible]
Maximum Recommended Cruise	[illegible]	[illegible]
Maximum Recommended Cruise	242 mph	388 km/hr
RANGE	[illegible]	[illegible]

RATE-OF-CLIMB AT SEA LEVEL:		
Twin Engine	1500 fpm	(457 m/m)
Single Engine	250 fpm	(76 m/m)
SERVICE CEILING.		
Twin Engine	26,500 ft	(8077 m)
Single Engine	12,100 ft	(3688 m)
TAKEOFF PERFORMANCE:		
Ground Run	1760 ft	(536 m)
Total Distance Over 50 ft Obstacle	2430 ft	(741 m)
LANDING PERFORMANCE:		
Landing Roll	765 ft	(233 m)
Total Distance Over 50 ft Obstacle	1840 ft	(561 m)
EMPTY WEIGHT: (Approximate)	3697 lbs	(1627 kg)
BAGGAGE ALLOWABLE:	930 lbs	(422 kg)
WING LOADING:	32.47 lbs/ft²	(159 kg/m²)
POWER LOADING:	9.48 lbs/hp	(4.75 kg/hp)
FUEL CAPACITY: Total		
Standard	102 gal	(386 L)
Optional	143 gal	(541 L)
Standard & Optional & Wing Lockers	184 gal	(697 L)
WING SPAN:	38' 1"	
LENGTH OF AIRPLANE:	34' 4"	
PROPELLER		
Constant Speed, Full Feathering		
Two Blade, Diameter	81.0 in	(2.06 m)

Specifications and Performance Subject to Change Without Notice

1972 PRESSURIZED 340 RANGE PERFORMANCE

(Recommended Lean Mixture)

Number of People	1	2	3	4	5	6
Takeoff Weight - Lbs	[illegible]	5563	5768	5973	5975	5975
Usable Fuel - Lbs	1080	1080	1080	1080	872	672
	Statute Miles	Statute Miles	Statute Miles	Statute Miles	Statute Miles	Statute Miles
Range at 75% Power, 20,000 Ft, Cabin Altitude 8000 Ft	[illegible]	1133	1129	1123	872	619
Range at 65% Power, 20,000 Ft, Cabin Altitude 8000 Ft	1220	1213	1205	1197	926	653
Range at 55% Power, 20,000 Ft, Cabin Altitude 8000 Ft	1295	1284	1273	1257	969	683
Range at 75% Power, 16,000 Ft, Cabin Altitude 5200 Ft	1206	1102	1100	1094	853	612
Range at 65% Power, 16,000 Ft, Cabin Altitude 5200 Ft	1191	1184	1178	1170	911	649
Range at 55% Power, 16,000 Ft, Cabin Altitude 5200 Ft	1269	1258	1249	1242	956	680

The above ranges allow for takeoff, climb with 75% power at 130 mph indicated airspeed, cruise, 45 minutes reserve fuel 88 lbs, at 40% BHP and [illegible]

[illegible]

Cabin altitude is based on a maximum differential of 4.2 psi.

Step 4.- Determine range of a turbofan-powered derivative at the original gross weight: Subtract the nacelle wetted area from the original airplane, and add an estimated wetted area for turbofan nacelles--7.4 m^2 (80 sq ft). Obtain a new empty weight by adding the estimated installed weight of two turbofans--317.5 kg (700 lb)--to the new structure-plus-equipment weight. Assuming a full cabin payload, obtain a new fuel weight at 2710 kg (5975 lb) gross weight--689 kg (1518 lb). Based on the estimated wetted-area drag coefficient and the original induced drag coefficient, calculate the drag at 648 km/hr (350 kts) and 7315 m (24,000 ft). Based on the thrust specific fuel consumption (TSFC) results of preliminary engine cycle analysis, and with an estimated allowance for takeoff and climb fuel, calculate a cruise range (overhead-to-overhead to dry tanks). Estimated range is 1355 km (842 miles).

The comparable range of the Model 340 with six people aboard, at 75 percent power and 6096 m (20,000 ft), is 996 km (619 statute miles), and 45 minutes fuel reserve at 40 percent power. Step 4 was repeated for higher wing loadings, and greater ranges were calculated for the turbofan-powered derivatives, at the original Model 340 gross weight. The principal result of this analysis was the determination that the postulated airplane performance criteria could be met by an airplane with a gross weight of about 2722 kg (6000 lb), having engines with approximately 1779 N (400 lb) of cruise thrust. This permitted early candidate-engine definition work to proceed with baseline engine sizes that would require little scaling in the later analyses.

Further analysis of this type was done with four candidate engine cycles and a normalized airplane configuration and mission. In this study, a graphical sizing analysis was used to obtain the airplane "solution" gross weight. The assumptions in the following list were used:

(1) Constant range = 1448 km (900 statute miles) (overhead to overhead/to dry tanks)

(2) Constant payload = 5443 kg (1200 lb) [6.(170 + 30)]

(3) Constant equipment weight = 4536 kg (1000 lb) [equipment not variable with W_g]

(4) Constant structure fraction = $\frac{W_s}{W_g} = \frac{1557}{5975} = 0.261$

(5) Maximum propulsion fraction = $\frac{W_p}{W_g} = \frac{2218}{5975} = 0.371$

(6) Constant engine $W_{eng}/F_{SLS} = 0.25$ $(\frac{F_{SLS}}{Wt} = 4, \text{installed})$

(7) Constant takeoff fuel weight = 454 kg (100 lb)

(8) Constant $C_{Dwet} = 0.004$

(9) Constant $W/S = 2155\ N/m^2$ $(45\ lb/ft^2)S_{wet}$

(10) Constant $S_{wet} = 2.97S + 420$

(11) Constant $C_{Di} = \frac{C_L 2}{\pi ARe} = 0.0497\ C_L^2$

(12) Engine performance characteristics from preliminary candidate engine cycle analysis:

Engine	$TSFC_{cruise}$	F_{cruise}/F_{SLS}	$TSFC_{installed}$	$\frac{F_{cruise\ installed}}{F_{SLS}}$
1	0.86	0.271	0.955	0.2445
2	0.79	0.2642	0.876	0.2375
3	0.75	0.260	0.832	0.2330
4	0.71	0.2565	0.788	0.2295

(13) The propulsion system weight relationships:

$$W_p = W_{eng} - 454\ kg\ (100\ lb)$$

Where: $$W_{eng} = W_{cruise} \times \frac{F_{cruise}}{W_{cruise}} \times \frac{F_{SLS}}{F_{cruise}} \times \frac{W_{eng}}{F_{SLS}}$$

$$\frac{F_{cruise}}{W_{cruise}} = 1 \div \text{lift/drag (at start of cruise)}$$

$$W_{fuel} = \text{drag} \times TSFC \times \theta$$

$$\theta = \frac{\text{range}}{\text{cruise speed}} = 2.23 \text{ hours}$$

(14) Finally, the gross weight equation, to be solved graphically or iteratively by assuming several gross weights for the structure weight fraction in the right side of the equation and calculating the propulsion weight from preceeding assumptions:

$$W_g = \underbrace{1200}_{\text{Payload}} + \underbrace{1000}_{\substack{\text{Fixed} \\ \text{equip.}}} + \underbrace{100}_{\substack{\text{Takeoff} \\ \text{fuel}}} + \underbrace{0.261\ W_g}_{\substack{\text{Structure} \\ \text{weight}}} + \underbrace{W_p}_{\substack{\text{Propulsion} \\ \text{weight}}}$$

Based on these assumptions and the calculation procedures previously described, the graphical gross-weight solutions, together with drag and engine static thrust solutions, were obtained as shown in Figure 2.

Following this analysis, NASA obtained a three-view general arrangement drawing, a speed-power polar, drag polars (five configurations), and a calculated group weight statement of the Model 340 from the Cessna Aircraft Company. These data were incorporated in the NASA aircraft synthesis computer program that was being developed concurrently with these preliminary studies. This data was also used in deriving a baseline airplane for use in the initial engine/airplane performance analysis to be conducted in Phase II.

Engine cycle analysis and sizing studies.- A preliminary examination was conducted of 12 candidate turbofan cycles. The principal cycle variables--fan pressure ratio, core pressure ratio, and turbine inlet temperature--were chosen to provide substantial spread in the design-point cruise TSFC and specific thrust ($F/\dot{W}_a$). Efficiency and loss assumptions made for these cycles reflect the levels currently attainable. The cycle variables were not chosen to provide a complete matrix of possible cycles. For example, turbine inlet temperature was chosen as a function of cycle pressure ratio only to provide a nearly constant percentage of maximum cycle thermal efficiency attainable at each selected pressure ratio. The assumptions and results of this parametric analysis are listed in Table IV.

The performance specifics of these cycles fell in groups that correspond to certain cycle characteristics. For example, there are four TSFC groups that correlate closely with overall cycle pressure ratio, and three $F/\dot{W}_a$ groups that correlate closely with fan pressure ratio. This grouping occurs when each turbofan cycle is optimized--that is, when the bypass ratio that provides the lowest TSFC for each cycle is determined. In general, the specific thrust of an optimized turbofan cycle is primarily a function of the fan pressure ratio, and the TSFC is then primarily a function of internal cycle quality; i.e. core pressure ratio, turbine inlet temperature, component efficiencies, and cycle pressure losses.

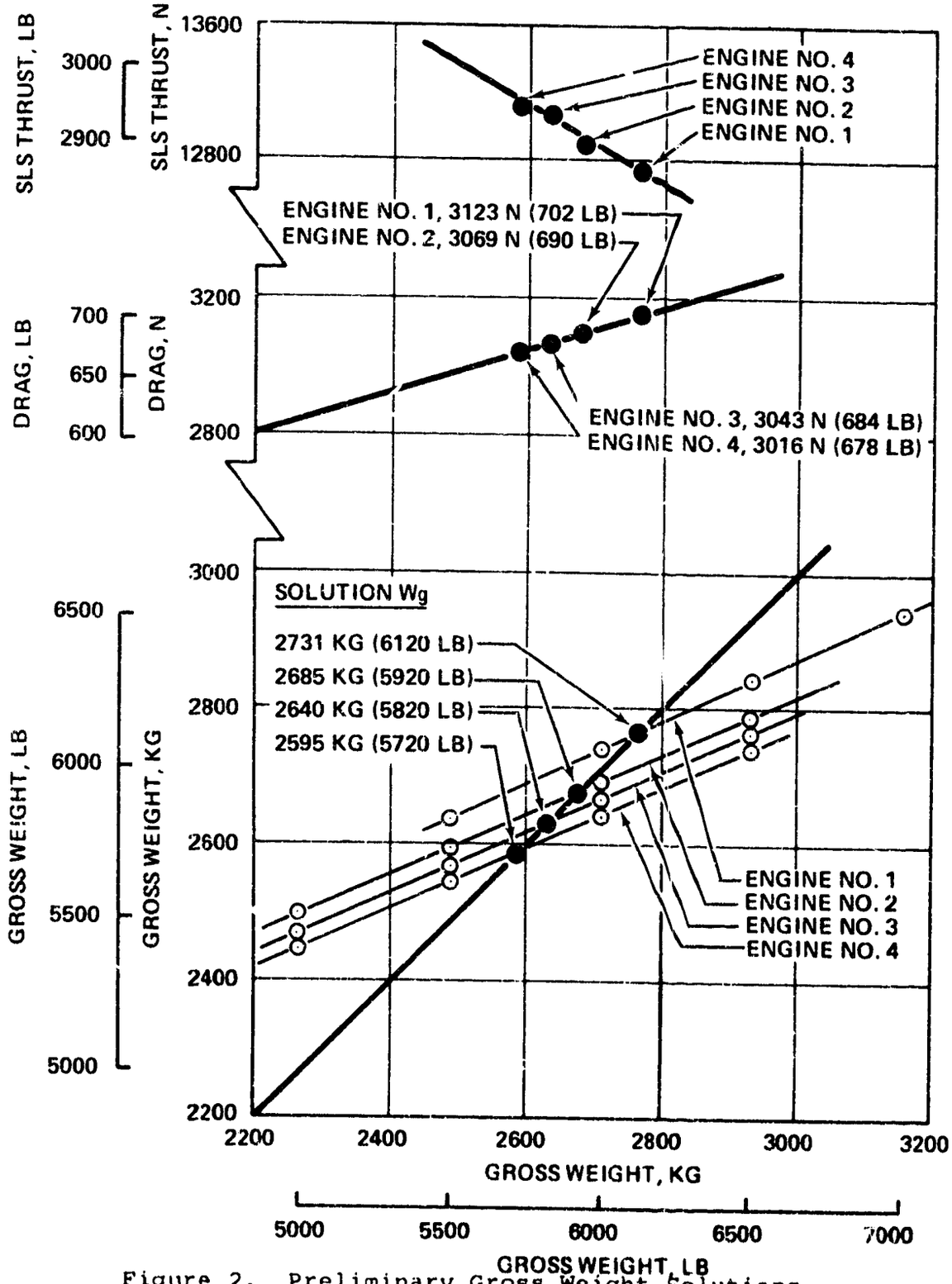

Figure 2. Preliminary Gross Weight Solutions for Four Engine Candidates.

TABLE IV. PRELIMINARY CANDIDATE TURBOFAN CYCLES.

	Fan Pressure Ratio											
	1.30:1				1.40:1				1.50:1			
Core compressor pressure ratio	4:1	5.5:1	7:1	9:1	4:1	5.5:1	7:1	9:1	4:1	5.5:1	7:1	9:1
Core adiabatic efficiency	0.84	0.82	0.81	0.80	0.84	0.82	0.81	0.80	0.84	0.82	0.81	0.80
Cycle pressure ratio	5.2:1	7.15:1	9.1:1	11.7:1	5.6:1	7.7:1	9.8:1	12.6:1	6:1	8.25:1	10.5:1	13.5:1
Turbine inlet temperature (°K)	1005	1060	1116	1172	1005	1060	1116	1172	1005	1060	1116	1172
(°F)	1350	1450	1550	1650	1350	1450	1550	1650	1350	1450	1550	1650
Specific thrust, F/W_a - (N-s kg)	100.2	96.7	94.4	92.6	131.4	126.5	123.5	121.0	161.4	155.0	151.5	148.0
lb/lb sec)	10.22	9.86	9.63	9.44	13.40	12.90	12.59	12.34	16.46	15.81	15.45	15.09
TSFC (kg N-hr)	0.088	0.080	0.076	0.071	0.088	0.081	0.076	0.072	0.089	0.081	0.077	0.073
(lb/hr lb)	0.865	0.788	0.747	0.700	0.864	0.790	0.749	0.710	0.869	0.796	0.757	0.717
Bypass ratio	4.86	5.88	6.72	7.67	3.45	4.15	4.76	5.39	2.55	3.09	3.55	4.05

All cycles have the following additional efficiency and pressure loss assumptions:

Fan efficiency	0.88
Combustor efficiency	0.98
HP turbine efficiency	0.88
LP turbine efficiency	0.90
Mechanical efficiency (both spools)	1.00
Jet velocity coefficient (both)	0.96
HP compressor bleed	0.03
Ram recovery	1.00
Combustor pressure loss	0.05
Fan duct pressure loss	0.03
Exhaust duct pressure loss	0.02

All values at cruise design point - 0.8 Mach (350 kts) and 7315 m (24,000 ft)

The four cycles in the intermediate specific thrust group offered a representative spread in cycle quality and resultant cruise TSFC. These cycles were expanded to include installation losses--i.e., nacelle drag charged to the engine performance. The results were then applied to the preliminary airplane sizing procedure described earlier. This exercise confirmed that turbofans of about 1779 N (400 pounds) of cruise thrust [6672 N (1500 lb) SLS] have sufficient size to meet the performance targets of the airplane prescribed for this study. From this group of four cycles, the 9.8:1 pressure ratio cycle was chosen as representative of moderate quality and cost.

Two distinctly different engine configuration studies were initiated for the 9.8:1 cycle. The first, an all-axial configuration, is depicted in Figure 3. The engine layout shows a single-stage 1.4:1-pressure-ratio fan, a seven-axial-stage, 7:1-pressure-ratio high-pressure compressor, an annular vaporizer combustor, a two-stage high-pressure turbine, and a three-stage low-pressure turbine. The second configuration is illustrated in Figure 4. It shows a 1.4:1-pressure-ratio fan, followed by two substages on the fan spool with 1.4:1 pressure ratio, a 5:1-pressure-ratio centrifugal high-pressure compressor, a reverse-flow combustor, a single-stage high-pressure turbine, and a four-stage low-pressure turbine. Both configurations were sized for 1779 N (400 pounds) thrust (uninstalled) at the cruise design point.

The component designs and configurations used in these conceptual engines are representative of current technology and design practice. However, because they are new and without performance maps, no attempt was made to obtain off-design or flight performance for these engines. The layouts were prepared to provide size and configuration baselines for initial component manufacturing investigations and cost analyses. Because viable component configurations are represented in these two layouts, later candidate engine designs were derived for the most part from these configurations.

While performing the parametric engine cycle analysis and sizing studies, a parallel effort was conducted to investigate a new methodology for turbofan cycle and engine optimization. As a result of work completed prior to this study, a less tedious cycle optimization method was considered possible, based on separate evaluations of propulsive and thermodynamic efficiencies. While the methodology is not fully developed, it is more rational, less time-consuming, and less expensive than conventional extensive parametric analysis procedures. The results of this investigation are submitted in Appendix A.

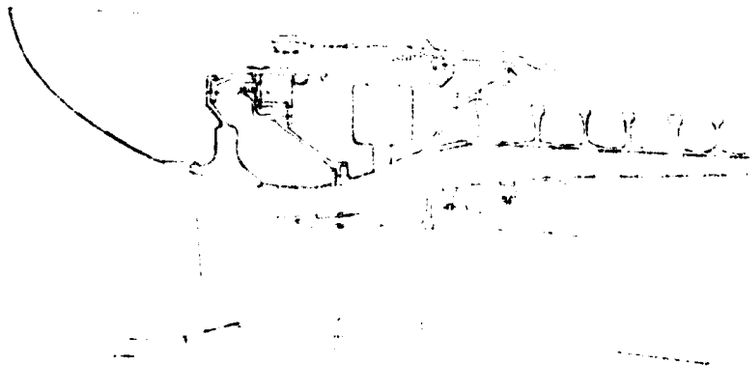

FOLDOUT FRAME

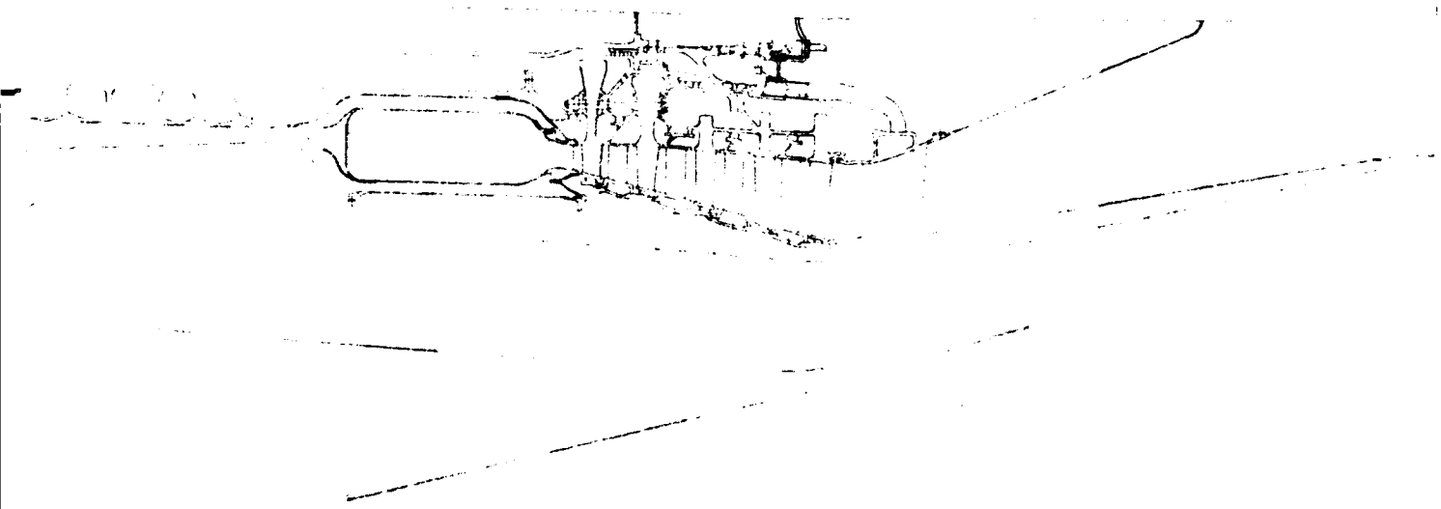

Figure 3. Turbofan Configuration Study Layout with All-Axial Core Compressor.

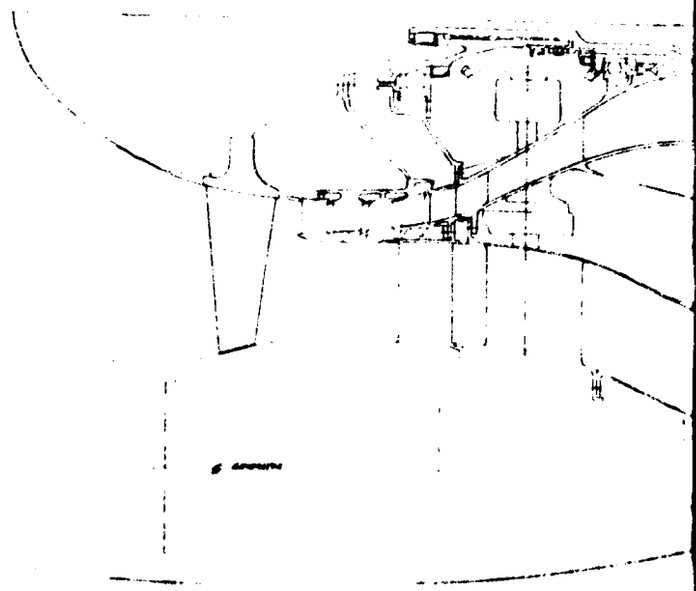

FOLDOUT FRAME

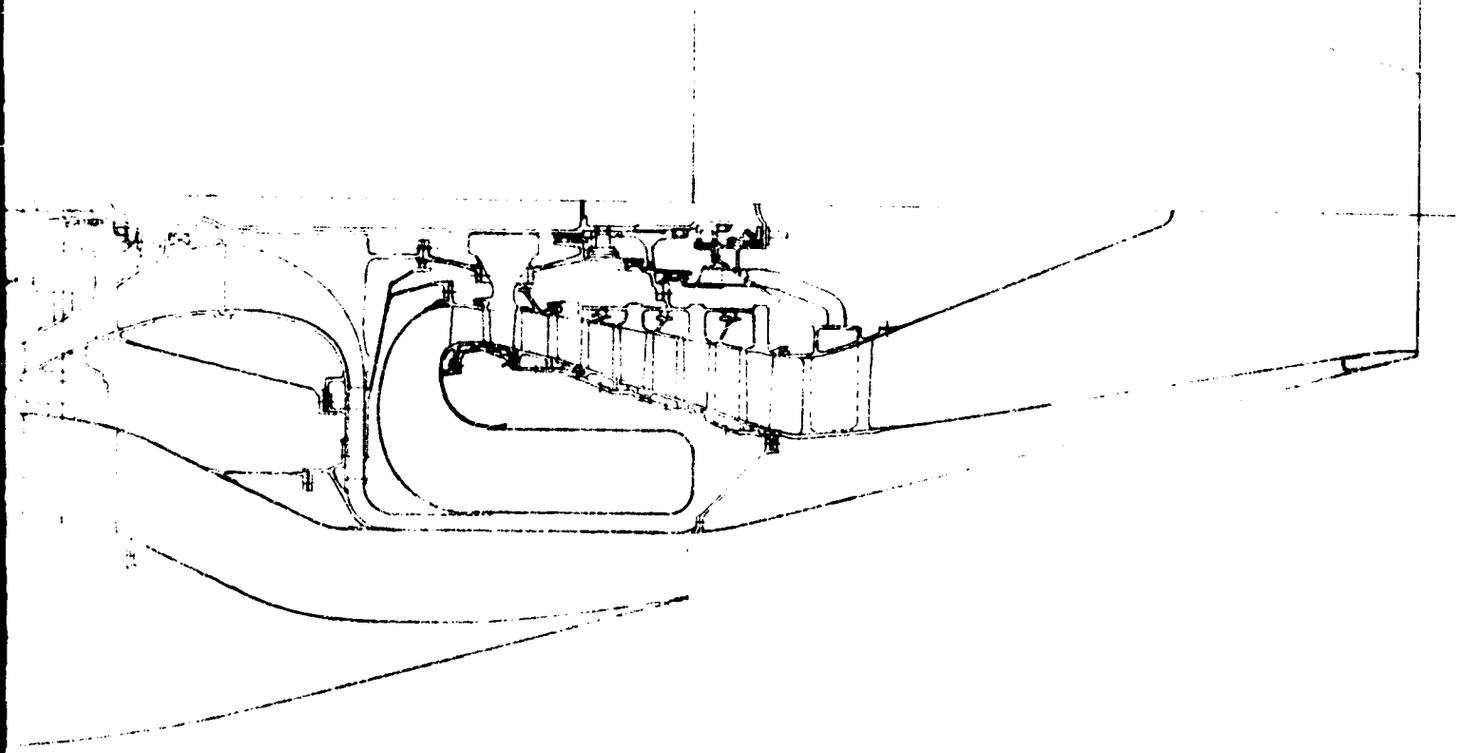

Figure 4. Turbofan Configuration Study Layout with Centrifugal Core Compressor.

Engine Cost Reduction Studies

Component cost distribution analysis. - Current engine component cost data acquired from three AiResearch-designed and -manufactured engines--a turbofan, a turboshaft, and a turbojet--was used in a component cost-distribution analysis. Pareto distribution curves of component costs associated with these engines, which account for about 80 percent of the total engine costs, are presented in Figures 5, 6, and 7.

The Pareto distribution curve was chosen to present the cost data because it provides continuing incentive for productive cost-reduction efforts. The curve is prepared by subtracting the percentage cost of the most expensive component from 100, plotting the result at an even increment to the right of the ordinate, repeating with the subtraction of the next most expensive component, and so on. As a result, the shape of the curve remains the same after cost-reduction efforts have yielded one or more lower cost components. When the most expensive component is cost-reduced, the next most expensive component takes its place and a new cost-reduction effort is initiated. For greatest cost-reduction yield, the component at the left of the curve is addressed with the greatest emphasis.

With the exception of special starting and electric power generation systems used on the turbojet, the following eight engine sections and systems are the common major cost items on the three engines investigated:

- Turbine flow-path section
- Compressor flow-path section
- Fan stage
- Combustor section
- Structural housings and frames
- Speed-reduction gearbox
- Fuel control
- Lubrication system

These items were subjected to materials and manufacturing cost-reduction investigations. The results of the investigations were applied in later definitions of candidate engines. It should be noted that the three engines from which this component cost data was prepared are economical aircraft engines in the context of the total requirements for each engine. Each is a current-technology engine designed to definite contemporary requirements. The designers were cognizant of modern materials and current manufacturing technology, and applied this knowledge to the design of cost-effective engines that met these requirements. For example, the

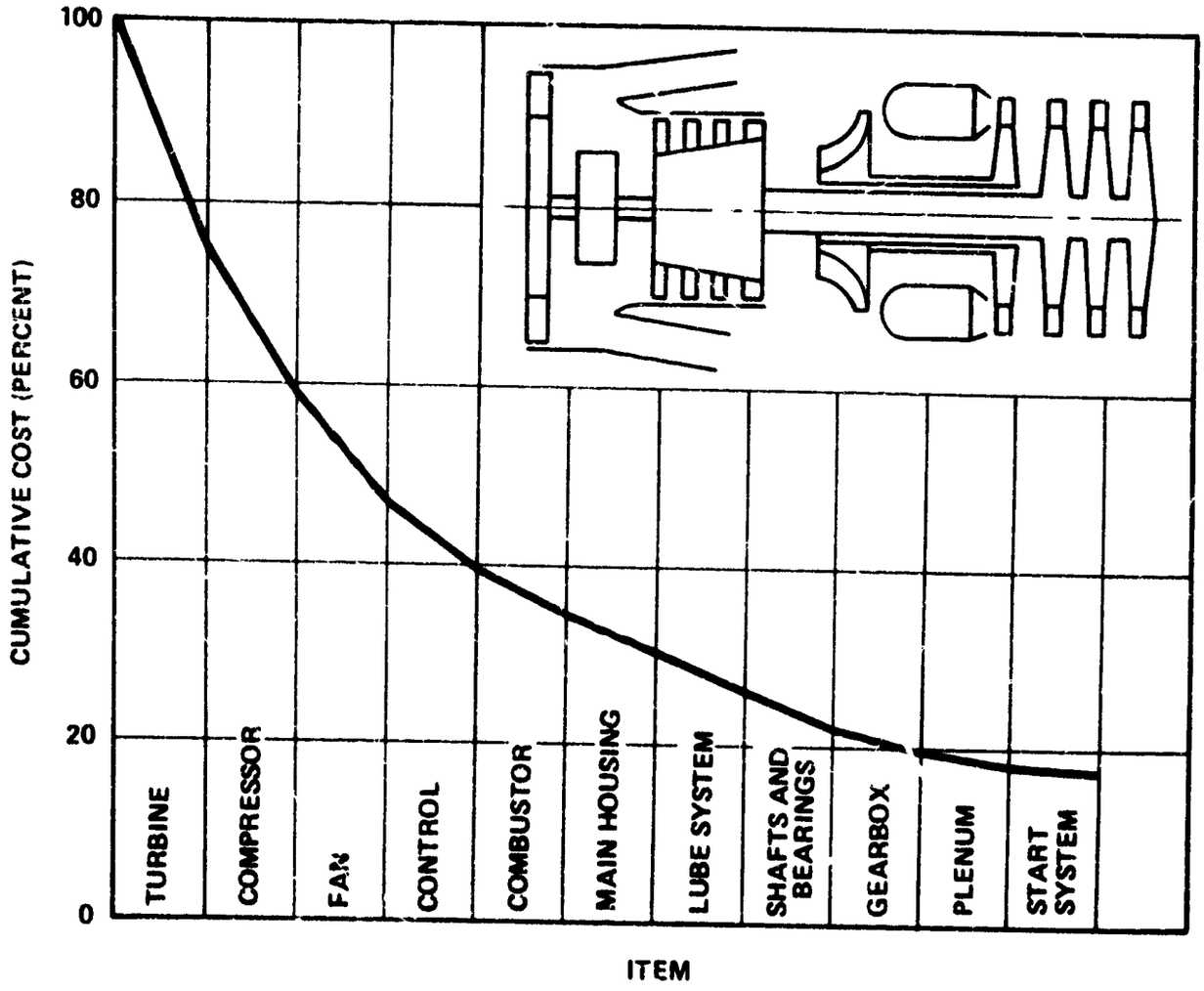

Figure 5. Pareto Distribution Curve for a Turbofan Engine.

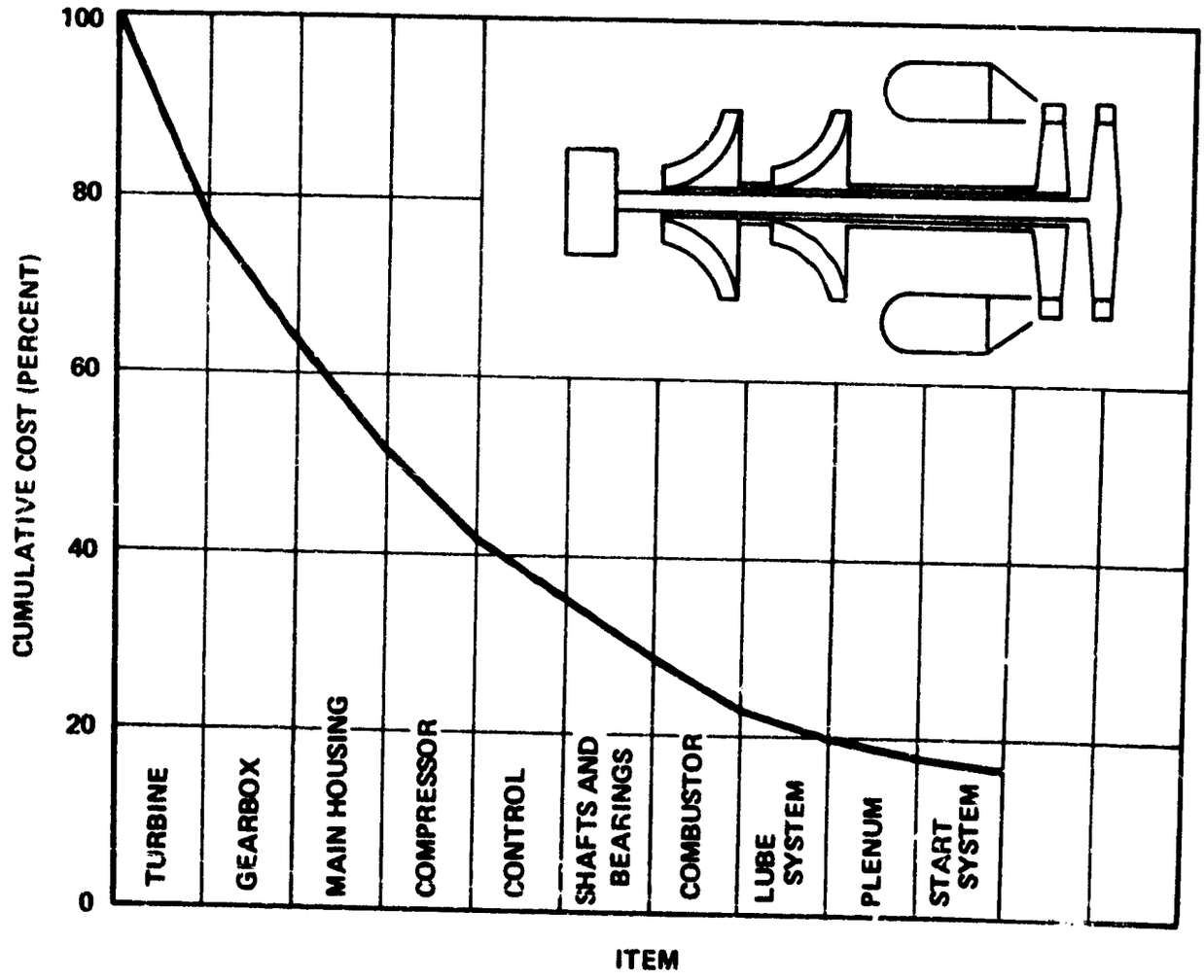

Figure 6. Pareto Distribution Curve for a Turboshaft Engine.

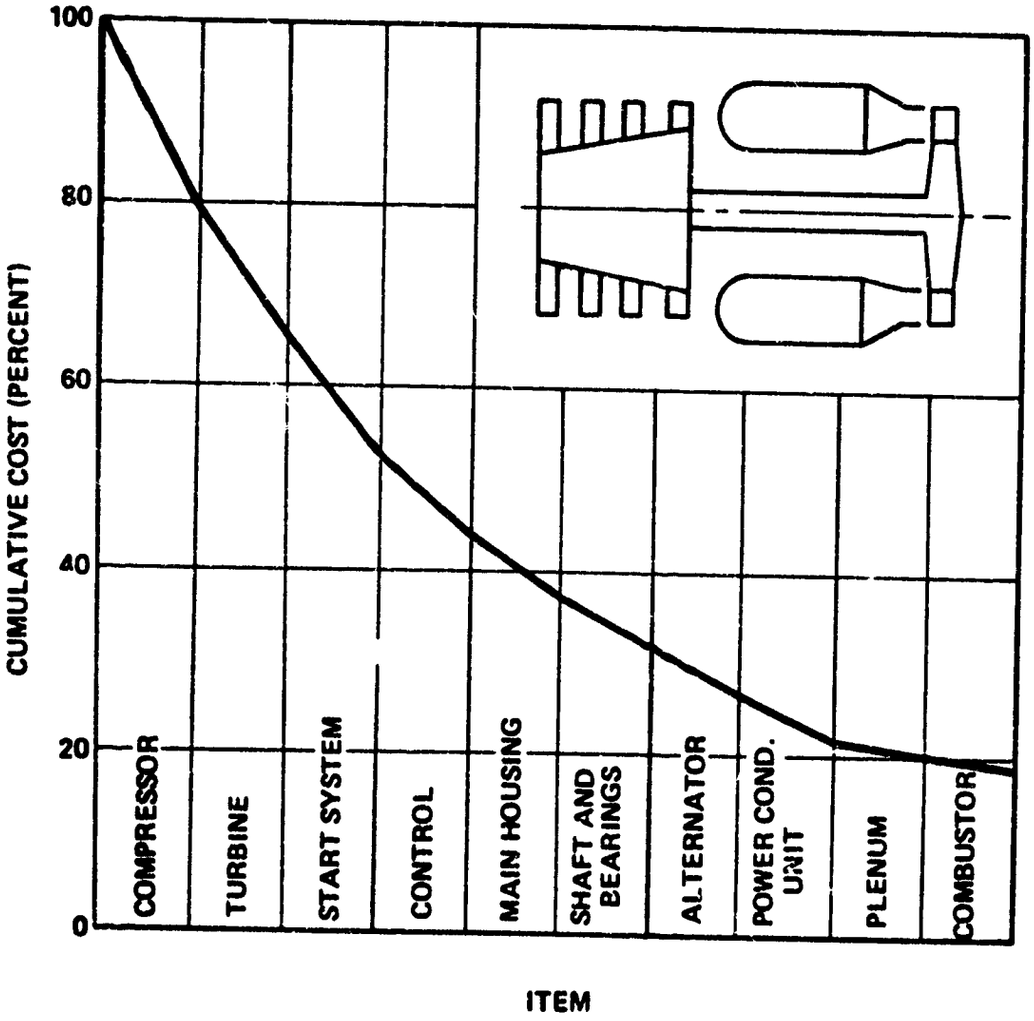

Figure 7. Pareto Distribution Curve for a Turbojet Engine.

turbojet was designed to meet the propulsion requirements of a tactical missile. Because of the low-altitude, high-subsonic-flight envelope of the missile, the engine weight is of secondary importance. It was decided by the designers, in deference to cost effectiveness, that the main structural frame of the engine should be a heavier than normal, but very low cost ductile iron casting. Since cost-effective techniques were practiced in the design of each of the three engines evaluated, the materials and manufacturing methods established for those engines were adopted as base lines for this study.

Materials and manufacturing methods investigations. - Initial efforts were directed to an investigation of alternative materials and manufacturing methods for the fabrication of turbine, compressor, and fan stages, with emphasis on the rotating components. The procedures adopted in the investigation were (a) to list the viable alternatives, (b) assess their applicability, and (c) generate new cost estimates or obtain them from appropriate suppliers. Because of the complexity of some fabrication approaches and the proprietary nature of others, in-depth discussions were held with investigators and developers of credible new methods and processes. The costs of the alternative materials and methods are listed in the following paragraphs as values relative to the base lines chosen. No attempt was made to temper optimistic cost projections or to assess the impact of development costs on unit cost. All estimates were based on a production rate of 1000 engines per year.

Turbine investigation. - The most cost-effective turbine manufacturing method for small engines (that do not require turbine blade cooling) is the precision investment casting of blades and disks in an integral configuration. This method is applicable only when the turbine configuration and rotor speed permit disk stresses that are somewhat lower than those normally allowed in forged disks. (Typically, allowable average tangential stresses are 55,000 and 65,000 pounds per square inch, respectively.) This integral configuration normally costs less than half that of the older configuration with individual cast blades attached to a forged disk by precision-ground fir-tree attachments. The development of larger integral castings is a continuing process for stators as well as rotors, and for compressor stages as well as turbine stages. While many castable alloys are available, turbine designers usually select INCO 713C or IN-100 because of their excellent high-temperature physical and mechanical properties. Although they are nickel-base alloys, the raw material costs are moderate. They have good castability, resulting in good yields. In order to employ a lower cost alloy than INCO 713C or IN-100, the turbine designer would have to design to a substantially lower turbine inlet temperature, thereby increasing the size of the engine for a given power output.

The following are alternatives to the base line INCO 713C/ IN-100 with savings potential:

(a) Dual-property or bi-cast wheels--separately cast blades, with the disk forged or cast around the blade to provide attachment. This method decreases scrap cost per misrun blade.

(b) Individually cast blades with a non precision-attachment shape activated-diffusion-bonded to a cast hub to reduce scrap cost.

(c) Integrally cast wheels with lower quality standards to accept misruns of some blades to increase the casting yield.

(d) Use of alloys that are more highly corrosion resistant, such as IN-738 or IN-792, to replace IN-100 and INCO 713C and to eliminate corrosion-resistant coatings.

(e) The use of revert material in the preparation of master heats to lower the cost of using all virgin material for castings.

The cost-saving potential of Alternative (a) is shown in Figure 8. In this case, the base-line cost was assumed to be higher than normal, reflecting the large scrappage allowance experienced in some turbine designs. The cost-saving potential of these methods is significant, especially when the engine design dictates a turbine with a large number of thin, high-aspect-ratio blades that are prone to misruns. However, a suitable attachment geometry must be developed to avoid an attendant large penalty in disk weight. This weight penalty is caused by the disk size increase that is required to carry the high "dead-rim" load inherent in the separate-blade method. The remaining alternatives must be considered in any new turbine design. However, each is accompanied by an engine weight or performance penalty, which can be traded off only after an in-depth analysis of each case.

Compressor investigation. - One of three compressor configurations is used in contemporary small gas turbine engines: (a) one- or two-stage centrifugal, (b) one or more axial stages plus a centrifugal stage, or (c) multiple axial stages. Each configuration has a preferred material and manufacturing method. The latest small-engine designs, using all axial or axial plus centrifugal compressors, were devised for integral-wheel castings. The casting material is usually the precipitation-hardening steel alloy 17-4PH. It is chosen for its very good properties and castability versus those of alternative alloys.

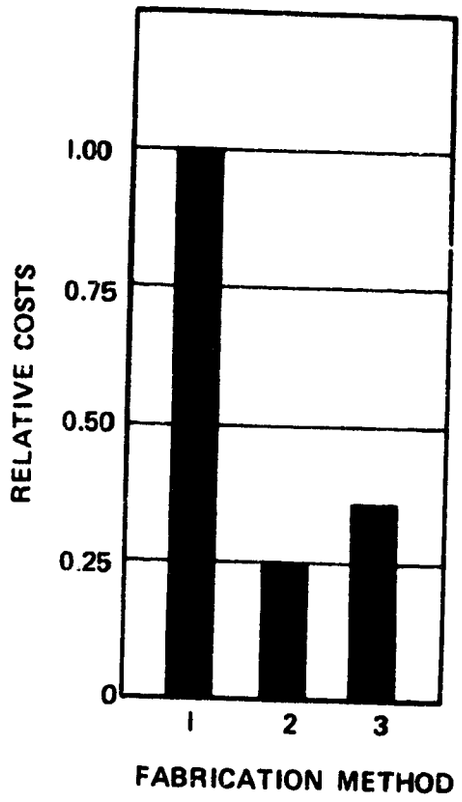

1. BASE-LINE INTEGRALLY CAST IN-100
2. DUAL PROPERTY, FORGED WASPALOY DISK/CAST IN-100 BLADES
3. BI-CAST, SEPARATELY CAST IN-100 BLADES/CAST DISK IN-100

Figure 8. Relative Costs To Produce a 9-Inch-OD Superalloy Axial Turbine Wheel with 50 to 60 Blades in Quantities of 1000 Wheels/Year (Tooling Costs Excluded).

Centrifugal compressors are generally precision-machined from titanium forgings. Tip speeds of centrifugal components are usually much higher than those of axial components. Consequently, stresses would be prohibitively high, and weight could multiply four times if centrifugal components were made of steel.

In lower tip-speed, lower pressure ratio designs, steel can be used with smaller penalties. For these applications, the alternatives described in Figure 9 were investigated. A large part of the cost of the forged and machined titanium base-line configuration is the hand finishing required to smooth the airflow passages. The lower cost of the separate-blade method requires that the blades be precision-forged or cast to size to avoid subsequent hand finishing. Because of the large size and complex shape of centrifugal compressor blades, it was determined that this would require extremely expensive and time-consuming development. These methods also incur the dead rim load weight penalty described for the turbines. In addition, the design of a reasonable blade root or attachment configuration is doubtful because of the complex curvature required in the blade when transitioning from axial to radial. The fifth alternative shown in Figure 9 is, of course, not new to compressor design. The precision investment casting has the lowest cost for low-tip-speed, low-pressure-ratio centrifugal components that follow multistage axial compressors.

It could not be shown that axial compressors could be manufactured for less cost by methods other than the precision investment casting method. Sheet metal construction was investigated as well as the separate blade methods described previously. These alternatives were judged to be more expensive, and incurred either weight or performance penalties when compared with high-yield, multiple-stage investment castings. This determination led to the consideration of methods to provide further reductions in the cost of investment castings.

The manufacturing labor cost distribution for a typical integral wheel casting is illustrated in Figure 10. This Pareto curve shows that a small number of the cost increments account for a large percentage of the casting cost. The scrap allowance for a typical 60-percent casting yield is the largest increment. Improvement of the yield of a given casting can be accomplished by several means:

(a) Blade thickness can be increased to ensure consistent filling of the mold blade cavities

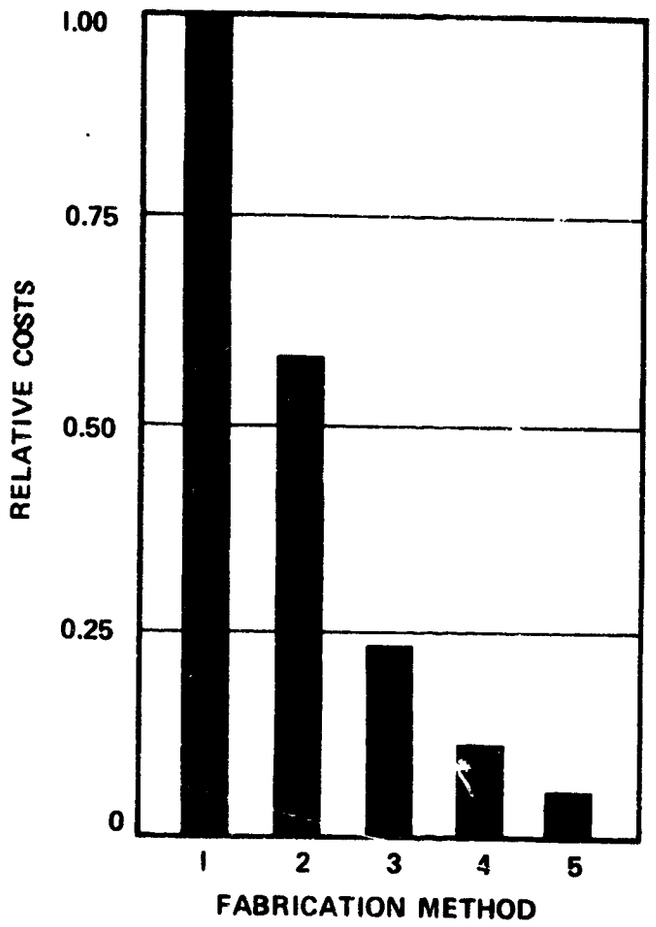

1. BASE-LINE CONVENTIONAL Ti FORGING PRECISION-MACHINED ON 5-AXIS MACHINE
2. SEPARATELY FORGED Ti BLADES/HUB FORGED AROUND BLADES USING DUAL PROCESS
3. FORGED CRES BLADES/FORGED STEEL HUB, DUAL PROCESS
4. CAST CRES BLADES/FORGED STEEL HUB, DUAL PROCESS
5. PRECISION INVESTMENT CASTING, CRES ALLOY

Figure 9. Relative Costs To Produce a 9-Inch-OD Radial Compressor Wheel in Quantities of 1000 Wheels/Year (Tooling Costs Excluded).

(b) Closer quality control of the various casting process steps

(c) Increased automation in process steps to improve consistency

(d) Relaxed quality standards for casting acceptance

By these means, an improvement from 60 to 85 percent in casting yield may be achieved.

The use of revert material could provide a substantial cost reduction for investment castings. Typically, there is as much material in discarded gating and sprues as in the finished part. A substantial cost reduction can be effected by using some of this material in combination with virgin material and accepting lower metallurgical and mechanical-property standards.

The use of reusable rubber investment patterns (RIP) in place of wax patterns provides further opportunities for reducing the cost of investment castings. Rubber patterns have been developed for low-solidity axial compressor wheels cast in aluminum. It is feasible that with novel design and considerable development, RIP would be applicable to high-solidity steel compressor and superalloy turbine wheels. RIP could provide a significant cost-reduction increment for small wheels in which the wax pattern represents a large percentage of the total casting cost.

The combined effects of improved yields, use of revert material, and employment of reusable investment patterns on casting costs are shown in Figure 11. This figure illustrates the cost-reduction potential in the investment-cast integral-stage process. The cost-effectiveness of investment castings for small engines can be improved by these developments and techniques. This should permit substantial reductions in the cost of compressors, as well as turbines. However, the cost-reduction developments would be expensive, and a large production base would be necessary to amortize these developments economically.

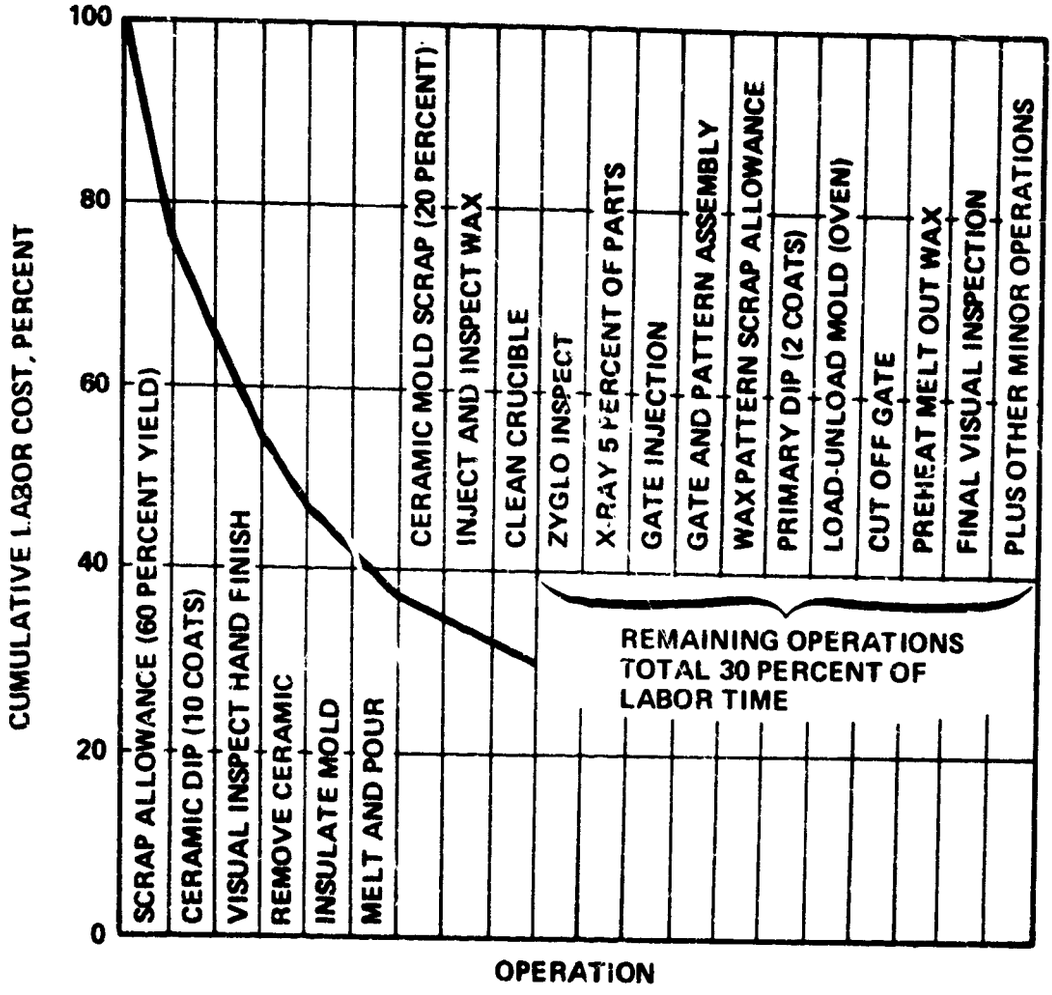

Figure 10. Pareto Distribution Curve for a Typical Precision Investment Cast Wheel.

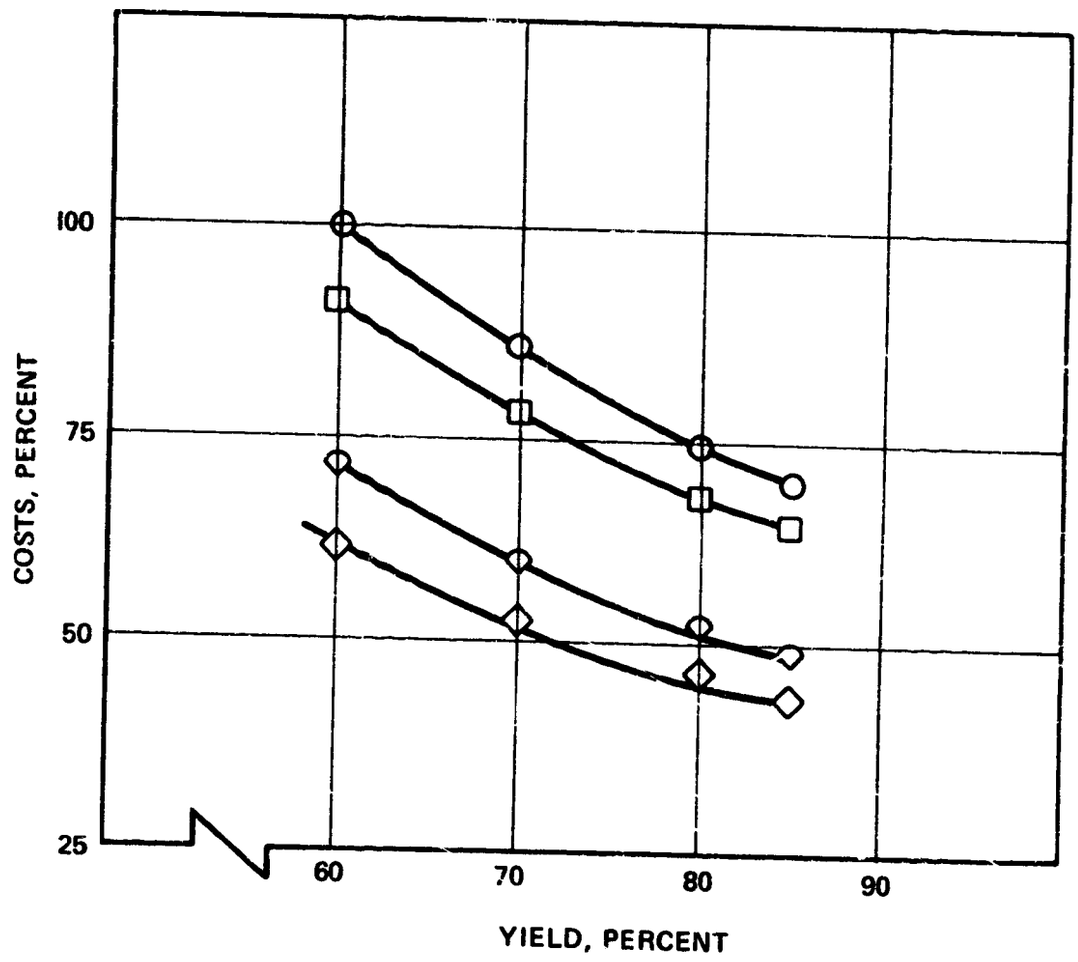

Figure 11. Cost Versus Yield for a Typical 9-Inch-OD 17-4PH Integral Wheel in Quantities of 1000 Wheels/Year (Tooling Costs Excluded).

Fan investigations.- Because the fan is the heaviest single component in a high-bypass-ratio engine, it is a large determinant of engine thrust-to-weight ratio. Typically, the fan has a hub/tip radius ratio of 0.5 or less and a tip speed of 396 to 457 m/s (1300 to 1500 ft per second). In meeting these design constraints, titanium has a stage weight advantage of up to 4:1 over steel. In turbofan engines designed and produced to this date, the advantages provided by titanium have proven to be cost-effective. Because stage weight is approximately proportional to blade chord, substantial weight savings are effected by the use of blade-to-blade vibration dampers, which permit reduction of chords up to one-half per row of dampers. This fan weight-reduction method has also proven to be cost-effective.

The low hub/tip radius ratio and high tip speeds of fans are dictated by several engine design considerations. These fan design constraints in turn dictate the fan blade geometry. Low thickness/chord ratio (0.035-0.040 at the tip), and small leading- and trailing-edge thicknesses are required for good aerodynamic efficiency at transonic fan speeds. The resultant blade geometry causes high bending and vibratory stresses in addition to high centrifugal stresses. Great care is required in fan detail design, and precision is required in fabrication to ensure structural integrity of a suitably lightweight design. An additional burden is placed on the fan design by the integrity requirements of the bird-ingestion criteria specified for FAA certification.

Because of the foregoing considerations, the conventional titanium fan with part-span dampers was established as the base line for the investigation of alternative materials and manufacturing methods. Fabricability and cost were the judging criteria used for the alternatives assessed in the investigation. It was acknowledged that the replacement of forged titanium in a fan design would require an extensive and costly design and development program.

The fan design, materials, and fabrication alternatives investigated and the estimated costs relative to the titanium base line are listed in Figure 12. The precision investment cast steel (CRES) blades and precision-forged aluminum blades proved outstanding examples of cost-reduction potential, and were identified for later engine/airplane cost trade-off and sensitivity analyses.

The results of engine cost-reduction studies conducted in Phase I are:

(a) The turbine, compressor, and fan sections were identified as the most expensive turbofan components, and would therefore yield the greatest return to cost-reduction efforts.

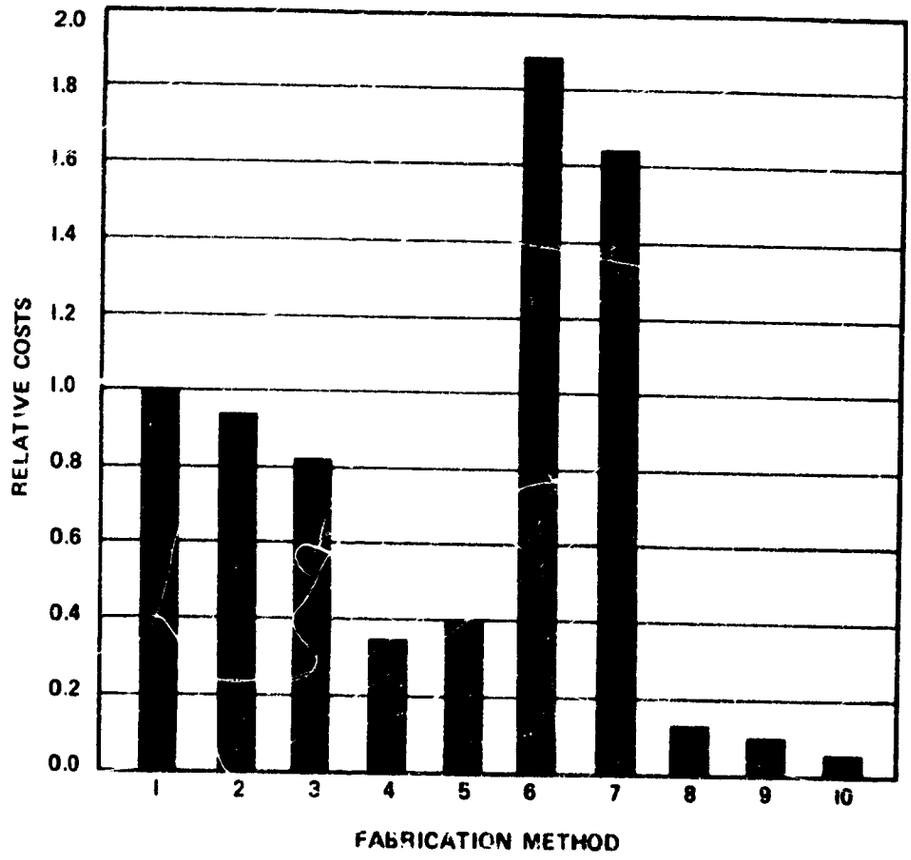

1. CONVENTIONAL FORGED AND PRECISION MACHINED Ti ALLOY WITH DAMPERS
2. PRECISION FORGED AND MACHINED Ti ALLOY WITH DAMPERS
3. PRECISION FORGED AND MACHINED Ti ALLOY, NO DAMPERS
4. PRECISION FORGED AND MACHINED CRES ALLOY, NO DAMPERS
5. SHEET METAL UNIFORM X-SECTION CRES ALLOY, NO DAMPERS
6. METAL MATRIX Ti OR Al COMPOSITE, NO DAMPERS
7. Ti ALLOY SPAR, COMPOSITE SHELL, NO DAMPERS
8. HOLLOW PRECISION CRES ALLOY CASTING, AIRMELT
9. SOLID PRECISION CRES ALLOY CASTING, AIRMELT
10. PRECISION FORGED ALUMINUM ALLOY, NO DAMPERS

Figure 12. Relative Costs To Produce a 5- to 6-Inch Fan Blade in Quantities of 15,000 to 30,000 per Year (Tooling Costs Excluded).

(b) The investment-cast integral-wheel method was identified as the lowest cost of the alternatives investigated for the manufacture of turbine and compressor rotors and stators.

(c) Means were identified whereby the cost of investment-cast turbomachinery can be further reduced when sufficiently high production rates are attained to offset and amortize the cost of engineering and development.

(d) Substitution of steel investment castings for forged titanium fans and centrifugal compressors showed the most significant cost savings of all alternatives investigated. However, due to large weight penalties, the cost-effectiveness of this substitution can only be determined by aircraft sensitivity analyses.

Preliminary Candidate Engine Definition

Engine configuration studies. - The aircraft gas turbine engine has occupied the minds of engine designers for over 30 years. Thousands of engine configurations have been designed, built, and demonstrated. Hundreds of engine designs have been produced in quantity, and a few remarkable engines that were timely and correct in the total-design context have been produced in quantities of tens of thousands. The essence of these successful, classic engines is that they were "designed with intent." The designers' intent was manifested most obviously in engine configuration and detail mechanical design. Successful engines invariably exhibit excellence in these design characteristics.

The cycle and performance characteristics of turbine engines are the traditional criteria by which engines are judged and compared. However, it is the configuration and mechanical design features that set engines apart. These features provide lightness, compactness, durability, reliability, maintainability, and manufacturing economy. These qualities in turn provide the total excellence required to ensure the longevity of an engine on the production line.

While the aircraft gas turbine has substantially evolved and matured in the past 30 years, engine design remains an art. This is evidenced by the fact that competing engines with essentially the same cycles, designed by companies cognizant of the same technology, typically show substantial differences in configuration and detail design. Despite these differences, obvious design principles have evolved and have been identified by today's engine designers and informed customers. To ignore these principles in a new engine design would result in an engine that would not be totally responsive to the needs of the customer.

These principles were applied in the candidate engine definition work of this investigation. Pertinent design principles were identified in many new engines and assessed for applicability to the candidate engines. Component configurations and arrangements were evaluated that would facilitate adherence to these principles.

The most significant principle exhibited in most new engines is that aero-component design was manipulated to achieve engine arrangements that minimize expensive, parasitic internal machinery, such as bearings, seals, splines, couplings, gears, shafts, lubrication systems, and special nuts and devices that are necessary in engines. Thus, it has been shown by example, that by appropriate fan, compressor, and turbine design, the amount and complexity of this machinery can be substantially reduced.

The two-spool configuration (consisting of separate fan and core spools) is the accepted, conventional turbofan engine configuration. The two spools of this configuration can each be carried on a pair of bearings, in only two sump cavities, and supported by just two structural engine frames. First-generation turbofans lacked the aero-component characteristics that make this simple arrangement possible. Typically, seven engine main bearings supported by four frames were utilized because the high-pressure rotor (or core spool) was designed for high speed and required three small-diameter bearings for support. The result was a long, small "hole" through the core. Consequently, the low-pressure rotor (or fan spool) required the support of four bearings along its length in order to maintain required shaft dynamics and critical speed margins.

There are several recent examples of turbofan design in which the four-bearing, two-frame arrangement was accomplished. Typically, these engines have core compressors with higher inlet hub/tip ratios, which result in low values of rotor speed per unit of airflow. These compressors are also shorter in length. At a high hub/tip ratio, the average blade tangential velocity is greater, permitting higher pressure ratio per stage of compressor. Therefore, fewer stages are required for a specified overall pressure ratio. A further shortening effect is that at high hub/tip ratio, the blade radial heights are small; then, with conventional aspect ratios, the blade chords and axial stage lengths are less. Bearing technology has also played a part in the achievement of the new four-bearing, two-frame engines. The speed capability of bearings is usually defined in terms of the product of the bearing bore diameter, in millimeters, times the design limit speed, in revolutions per minute, and is referred to as the "DN value." Typical design DN values in older engines were from 0.75 to 1.25 million. Intensive bearing, seal, and lubrication design and development efforts have raised DN capability in new engines to about 2 million. The value targeted for current continuing efforts

is over 3 million. Together, the high hub/tip ratio compressors and high DN value bearings have permitted engine designers to maximize the core "hole" diameter, minimize its length, and thereby accomplish the lightweight, economical four-bearing, two-frame configuration.

The design principles outlined in the previous paragraphs were adopted for the candidate engine conceptual design work of this study. The engine basic layout studies, shown in Figures 3 and 4, were prepared in accordance with these principles. These layouts served to identify general component characteristics and design limits that might prevent adherence to these principles in small engines.

Typically, small engines are burdened by several size-related limitations that prevent greater attainments in their performance specifics. The following examples illustrate those limitations:

- Aerodynamic losses rise rapidly at Reynolds numbers below 2.5×10^5, thus adversely affecting the efficiency of small aerodynamic components.
- Manufacturing tolerances common to large engines cause greater deviation from the nominal when applied to small engines, with a further debasing effect on efficiencies through greater losses, leakages, etc.
- Some aero- and thermodynamic processes do not scale linearly--for example, combustion, which is largely a volume-related process. Thus, small engines typically have disproportionately large combustors, while meeting the same loading criteria as large-engine combustors.

The economic limitations of small engines, of course, prevent the finesse in detail design execution exhibited in large engines. A bolted-flange connection scaled down from a large engine, although mechanically satisfactory, would be prohibitively expensive due to the costly preparation of a great number of small holes and installation of a large number of small nuts and bolts. Thus, small engines have disproportionately large and heavy flanges. Similar considerations throughout a small-engine design serve to compromise the size, weight, and finally, engine performance specifics.

The engine configuration studies conducted in Phase I encompassed general engine design principles and specific constraints and requirements applicable to small turbofan engines. These initial studies provided the basic design data and philosophy required for early definition of the candidate engines that were designed and evaluated in Phases II and III.

Component configuration studies.- Myriad aerodynamic component configurations can be found in the small gas turbine engines produced today. The synthesizing effect of designing a large number of engines over a long period of time has not evolved a "best" set of component configurations for small engines. Designers of large engines consistently choose straight-through flow paths, with axial-flow components arranged in tandem or in series. In large engines, this arrangement minimizes the amount of metal required to effect the necessary aero- and thermodynamic processes since it provides the highest performance specifics, together with lowest manufacturing cost. This is not a true or practical philosophy for small-engine designs. Many small engines proven to be cost-effective and adequate in performance have tortuous flow paths. Radial-inflow inlets, centrifugal compressors, reverse-flow combustors, radial-inflow turbines, and right-angle exhausts have been used together in successful small engines.

Designing a small engine with a minimum amount of metal and a simple flow path does not ensure high performance and low cost. In fact, a complex and variable set of rules governs the flow-path shape and component configurations. The rules are, however, flexible and subject to wide interpretation. For example, the policy of one engine manufacturer prohibits axial compressor stages with blade heights of less than 15.24 mm (0.6 inch), yet other manufacturers have designed and produced engines with smaller stages.

The selection of fan configurations for the candidate engines was more straightforward than was the selection of other engine components. In current fan design practice, the use of inlet guide vanes is avoided in deference to cost, simplicity, performance, and the advantage of not having static elements in the flow path ahead of the fan that require anti-icing. Current practice maximizes the flow per unit frontal area by using a low hub/tip-diameter ratio (0.35 to 0.50), with resulting tip relative Mach numbers of 1.2 or greater. Adiabatic efficiencies of 87 to 89 percent are attainable at pressure ratios above 1.5 in these designs. In current practice, the fan outlet stator vanes are spaced downstream by about two times the fan blade axial chord. This provides length for attenuation of the fan blade trailing-edge wakes and reduces noise generating interference between the wakes and the stator vane leading edges. This spacing has little effect on the fan stage efficiency.

The fan configuration and design principles outlined here were used in the preliminary design of fans for the candidate engines. Engine cycle and performance analysis showed that fan pressure ratios between 1.3 and 1.5 were required. Since pressure ratios greater than 1.5 are easily attainable in one stage, multiple-stage fans were not considered.

The size of the turbofan engines defined in this study did not limit the selection of compressor configurations. Initial airplane and engine sizing analysis indicated that engines with core-compressor corrected inlet flows of about 3.1 kg/sec (7 lb/sec) would be required. At this flow, either axial- or radial-flow compressors or combined axial/centrifugal compressors can be used. All three types are used in engines produced by AiResearch in this size class, with good efficiencies and operating characteristics demonstrated in each type. It was therefore determined that the candidate engines must include both axial- and radial-flow compressors.

An objective of this study was to determine which compressor type provides the most cost-effective engine, yielding the most economical airplane. Initial studies indicated that there was no advantage of one type over the other with respect to either cost or performance. Comparative analysis of representative engine designs was required to establish a "best" compressor configuration. Therefore, when candidate engine cycles were defined, engine designs were prepared with both axial and centrifugal compressors for each cycle. By this method, the effects of engine configuration, weight, performance, and cost differences could be determined from the results of the airplane synthesis and sensitivity analyses.

State-of-the-art combustor technology and performance attainments are generally independent from the overall combustor configuration. High-performance combustors are normally the product of detail design and development finesse. Various fuel-injection techniques are used successfully, including fuel pressure atomizers, air-assisted atomizers, air-blast atomizers, shaft-mounted slinger atomizers, and vaporizers. Low smoke and gaseous emissions characteristics have been demonstrated in most candidate configurations with the various fuel-injection techniques. However, future emissions requirements may dictate the use of a "best" combustor design and fuel-injection system. Advanced technology investigations indicate that an in-line, axial-flow, annular configuration providing a low value of liner surface-to-volume ratio will be required. The "best" fuel-injection system will probably evolve from current technology vaporizers, or from air-blast atomizers. The only apparent configuration-oriented cost advantage identified in this investigation favors combustors using vaporizers. Vaporizers are less costly than atomizing nozzles and require lower fuel supply pressure, resulting in a less expensive fuel pump.

Based on the foregoing considerations, it was determined that the candidate engine designs would have annular vaporizer combustors. Axial-flow engines would have an in-line configuration. Engines with centrifugal compressors would have the combustor wrapped around the turbine in a reverse-flow configuration. Based on an assessment of current attainments, the combustors would be sized for volumetric heat-release rates between 185 and 370 billion

J/hr/atm/m^3 (5 and 10 million Btu/hr/atmosphere/cubic foot). At these rates, it should be possible to design and develop combustors having low pressure loss, 0.2 temperature distribution pattern factor $\left(\frac{T_{max\ out} - T_{avg\ out}}{T_{avg\ out} - T_{in}}\right)$, essentially 100 percent efficiency, and good stability and relight capability throughout the airplane flight envelope.

There are few turbine configuration alternatives. The axial-flow configuration is the obvious choice for both compressor- and fan-driving turbines. A radial-inflow configuration would be suitable for driving a small, high-pressure-ratio centrifugal compressor in place of two axial stages. However, the inherent high tip speed and low outlet hub/tip-diameter ratio of the radial-inflow turbine results in a heavy disk, with a small center hole. As described previously, this small hole would inhibit the achievement of the four-bearing, two-frame engine configuration.

With conventional loadings and mechanical design, single-stage turbines can be designed to drive core compressors with up to 6:1 pressure ratio. Above this pressure ratio, single-stage designs would have high aerodynamic loading that would be time-consuming and expensive to design and develop. Accompanying high disk rim velocity would prohibit the use of the low-cost, integral-wheel casting method of manufacture. Therefore, it was determined that candidate engines with compressor pressure ratios up to 6:1 would have single-stage axial-flow compressor-driving turbines.

The multistage axial-flow configuration was chosen for the fan-driving turbine in all candidate engines. The principal configuration consideration was that given to the location and number of stages. A single- or two-stage design could be used, but would require a transition duct between turbines to match the turbine flow-path diameters. The cost, length, and weight of this duct could be avoided by using a close-coupled, three-stage design. Because of the small rim diameter and lower rim velocity of the three-stage design, the disks are lighter and less expensive and have large center holes that permit tucking the turbine-end bearings inside the fan turbine, thereby shortening the fan shaft. This configuration was judged to be best for all candidate engine designs.

Selected candidates for cycle studies.- Based on the engine cycle and airplane sizing analyses discussed previously, six engine candidates were selected for further definition in Phase II. The six engines were to represent three basic cycles. Two basic configurations were selected for each cycle. Tables V and VI present the cycle, performance and configuration characteristics that were judged to be appropriate to the candidates. It was

determined that the engines should be defined from off-the-shelf aerodynamic components, for which performance maps are available. With this approach, engine performance could be derived quickly, resulting in credible engine designs.

A single fan pressure ratio was chosen for the candidate engines consistent with optimum net propulsive efficiency and takeoff/cruise thrust matching considerations. A fan pressure ratio of 1.4 was a tentative choice, to be substantiated later by additional airplane takeoff and cruise performance analysis.

The cycle pressure ratio is the principal determinant of specific fuel consumption. Therefore, three core pressure ratios were chosen to provide a substantial spread in the cruise specific fuel consumption of the candidate engines.

The main effect of turbine inlet temperature in a turbofan engine is to size the engine core. When the engine thrust requirement, the fan pressure ratio, and the fan airflow have been established, the size of the core (and the resultant bypass ratio) is determined by the specific power of the core. The specific power, in turn, is determined partly by cycle pressure ratio, but mainly as a function of turbine inlet temperature. The thermal or internal cycle efficiency is also affected by turbine inlet temperature. While the tentative selection of turbine inlet temperature for the listed candidate engines was based on the foregoing considerations, higher temperatures (and consequently higher bypass ratios) were to be investigated in Phase II cycle analysis.

TABLE V. CANDIDATE ENGINE CYCLE AND PERFORMANCE CHARACTERISTICS*

	CYCLE		
	I	II	III
Fan pressure ratio	1.4	1.4	1.4
Core pressure ratio	4	6	9
Overall pressure ratio	5.6	8.4	12.6
Turbine inlet temperature (°K)	1005	1089	1172
(°F)	1350	1500	1650
Cruise specific thrust (approx.) (N-s/kg)	127.0	127.0	127.0
(lb/lb/sec)	13.0	13.0	13.0
Cruise TSFC (approx.) (kg/N-hr)	0.087	0.079	0.071
(lb/hr/lb)	0.85	0.77	0.70
Bypass ratio (approx.)	3.4	4.4	5.4

*All values at cruise design point: 648 km/hr (350 kt) and 7315 m (24,000 ft)

TABLE VI. CANDIDATE ENGINE CONFIGURATION CHARACTERISTICS

Configuration	1A (Axial)	1C (Centrifugal)	IIA (Axial)	IIC (Centrifugal)	IIIA (Axial)	IIIC (Centrifugal)
Fan	1 Axial	1 Axial	1 Axial	1 Axial	1 Axial	1 Axial
Compressor	4 Axial	1 Centrifugal	5-6 Axial	1 Centrifugal	5-6 Axial (With Fan sub-stages)	2 Centrifugal or (1 Centrifugal with fan sub-stages)
High-Pressure Turbine	1 Axial	1 Axial (Radial)	1 Axial	1 Axial	2 Axial	2 Axial
Low-Pressure Turbine	Multi-Axial	Multi-Axial	Multi-Axial	Multi-Axial	Multi-Axial	Multi-Axial

Acoustics Evaluation

Analytical method. - Before and during the course of the small turbofan engine study, acoustics efforts were directed toward the development and verification of analytical methods that permit:

- The determination of the primary aircraft/engine performance variables that cause or influence the generation or propagation of noise and the development of prediction techniques.
- The development of guidelines for changes in normal aircraft/engine equipment and components to control the generation or propagation of noise.
- The development of guidelines for the design and fabrication of acoustical attenuation devices to be installed in or attached to the aircraft/engine as either original equipment or retrofit to control the generation or propagation of noise.

Noise control can be implemented by overall sound power reduction, sound pressure reduction in the direction of maximum radiation, a shift of noise to less annoying frequency bands, a changing of the tonal combination to a less discordant quality, or a reduction in signal-to-noise ratios.

Major sources of aircraft engine noise are listed below and illustrated in Figure 13.

- Core exhaust stream
- Fan exhaust stream
- Compressor blades (inlet duct radiation)
- Fan blades (inlet duct radiation)
- Fan blades (fan exhaust-duct radiation)
- Turbine blades (core exhaust-duct radiation)

Minor sources of noise exist such as those radiating from the skin of engine nacelles and from the turbulent flow over flaps, spoilers, landing gear, and the like. The noise from these minor sources, however, is usually masked by the more intense noise from the major sources.

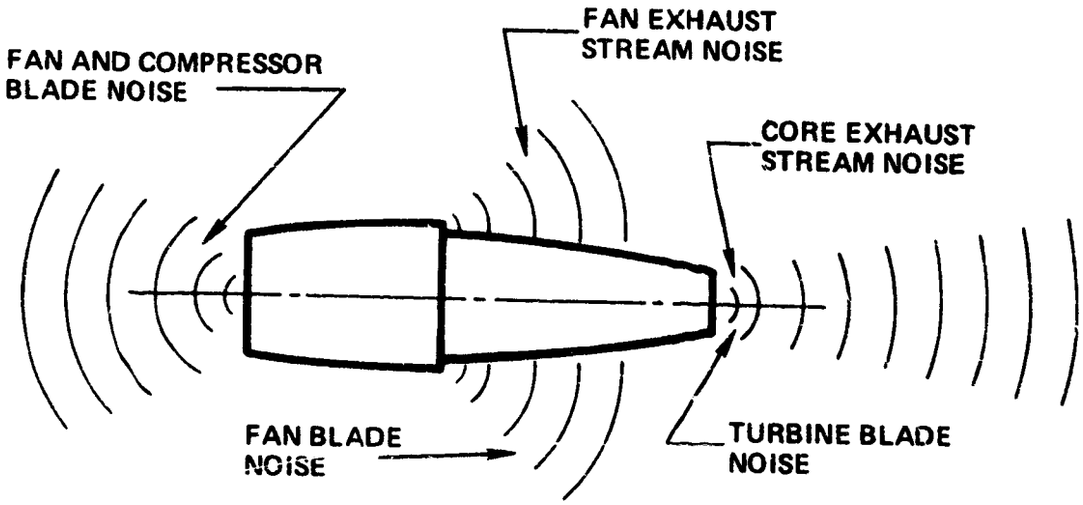

Figure 13. Major Sources of Noise from Aircraft Engines.

In order to adequately predict the flyover noise signature of a turbopropulsion engine, it is necessary to predict the contributions to that signature from each component. A family of computer programs have been completed so that these component noise predictions are made separately. This allows maximum flexibility for widely differing engine configurations and also later modifications of the individual prediction methods as improvements become available. The more important functions of the prediction method are discussed in the following paragraphs.

Fan and Compressor Noise. - The chain of compressor and fan noise radiation is developed in the following manner.

COMPRESSOR FLOW INVOLVES
UNSTEADY COMPONENTS

↓

UNSTEADY FLOW OVER THE
BLADES CAUSES FLUCTUATING FORCES

↓

FLUCTUATING FORCES PRODUCE NOISE

↓

NOISE COUPLES INTO INLET OR OUTLET DUCTING

↓

DUCT RADIATES SOUND INTO FREE AIR

↓

OBSERVED SOUND INTENSITY

Noise is initially generated by airflow fluctuations in the vicinity of the compressor stages. The sound results from a variety of different mechanisms--e.g., mass flow variations, the fluctuations and motions of aerodynamic pressure acting upon the blades, and the turbulent fluid motions themselves. Once generated, the sound escapes to the atmosphere. The most direct route is through the inlet and outlet flow ducts, although some of the acoustic energy escapes through the engine walls. Methods for external noise suppression rely upon attention to these transmission paths.

The noise spectrum basically consists of two distinct types of sound: harmonic (tonal) and broadband (random). The random sound extends over a wide range of frequencies, but tends to peak at very high frequencies, particularly in small turbofan engines. The tonal sound has one or more fundamentals corresponding to the blade passage frequencies of the compressor stages, together with associated harmonics. Broadband noise is attributable to the action of turbulence and other irregular flow disturbances upon the compressor blades.

The tonal spikes can be identified with the fundamental frequency of a rotating blade stage, as calculated by

$$F_i = B_i n_i$$

where F_i is the fundamental blade passage frequency of the i stage rotor, B_i is the number of blades on that rotor, and n_i is the rotational speed (revolutions per second) of that rotor.

Other combination tones, at sum and difference frequencies of the stage frequencies, can also be identified in the spectrum, although the exact mechanism of their combination is not well understood.

The tonal noise content at each of the stage frequencies is attributable to fluctuations of the fluid medium induced by the rotation of the stage rotor. These fluctuations can comprise additive components originating at the rotor blades, the inlet guide stators, and outlet stators of each stage. They can be mass-flow fluctuations, force (loading) fluctuations on the blades and vanes, or local fluid stresses around the rotor blades, giving rise to the familiar monopole, dipole, and quadrupole sound sources, respectively. The mass fluctuation terms arise solely due to rotor-stator interaction and consequently are closely dependent on details of the stage geometries and flow parameters. The force terms originate by two mechanisms. First, the rotor blades carry a steady pressure-loading field with them as they rotate, and this loading is imparted to the fluid medium periodically at any stationary point in the rotor plane. Second, a

nonsteady-load field is induced at the rotor and stator blades by time variances of the inflow velocity vectors. Each loading effect can be of primary significance. Usually the steady loads contribute predominantly only to the very low order harmonics of simple fan systems (with no inlet guide vanes or outlet guide vanes), and the unsteady loads contribute to all harmonics of complex stage systems. The latter effect is again closely dependent on stage geometry and flow parameters. The mechanisms by which the quadrupole (stress) acoustic sources contribute to the discrete frequency components have been studied, and it has been determined that the primary effect is due to an interaction between the periodic potential flow field and the turbulent velocity field surrounding the rotor disk. This quadrupole term becomes important when both the rotor blade number and Mach number are very high--such as in the case of transonic compressors.

The broadband base of the frequency spectrum is not so simply identifiable with blade-row design parameters. Its origin is a result of the highly random turbulent components of the flow field--giving rise both to random pressure loadings on the blades and vanes, and to fluid shear stresses similar to those of a jet stream. In multistage axial compressors, the turbulence from one stage is input directly to the following stage; and the resultant effect of all stages can induce a subjectively predominant noise content (when the random noise level in a critical bandwidth exceeds a discrete frequency level in the same bandwidth).

Each of the noise components, discrete frequency and broadband, undergoes a complicated transmission--through the stages and along the duct--before it is radiated to free space. Both dispersion and dissipation of the sound occurs to some degree in the transmission process. The observed characteristics of the noise will therefore differ from those predicted by simplified source models. The effects of duct transmission have been studied in some detail, and the energy coupling between the source and duct transmission modes has been demonstrated to be of primary importance to the radiated noise levels and directivity patterns. Each generated harmonic noise component, for example, can energize a very large number of transmission modes--each mode having a different coupling efficiency, transmission efficiency, and radiation efficiency at the energizing frequency. The final, observed sound harmonic level will be influenced by whichever mode gives a maximum at the point of observation. Movement to another observation location may mean that a different mode predominates or that the directivity pattern of the first mode is to be accounted for.

When the fan (or compressor) is operating at low tip speeds and has an extended inlet duct such as in "quiet-engine" designs, the cutoff effects of duct acoustics become extremely important in terms of radiated sound power level as well as directivity. In

these cases the sound energy is transmitted along the duct by a collection of modes, of which many are dispersive and some are propagative. The coupling of the sound source field to those modes depends on the frequency, phase, and spatial correlation between the sources and modes, and determines which modes will predominate at the duct ends, thereby controlling the radiated sound field. Calculations of the radiated sound pressures must therefore include the modal transposition of the in-duct sound field and the radiation properties of these modes.

Jet noise.- Fundamental to a study of jet noise is the theory that describes the process whereby the intense turbulence in the exhaust stream of a jet engine generates sound. The theory predicts that the sound from this turbulence will increase with the eighth power of flow velocity. This result has been verified experimentally in the laboratory and by measurement on turbojet engines over much of their operating range.

An eighth-power-of-velocity law suggests immediately that exhaust velocities need only be reduced by a small amount to obtain quite significant reductions in sound output. For example, a 25-percent reduction in exhaust velocity should effect a noise reduction of about 10 decibels; a 50-percent reduction would be accompanied by a 24-decibel reduction in noise.

In modern turbofan engines, thrust is developed by accelerating a larger volume of air/gas at a lower velocity than was typical of the older turbojet aircraft. While this has certainly resulted in lower jet noise levels, the exhaust flow as a noise source (particularly the engine core exhaust) cannot be ignored.

Three different computations are contained in the jet noise portions of the engine noise prediction program. They calculate the maximum-overall and one-third-octave-band spectrum for (a) supersonic jets, (b) subsonic jets, and (c) the directivities of both supersonic and subsonic flows. The first of these is generally based upon methods standardized by the SAE (Society of Automotive Engineers, Reference 3). In this calculation the peak overall sound pressure level ($OASPL_M$) along a sideline parallel to the jet axis is determined by the expression

$$OASPL_M = 10 \log_{10} f(U) + 10 \log_{10} \rho A - 20 \log_{10} (r/200)$$

where U = jet density, m/s (ft per sec)

ρ = jet density, per kg/m^3 (lb per cu ft)

A = effective nozzle area, m^2 (sq ft)

r = sideline distance, m (ft)

If the core exhaust velocity is less than 305 m/s (1000 feet per second), the noise field is influenced or dominated by internally generated core engine noise. However, a separate jet noise

prediction is generally based upon an extrapolation of the SAE noise curve.

It has been found (Reference 4) that the power level (PWL) of the jet can be found from

$$PWL = 10 \log_{10} \rho A + 10 \log_{10} f(U) + 50$$

and the space-average sound pressure level ($OASPL_A$), the sound pressure level that would result from an omnidirectional source of noise with the same sound power level, would be given from

$$OASPL_A = 10 \log_{10} \rho A + 10 \log_{10} f(U) - 6.5$$

The method of directivity calculation necessary to predict individual sound levels for any angle or position around the jet is defined in Reference 5. The effectiveness of this method is shown in Figure 14.

Combustor/turbine (core engine) exhaust noise. - As mentioned earlier, the rearward propagating noise from the core engine at the relatively low exhaust velocities of current and projected high-bypass-ratio engines will be dominated in many instances by disturbances produced upstream from the exhaust jet. These sources are generally dominated by the combustor design and operational parameters since both low-frequency combustion noise and the higher frequencies of the turbine broadband noise are dependent upon the turbulence level within the burning gases and upon the amount of turbulence-limiting between the combustor and the inlet to the first turbine stage.

A method developed at AiResearch predicts combustion noise employing a number of engineering parameters normally used to describe the physical characteristics of the combustor and the combustion process. While these parameters individually are not descriptive of the detailed flow, heat transfer, or chemical conditions that prevail from point to point within the combustor, collectively they have been shown to predict the order of magnitude of small engine combustor/turbine system acoustical performance. Thus, the development engineer can assess the acoustical performance of candidate systems prior to their development and actual test.

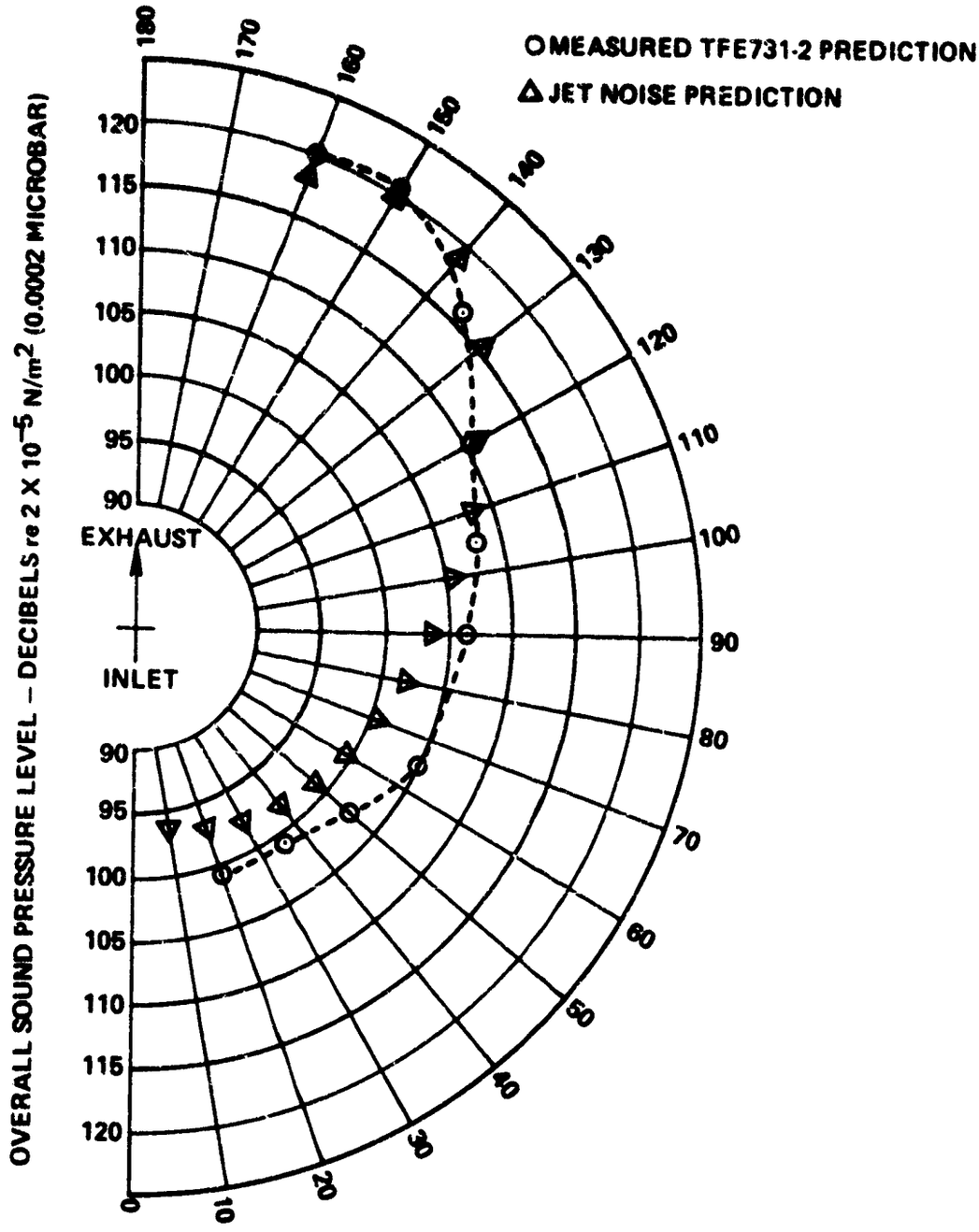

Figure 14. Comparison of Measured and Predicted Directivities for Jet Noise at 30.5 M (100 Feet).

Basically, the method unites the following:

Variable	Symbol
Acoustical power output, lb-ft per sec (watts)	p
Combustion energy release, lb-ft per sec	$\dot{W}$
Fuel-flow rate, lb per sec	$\dot{W}_f$
Airflow rate, lb per sec	W_a
Temperature, °R	T
Pressure, lb per sq ft	p
Typical combustor dimension, ft	D_e
Combustor discharge velocity	V_d

The sound power has been found to be proportional to the factor F, where

$$F = T_4 - T_2 \sqrt{V_d D_e} (1 + f_a) \frac{P_4}{T_4}$$

For engine combustion noise:

$$PWL = 40 \log_{10} F + B_1$$

For air-rig combustor noise:

$$PWL = 20 \log_{10} F + B_2$$

Further, from experimental data it was found that B_1 and B_2 were, respectively, 23 and 81 decibels (re 10^{-13} watts).[1] With these substitutions, the designer of small gas turbine engines is provided with a method to predict the acoustical power level generated by a given engine design and, further, to predict the effects of changing one or more design parameters. This method has proven useful for several families of small engines.

Gear system noise.- Gearbox noises evolve from the unsteady forces associated with tooth-meshing action and is a function of gear-tooth design, irregularities in the tooth profiles, and the flexibility of the gear teeth. The resultant unsteady forces excite the gear blanks and generate sound fields within the gearbox casing. Coupled with this, the vibrations are transmitted from the gear blanks to the shafts and shaft bearings and subsequently to the gearbox casing. Thus, the gearbox casing is excited both by directly transmitted mechanical vibrations and indirectly by the acoustic field generated within the casing. Both the sources of casing vibration result in noise radiating into the external field. For geared fans, this noise is also

predicted by the computer program. The logic diagram of this subroutine is shown i Figure 15.

Computer program for predicting noise from small turbine engines. - One of the key tools utilized during the small turbofan engine study was a computer program for predicting bare-engine noise generated by small turbine engines. This program was designed functionally so that the predictions of each of the component noise sources (fan, compressor, combustor, gears, etc.) were performed in separate subroutines. This allows wider latitude in the input of engine parameters for a study such as this, since it is possible to vary one engine component or parameter at a time.

The engine noise-prediction program considers the noise propagated forward and rearward by the various noise sources. It predicts the sound pressure level versus angular position (directivity) for each noise-generating mechanism and totals the predicted noise for each azimuth. These sound pressure level spectra are then extrapolated with the use of techniques described in Reference 6 to any desired distance, either radius or passby.

The basic logic of the fan/compressor noise-prediction routine is shown in Figure 16, while the logic sequence of the overall program is shown in Figure 17.

Noise goals. - Design goals for the small turbofan engine were 95 and 85 PNdB 152 m (500 feet) on either side of a line parallel to the aircraft takeoff path. Current Federal Aviation Regulations (Part 36) call for the sideline noise to be measured 0.25 nautical miles 463 m (1520 ft) from the takeoff path. The FAR Part 36 level is 102 EPNdB. With the assumption that the time duration and tone corrections to the PNdB unit cancel each other (usually a reasonable assumption for light aircraft), the PNdB and EPNdB levels can be compared.

On this basis, the current FAR Part 36 level corresponds to 112 PNdB at the 152-m (500-ft) sideline. Therefore, the two noise goals used for this study are from 17 to 27 PNdB under current regulatory levels. Since it is unlikely that the regulations will be lowered by more than 10 to 15 PNdB, it is suggested that the 95 EPNdB noise goal is more realistic for this study and should be the value employed in future noise-related work.

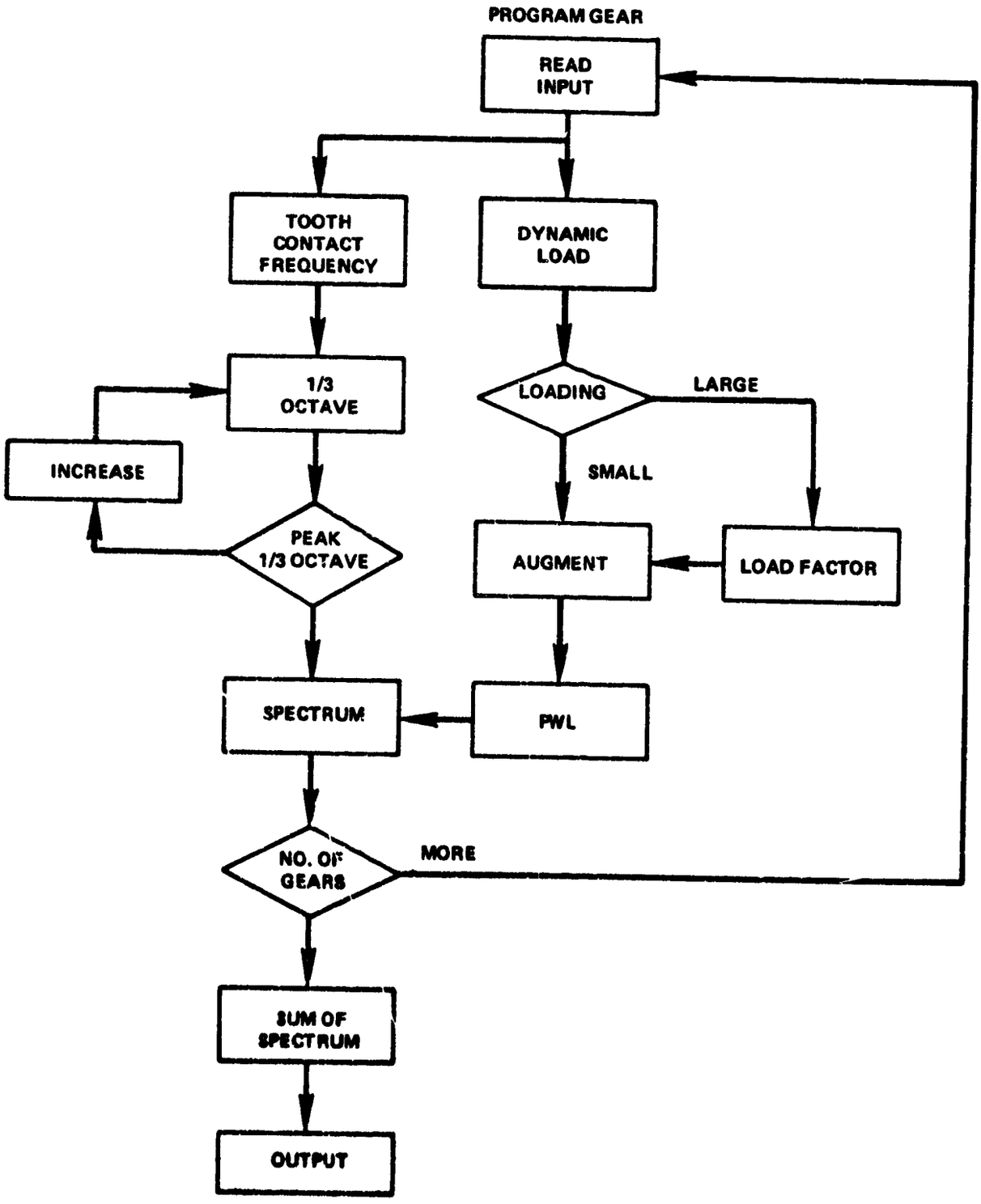

Figure 15. Gear Noise Subroutine.

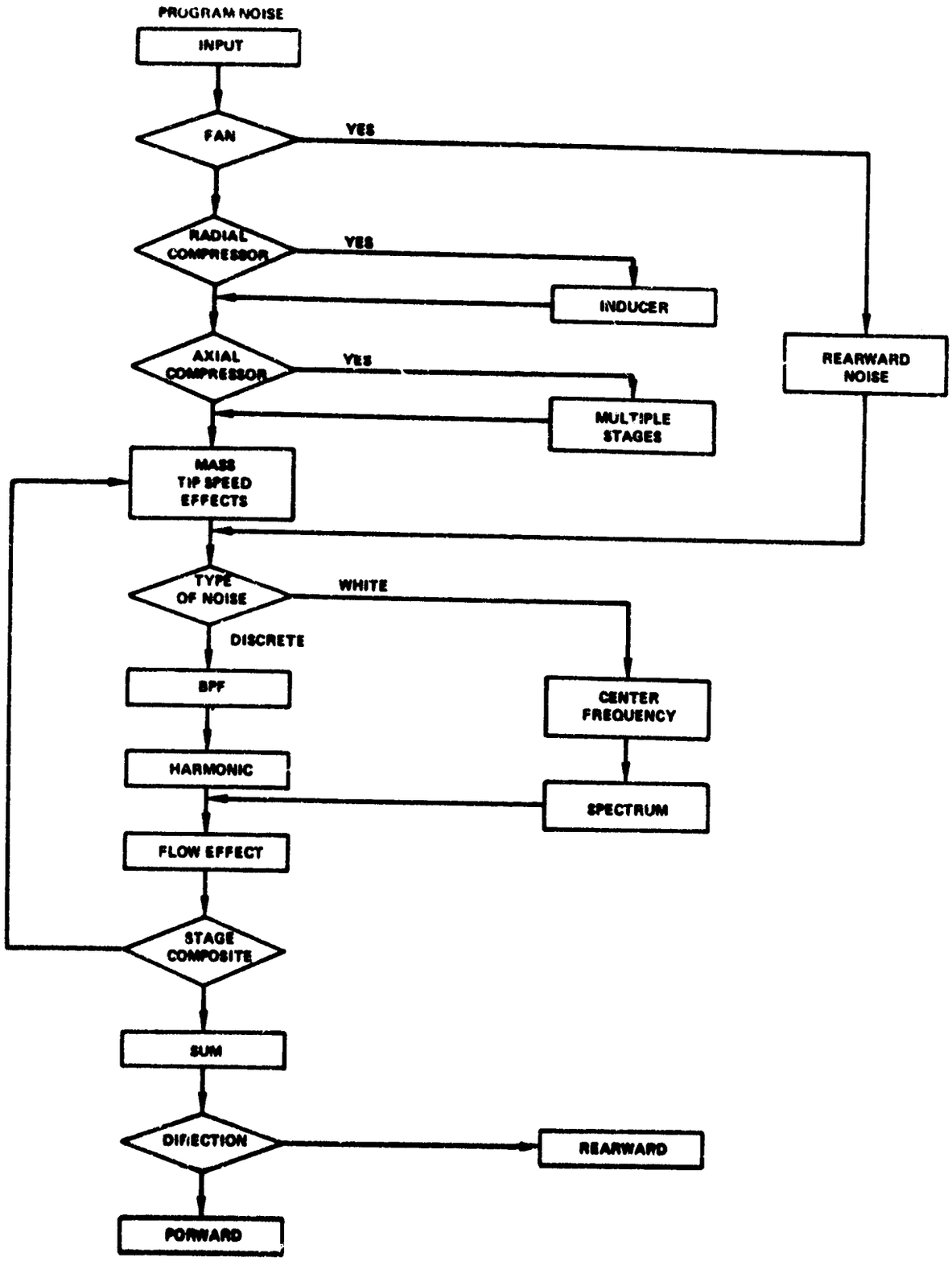

Figure 16. Fan/Compressor Impeller Noise Subroutine.

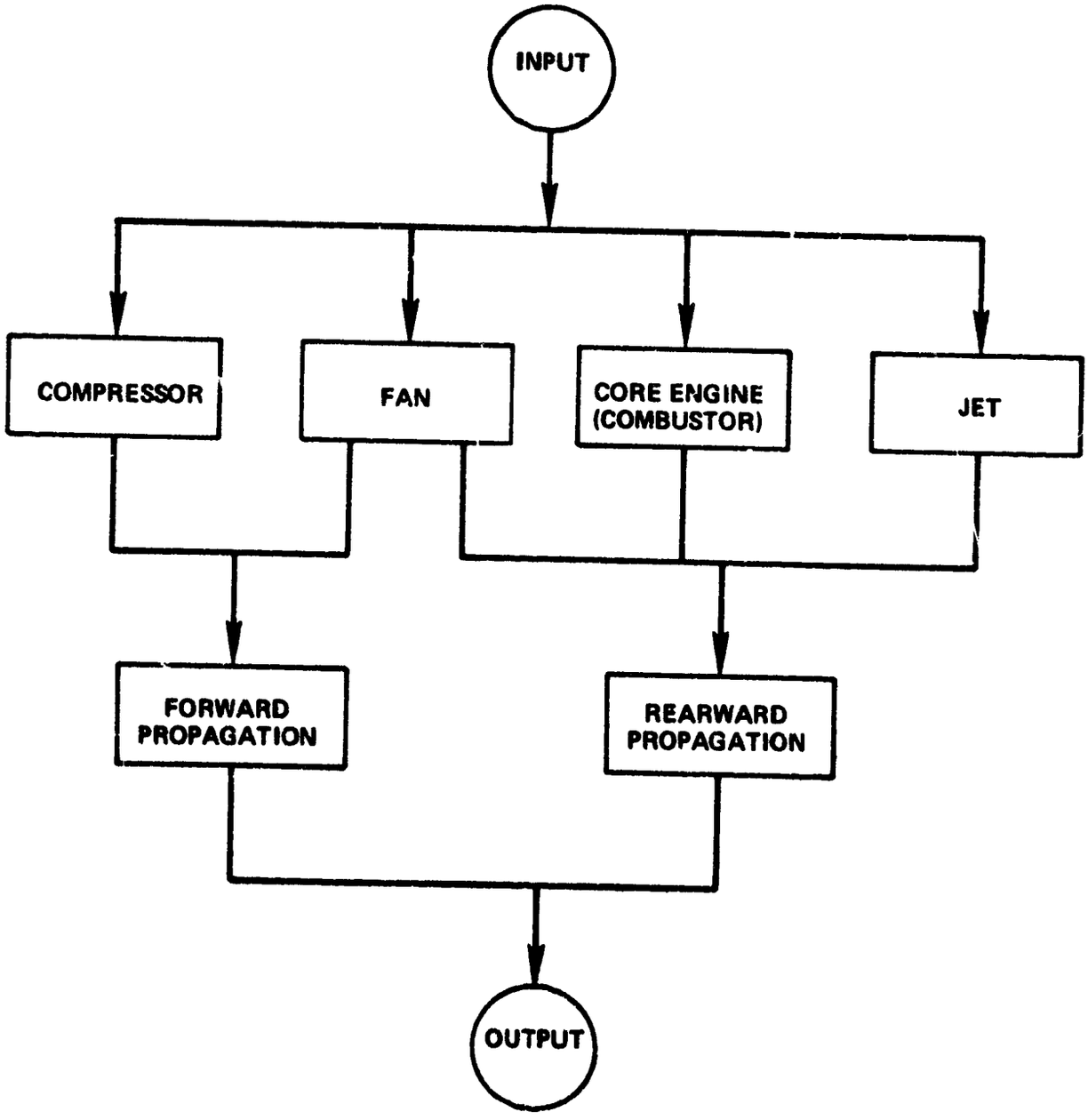

Figure 17. Overall Prediction Program.

PHASE II - ESTABLISHMENT OF CANDIDATE ENGINES AND AIRCRAFT SYNTHESIS COMPUTER PROGRAM

Candidate Engine Definition

Parametric cycle analysis. - Design-point cycles were derived from parametric cycle analysis, and then were used to obtain off-design performance for four engines having spreads in specific thrust and thrust decrement with flight speed. These engines, based on the gas generator components of the AiResearch Model TSE36-10 Turboshaft Engine, were used to evaluate thrust-decrement effects on takeoff and single-engine climb performance. The results of the design-point parametric analysis, with constant turbine inlet temperature, are presented in Figure 18. The design-point cycles were identified by selecting the fan pressure ratios that gave the lowest cruise TSFC for the four bypass ratios shown. The design point for all cycles was at cruise, 648 km/hr (350 kt) and 7315 m (24,000 ft).

While layout drawings were not prepared for these engines, their weights were estimated with the use of an engine weight-prediction computer program. Nacelle sizes were estimated from assumed fan flow characteristics. Airplane performance and mission analysis was then performed with appropriate engine scaling rules applied. The results indicated that although takeoff and single-engine climb performance was better with the higher bypass ratio engines, the lower bypass ratio engines provided greater range. The lighter weight and lower nacelle drag of the low-bypass-ratio engines offset the TSFC advantage of the high-bypass-ratio engines.

The BPR-5 engine was judged to have the best balance of takeoff, climb, and range performance. The fan pressure ratio is the principal determinant of these performance qualities. Therefore, it was decided that the fan pressure ratio (1.48) of the BPR-5 engine would be used in candidate engines IA, IC, IIA, and IIC.

Later in the program, it was considered desirable to perform an aircraft sensitivity analysis, and to evaluate the cost, noise, and performance characteristics of a high-bypass-ratio, low-fan-pressure-ratio engine. The BPR-9 cycle from this parametric analysis was used in the candidate engine, later identified as engine IIC/9BPR. The fan pressure ratio selected was 1.29.

Final candidate engine cycles. - With desirable flight speed, propulsive efficiency, and thrust-decrement characteristics identified, final cycles for candidate engines were derived from the guidelines developed in Phase I and from in-depth matching analysis of appropriately selected aerodynamic components. Final cycles differed in several minor details from the Phase I configurations listed in Tables V and VI. The most notable difference was the

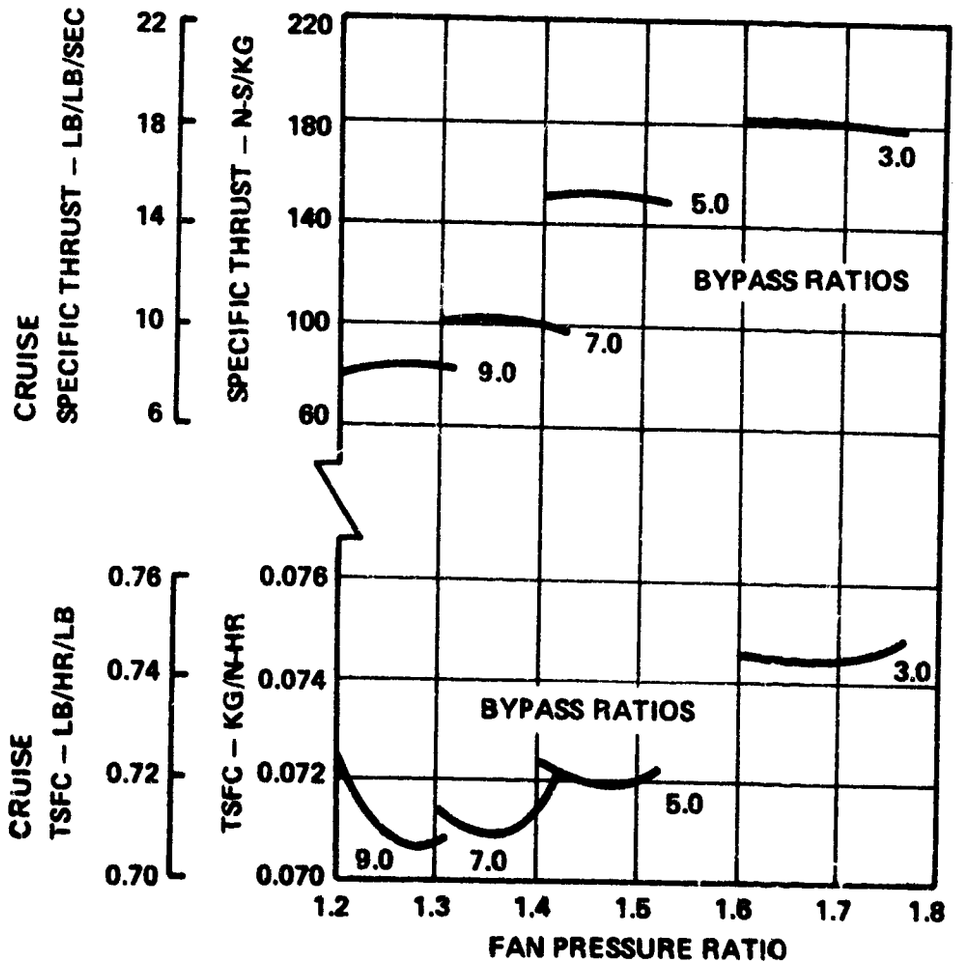

Figure 18. Parametric Cycle Analysis Results for Four Selected Bypass Ratios.

elimination of core-pressure-ratio-9 engine candidates IIIA and IIIC. These candidates were eliminated because suitable off-the-shelf components could not be obtained, and the derivation of new components would require an extensive expenditure of time. However, the candidate IIC/9BPR referred to previously was added, making a total of five candidate engines. These engines were to be defined in detail, and used in airplane synthesis and sensitivity analyses. The final cycle and performance characteristics of these engines are given in Table VII. Pertinent off-design flight performance is presented in Figures 19 through 33.

As shown in Table VII, there is no variation in turbine inlet temperature between the candidate engine cycles. A separate evaluation was performed of the effects of this important cycle parameter on engine performance and configuration. The engine IIA cycle was examined over a range of turbine inlet temperatures, with results plotted in Figure 34. The results showed that for TSFC-optimized cycles, there was only a 2.5-percent variation in TSFC, and a negligible effect on the thrust per total engine airflow. However, there was a substantial variation in thrust per core airflow and, consequently, in the bypass ratio of TSFC-optimized cycles. The prinicipal effect of turbine inlet temperature on a turbofan engine is to size the core. Since the engine weight is substantially affected by core size, it is obviously desirable to use the maximum turbine inlet temperature consistent with turbine stress, life, cost, and complexity considerations. The turbine inlet temperature of the candidate engines was chosen on this basis. The temperature is sufficiently low to avoid the requirement for costly turbine blade cooling and also to ensure long life, yet high enough to keep the engines in the small-core high-bypass-ratio context that ensures a good engine thrust/weight ratio.

Component definitions. - In order to obtain the most credible engine designs and performance data, the candidate engines were derived from existing AiResearch aerodynamic components, for which performance maps were available. In some cases, the components were modified in form or performance specifics. Corresponding adjustments were then made to the performance maps. The components required scaling and appropriate efficiency adjustments were made to reflect the changes in size. The components and the AiResearch engines from which they were derived are listed below for each candidate:

Engine IA

Fan - single-stage axial - TFE731-2 (modified)
Core compressor - 4-stage axial - ETJ331
Combustor - annular vaporizer - ETJ331 (modified)
Core turbine - single-stage axial - ETJ331
Fan turbine - 3-stage axial - TFE731 (modified)
Jet nozzles - from generalized convergent nozzle performance

TABLE VII. CANDIDATE ENGINE CYCLE CHARACTERISTICS.

	IA		IC		IIA		IIC		IIC/9EPR	
	*DP	SLS	DP	SLS	DP	SLS	DP	SLS	DP	SLS
Bypass ratio	5.5	5.14	5.5	5.14	5.17	5.37	5.02	4.75	9.1	7.84
Fan pressure ratio	1.48	1.39	1.48	1.395	1.47	1.40	1.48	1.40	1.29	1.25
Compressor pressure ratio	4.27	4.08	4.28	4.10	6.04	5.84	5.54	6.17	5.80	5.79
Turbine inlet (°K) temperature (°R)	1167 2100	1228 2210	1167 2100	1228 2210	1167 2100	1228 2210	1167 2100	1228 2210	1167 2100	1228 2210
Total airflow (kg/s) corrected (lb/sec)	28.35 62.5	24.59 54.21	28.00 61.71	24.40 53.80	28.83 63.55	25.52 56.27	26.46 58.33	23.19 51.12	42.21 93.05	34.44 75.93
Net thrust (N) (lb)	1779 400	5778 1299	1779 400	5796 1303	1793 403	6099 1371	1766 397	5649 1270	1833 412	6726 1512
TSFC (kg/N-hr) (lb/hr/lb)	0.085 0.831	0.049 0.484	0.084 0.820	0.049 0.478	0.075 0.738	0.043 0.417	0.079 0.770	0.046 0.452	0.073 0.718	0.038 0.372

*Design point is Mach 0.577 (350 kts) @ 7315 m (24,000 ft) standard day.

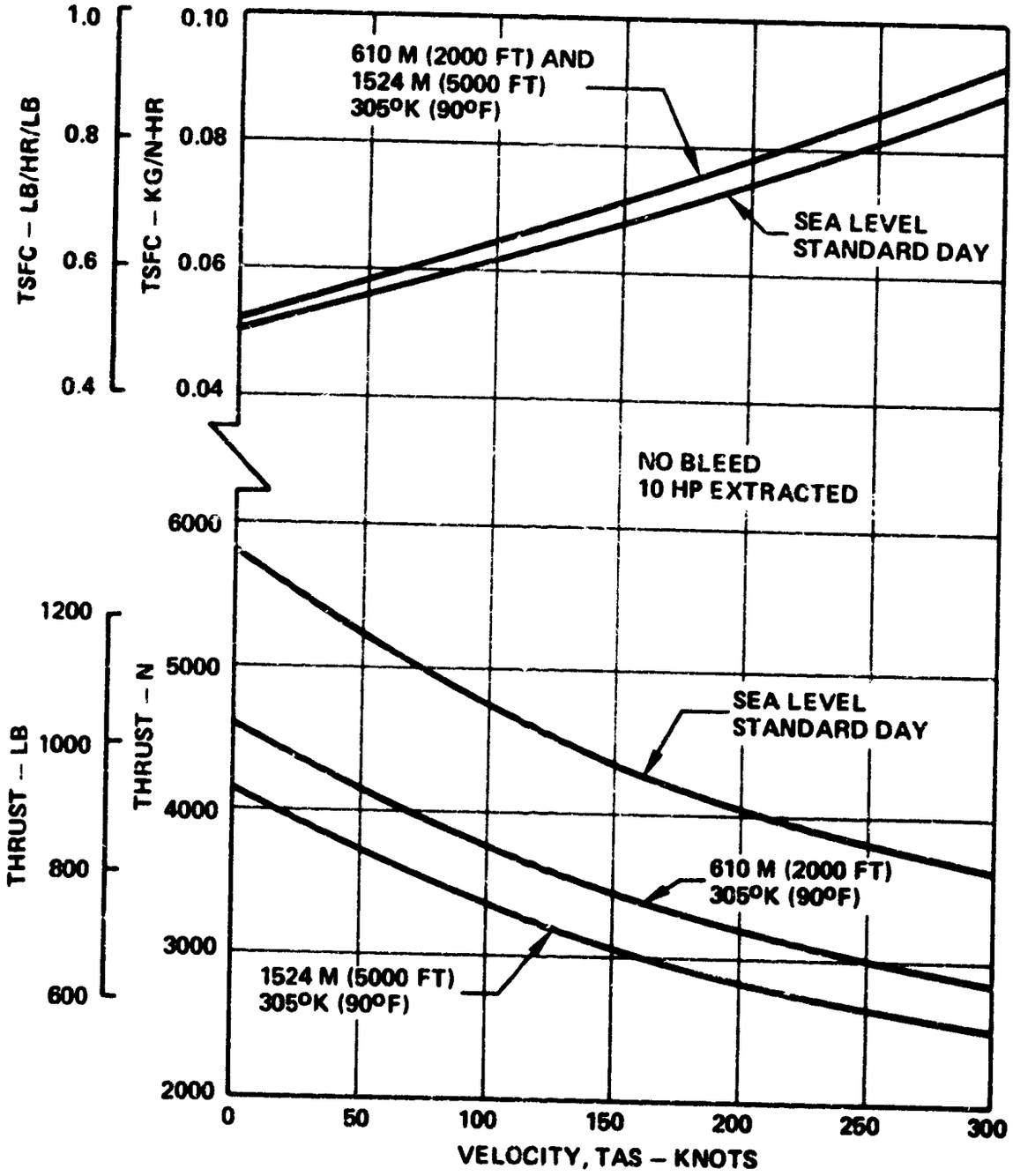

Figure 19. Full-Throttle Takeoff and Climb Performance, Candidate Engine IA.

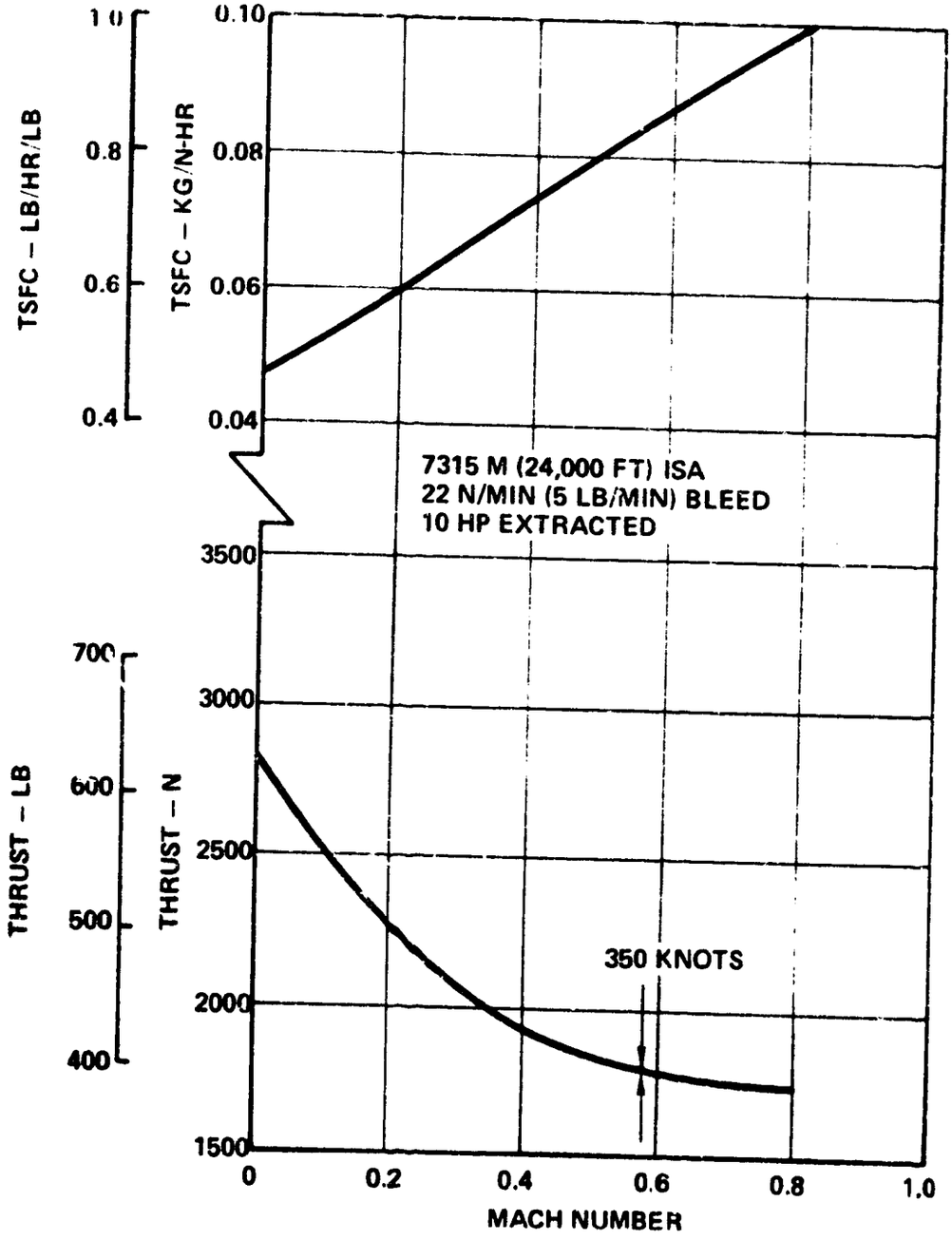

Figure 20. Full-Throttle Performance at Cruise Altitude, Candidate Engine IA.

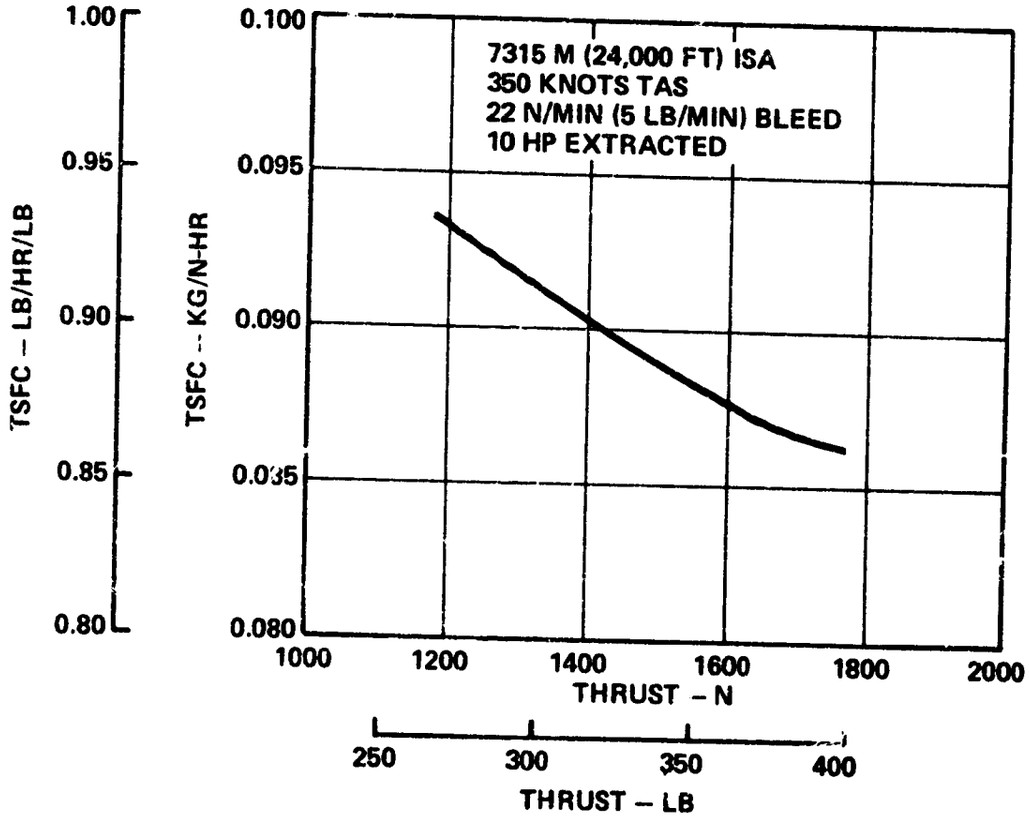

Figure 21. Part-Throttle Performance at Design-Point Flight Conditions, Candidate Engine IA.

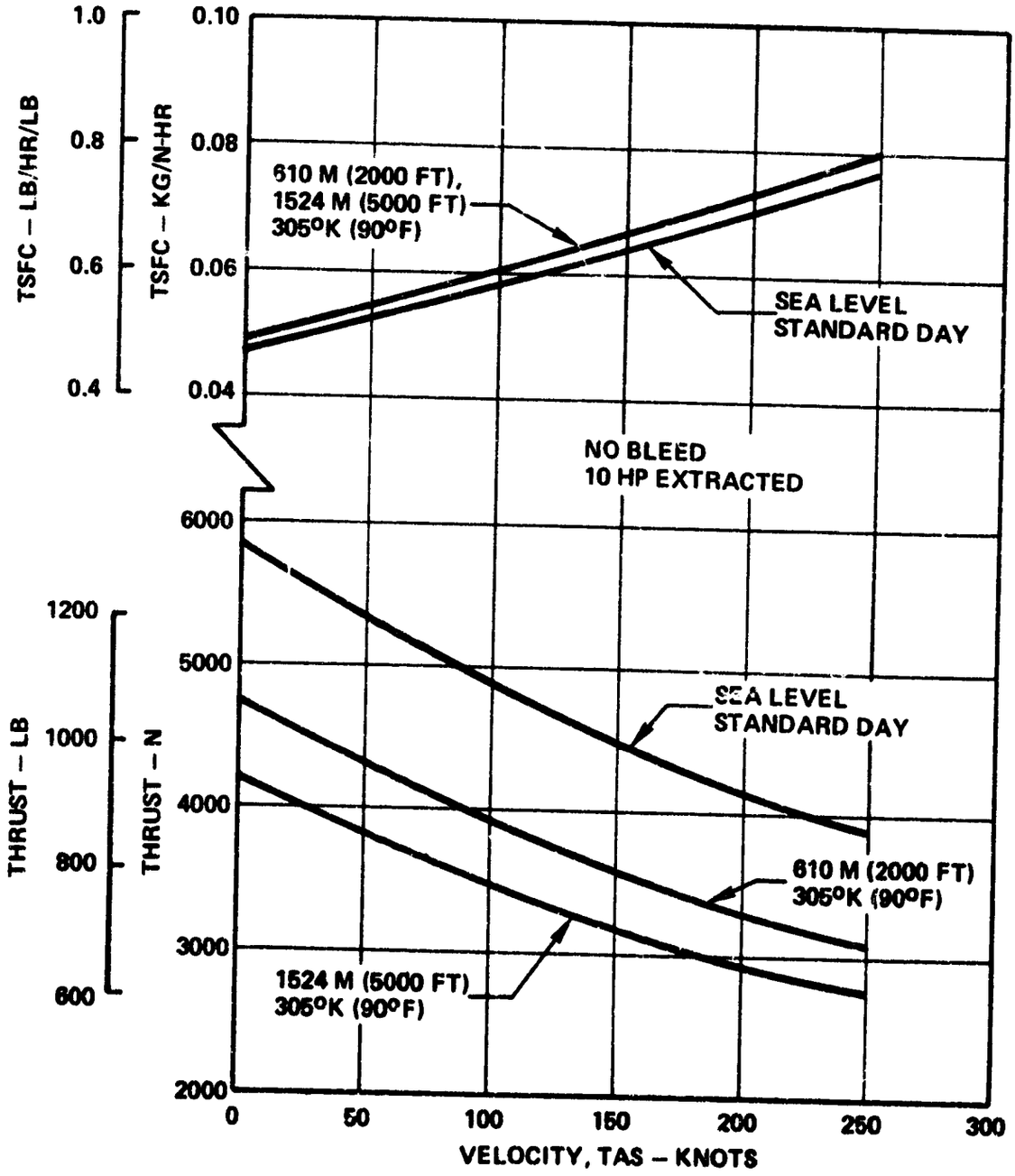

Figure 22. Full-Throttle Takeoff and Climb Performance, Candidate Engine IC.

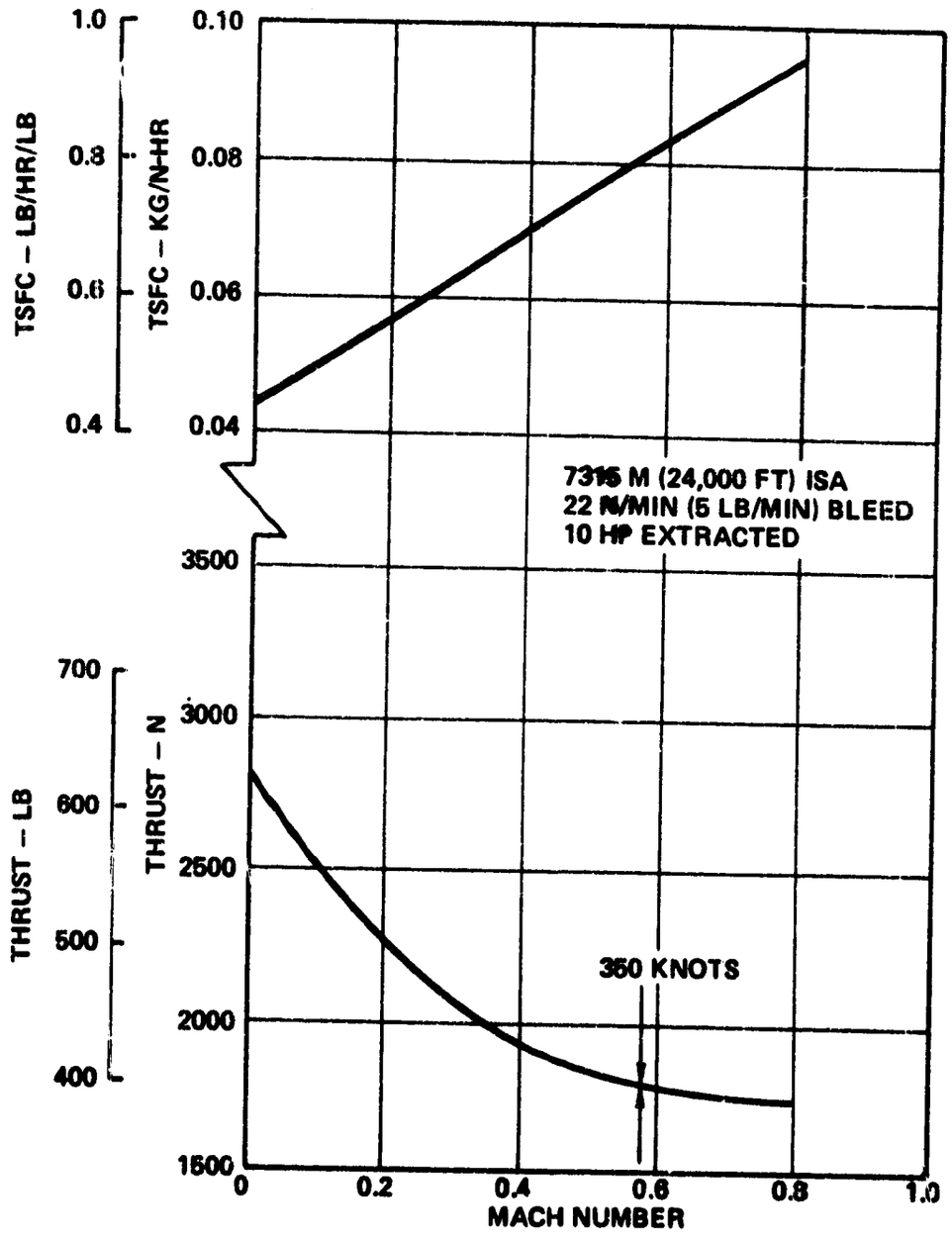

Figure 23. Full-Throttle Performance at Cruise Altitude, Candidate Engine IC.

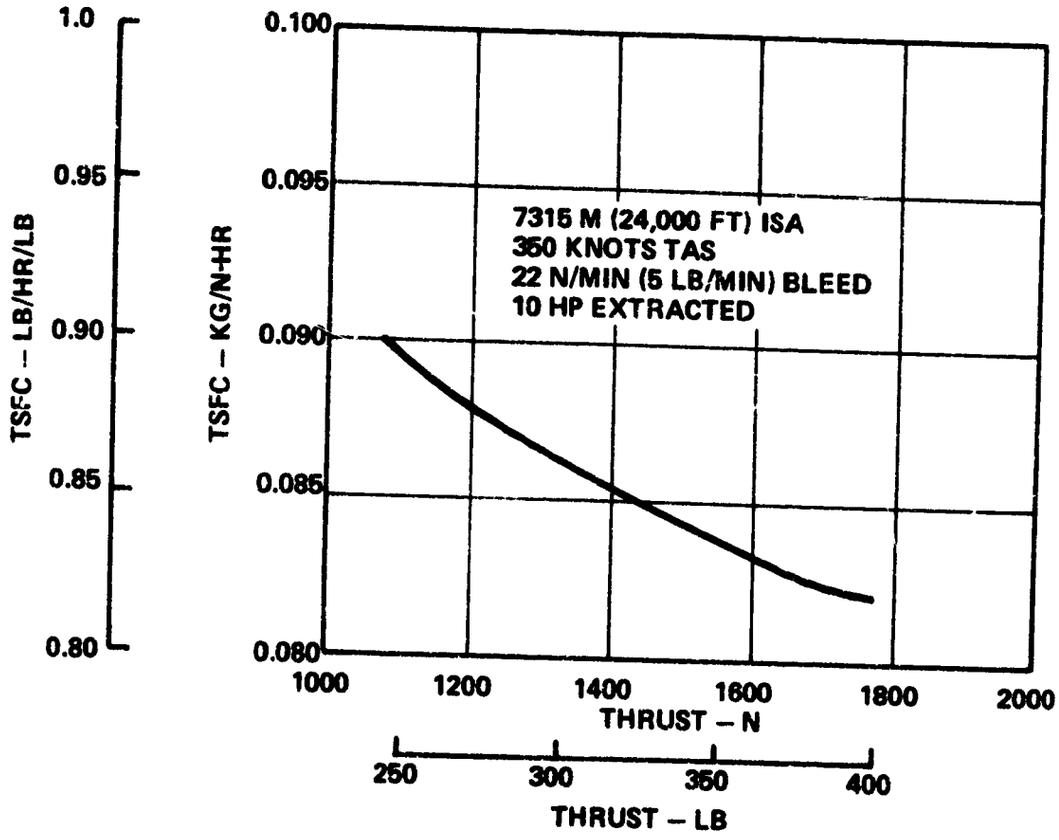

Figure 24. Part-Throttle Performance at Design-Point Flight Conditions, Candidate Engine IC.

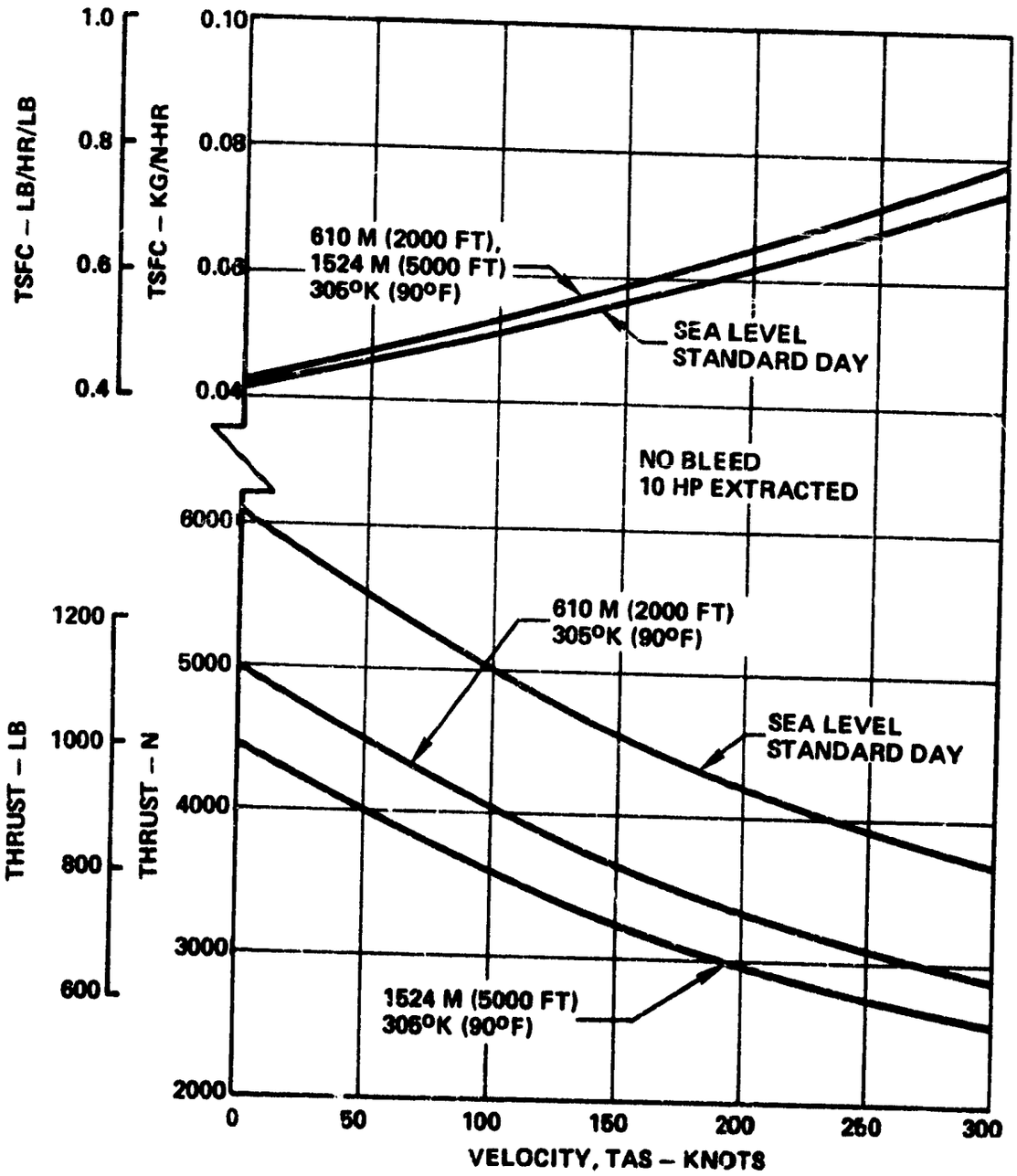

Figure 25. Full-Throttle Takeoff and Climb Performance, Candidate Engine IIA.

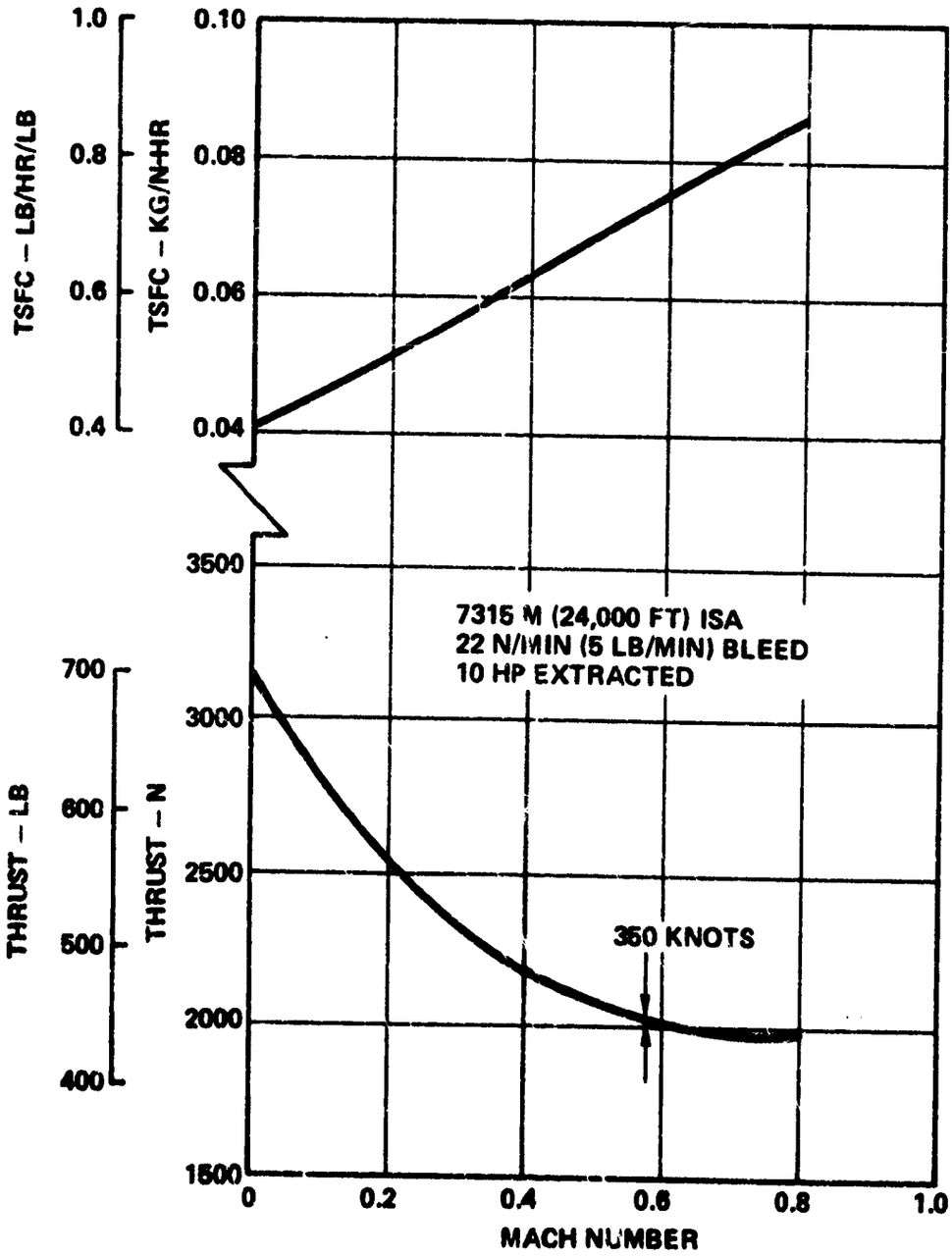

Figure 26. Full-Throttle Performance at Cruise Altitude, Candidate Engine IIA.

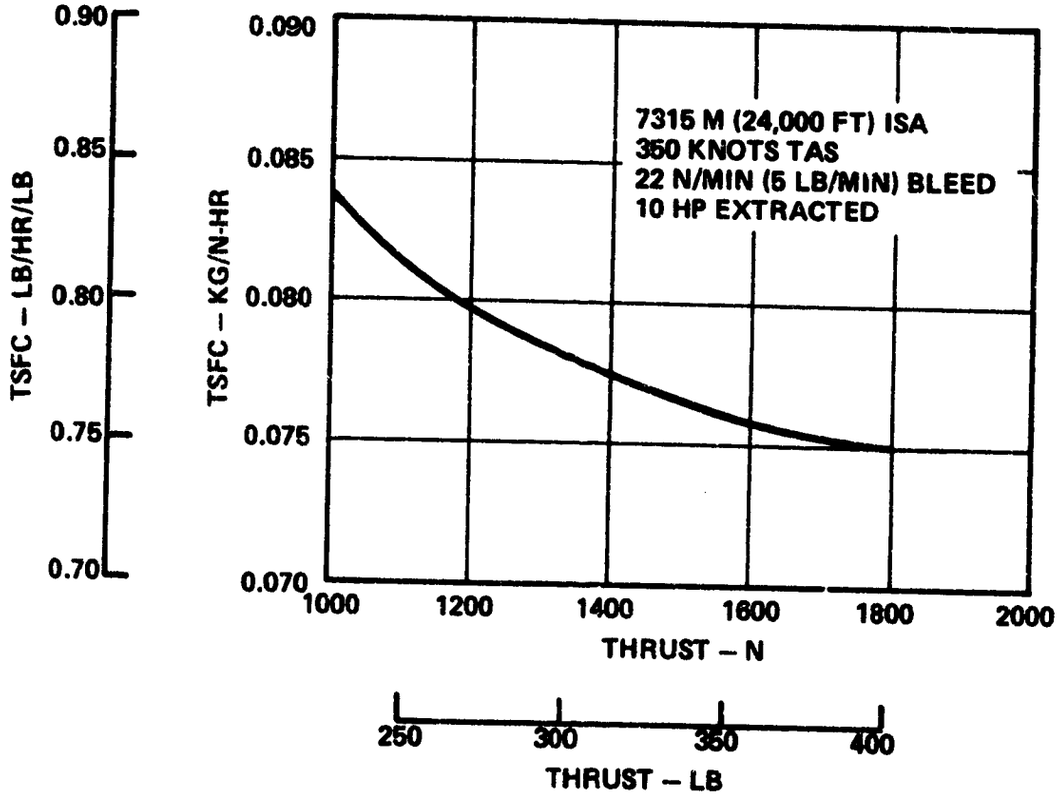

Figure 27. Part-Throttle Performance at Design-Point Flight Conditions, Candidate Engine IIA.

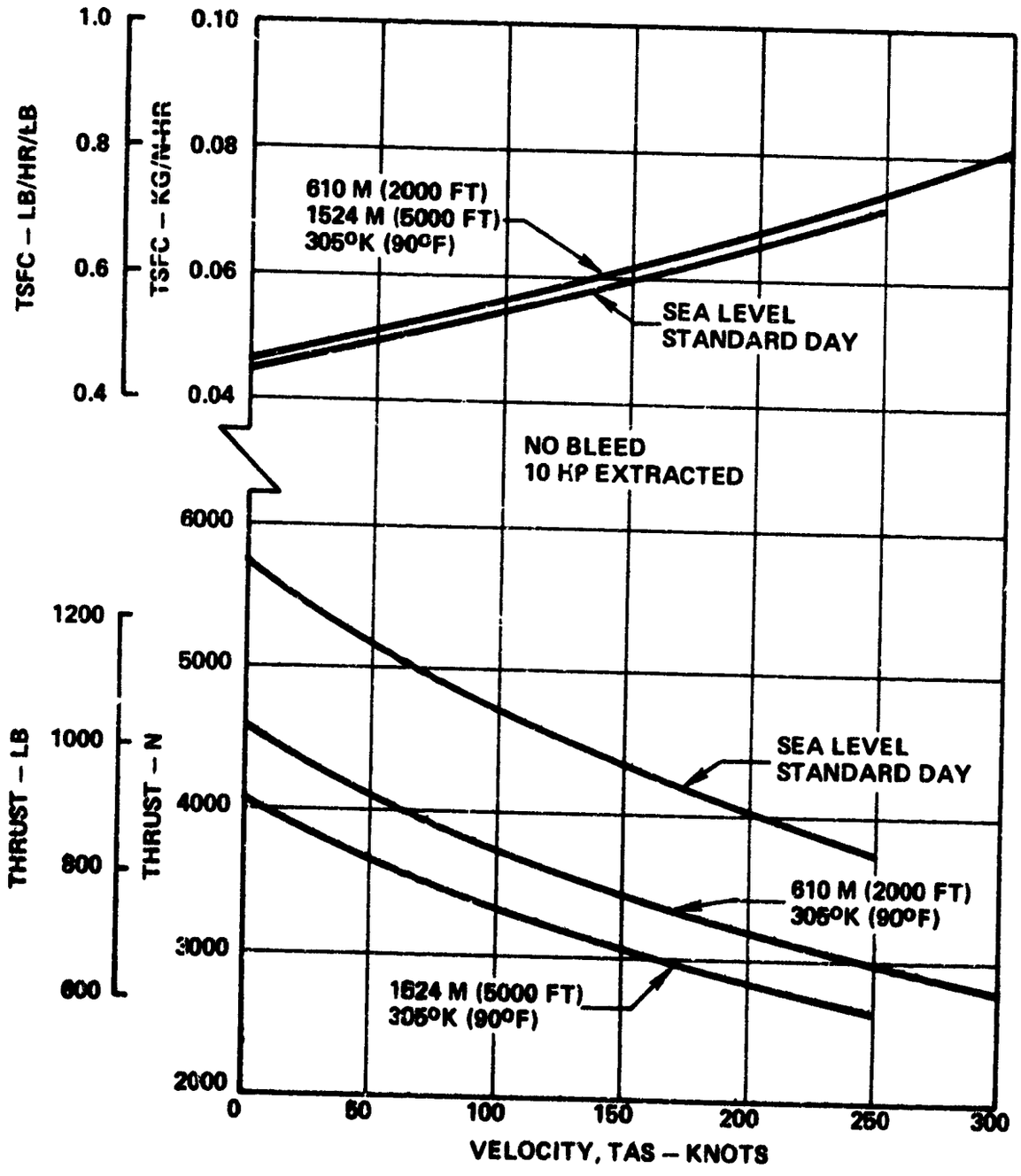

Figure 28. Full-Throttle Takeoff and Climb Performance, Candidate Engine IIC.

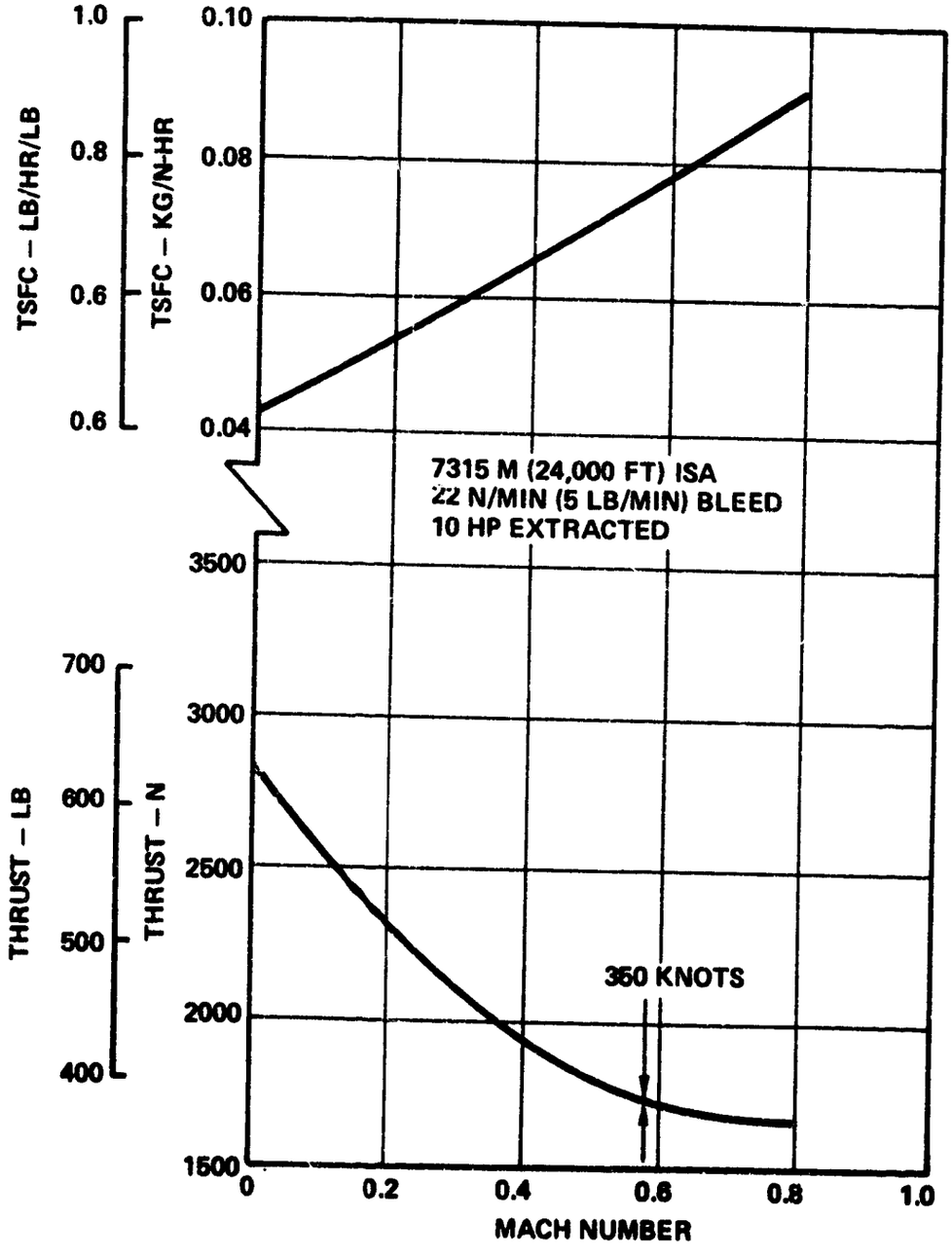

Figure 29. Full-Throttle Performance at Cruise Altitude, Candidate Engine IIC.

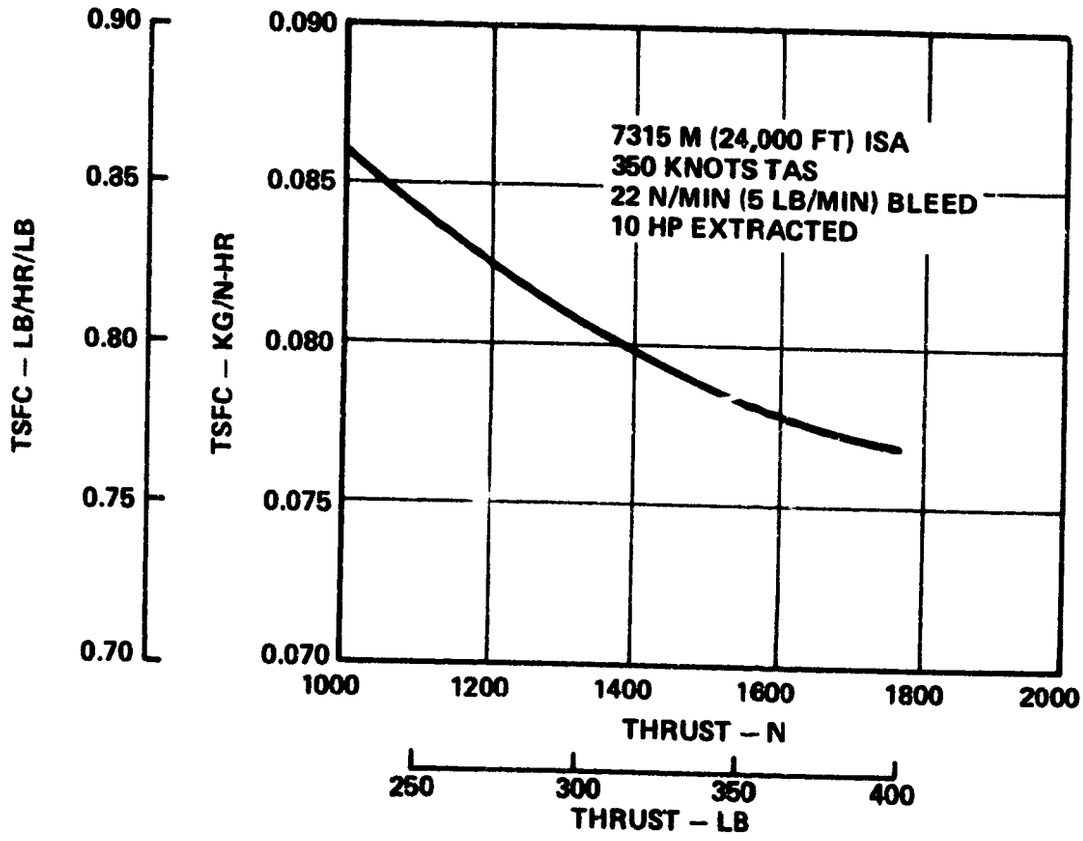

Figure 30. Part-Throttle Performance at Design-Point Flight Conditions, Candidate Engine IIC.

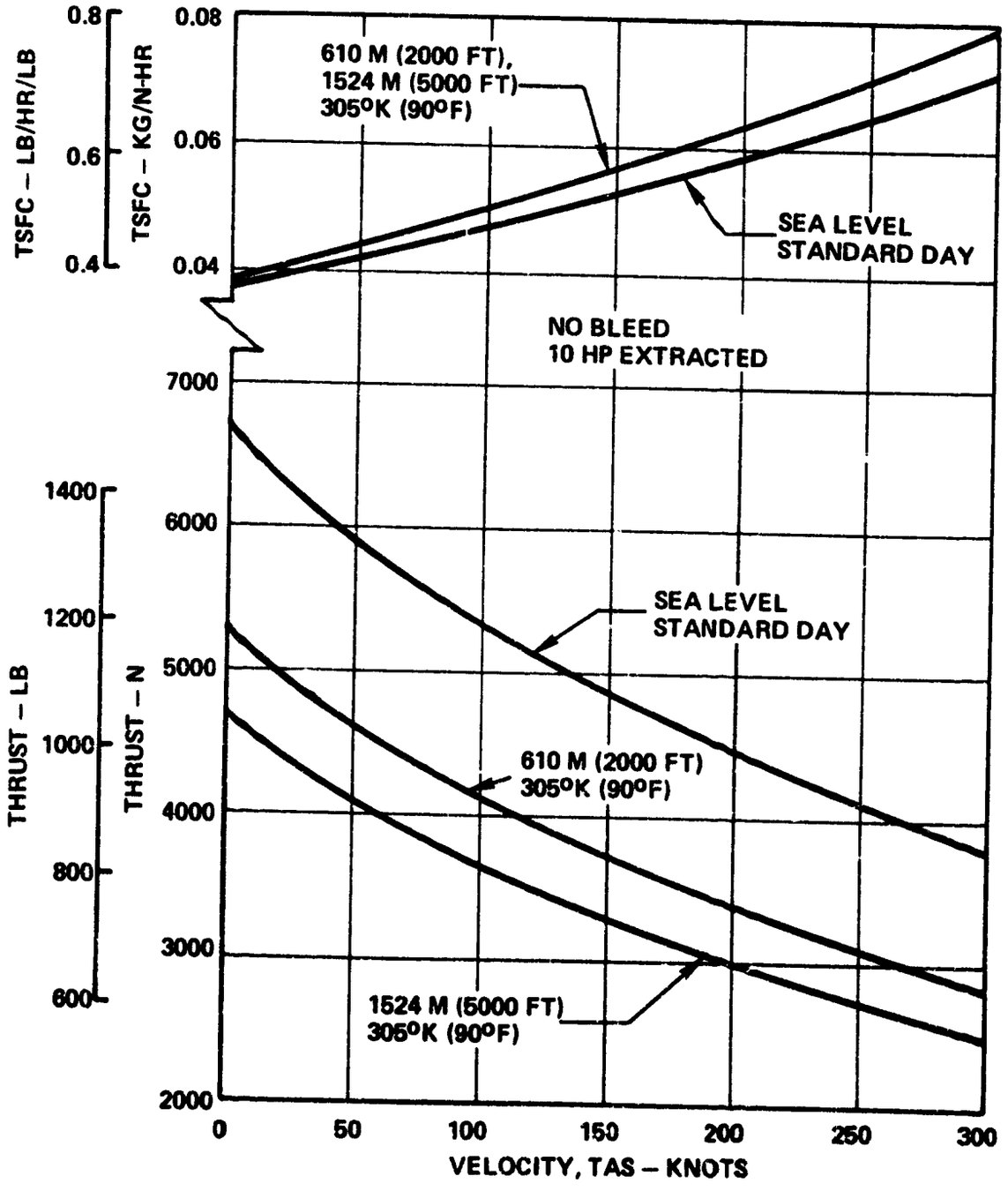

Figure 31. Full-Throttle Takeoff and Climb Performance, Candidate Engine IIC/9BPR.

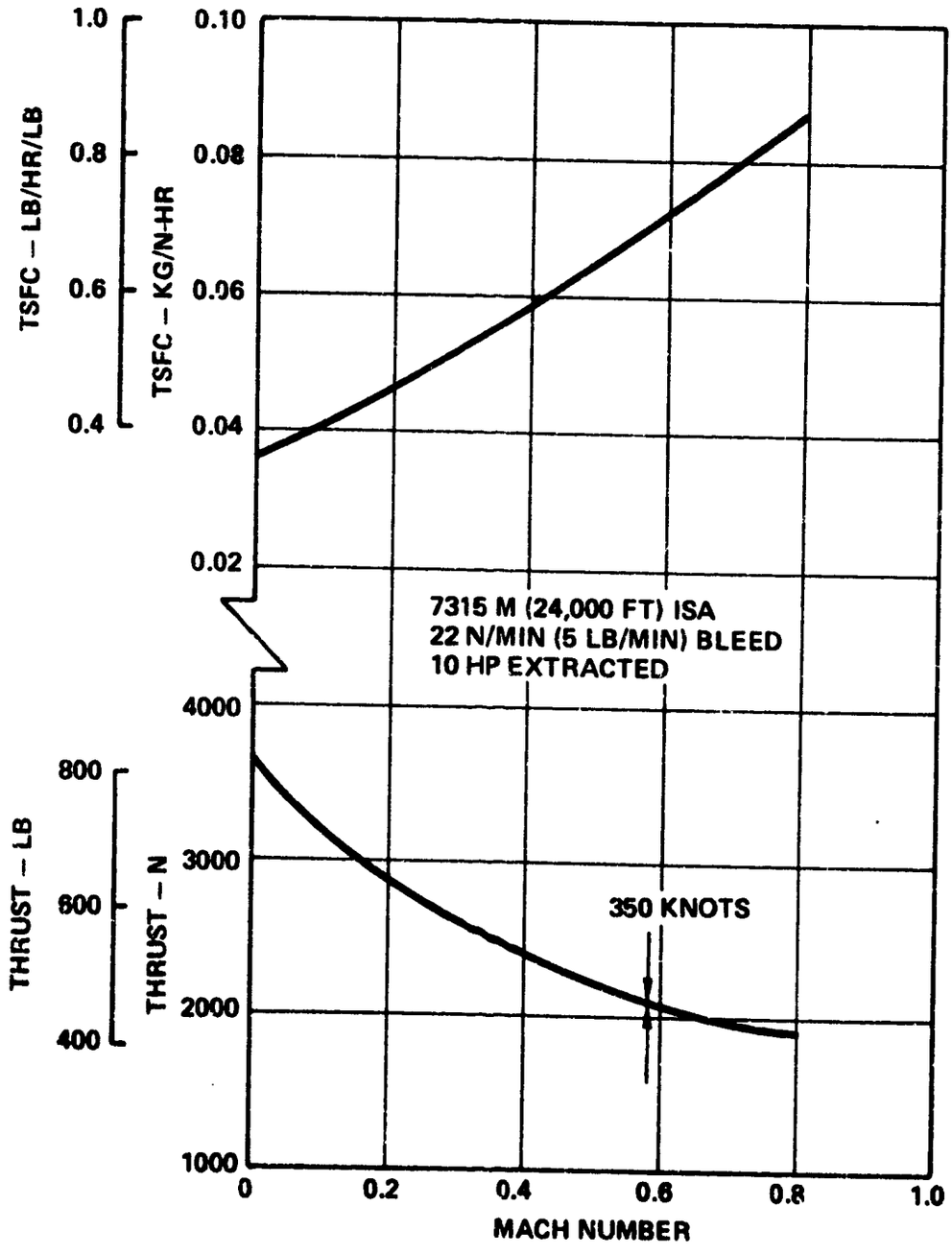

Figure 32. Full-Throttle Performance at Cruise Altitude, Candidate Engine IIC/9BPR.

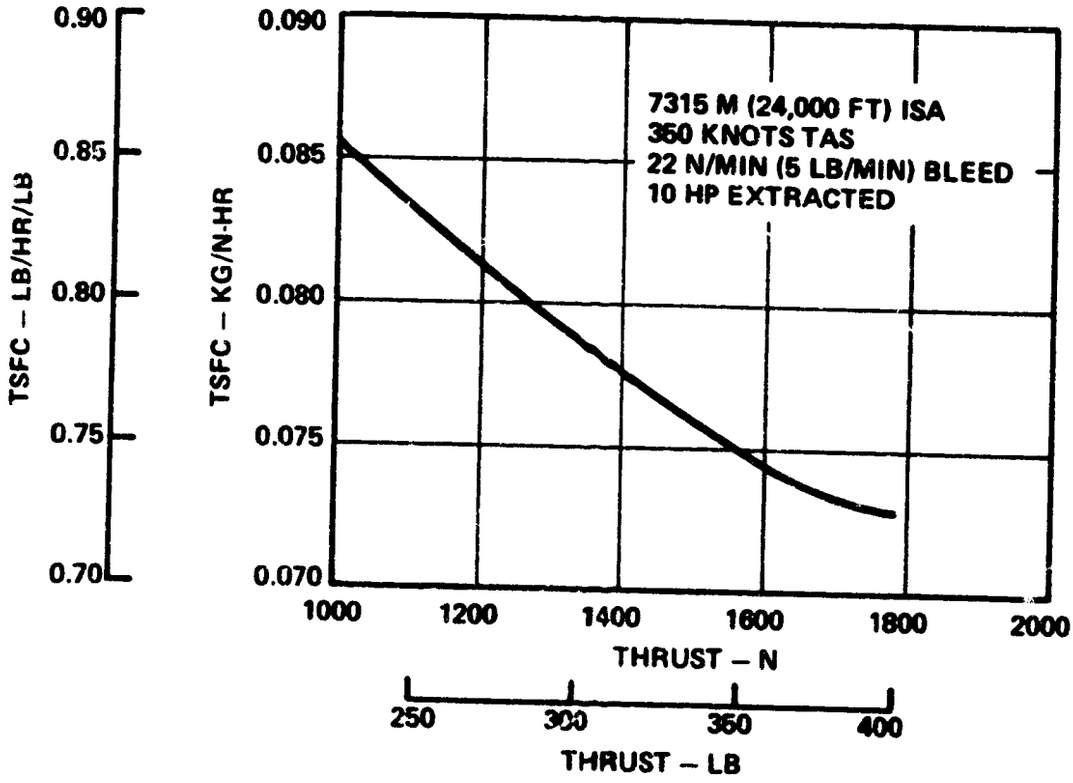

Figure 33. Part-Throttle Performance at Design-Point Flight Conditions, Candidate Engine IIC/9BPR.

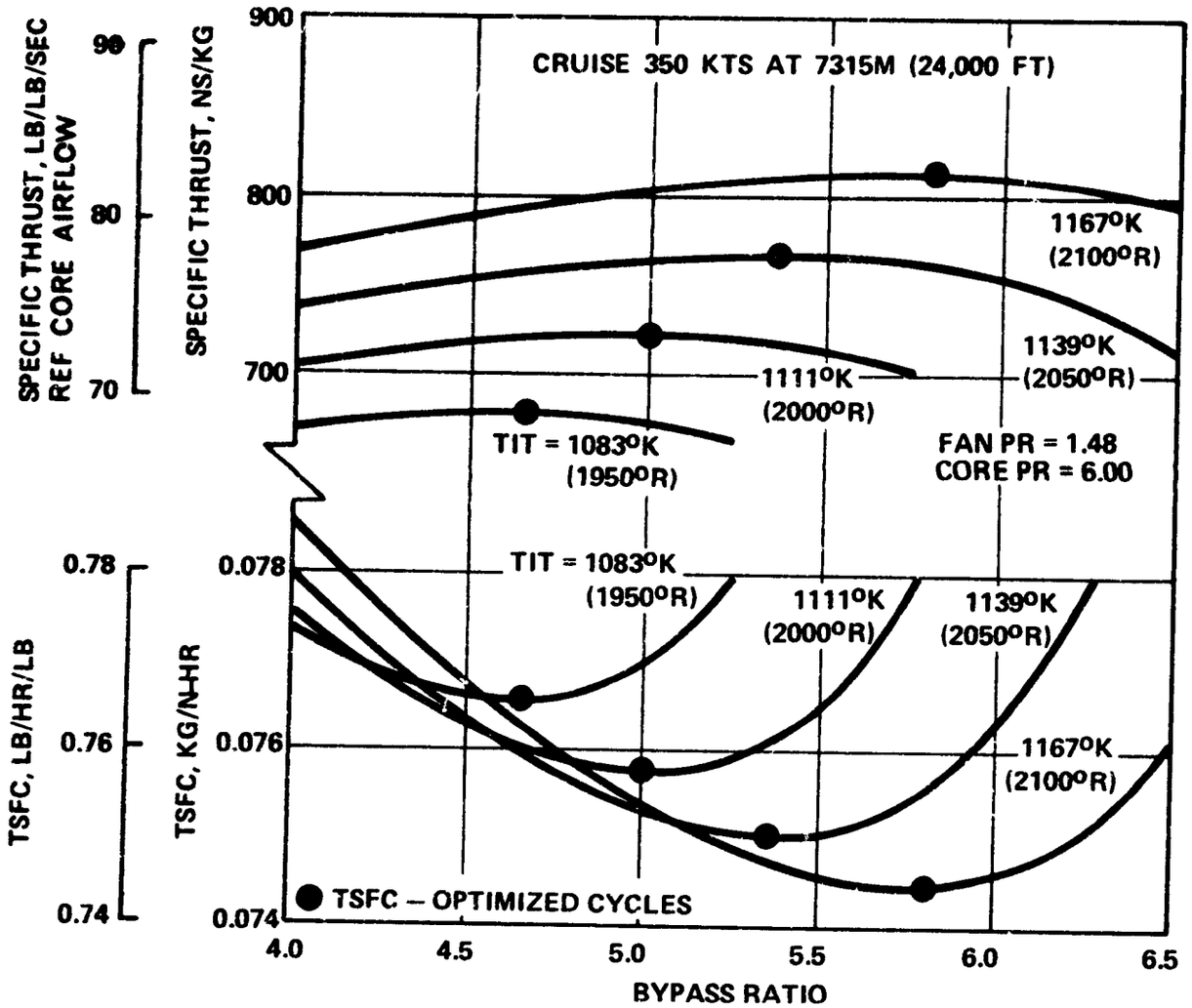

Figure 34. Effects of Cycle Temperature on Engine IIA.

Engine IC

Core compressor - single-stage centrifugal - TPE331 (modified)
Other components - same descriptions and derivations as IA.

Engine IIA

Core compressor - 5-stage axial - ATF3
Core turbine - single-stage axial - TSE36-10
Other components - same descriptions and derivations as IA

Engine IIC

Core compressor - single-stage centrifugal - TSE36-10 (modified)
Core turbine - single-stage axial - TSE36-10
Other components - same descriptions and derivations as IA

Engine IIC/9BPR

Fan - single-stage axial - TFE731-2 (modified)
Core compressor - single-stage centrifugal - TSE36-10 (modified)
Core turbine - single-stage axial - TSE36-10
Other components - same descriptions and derivations as IA

The derived components were modified substantially in mechanical design. However, care was taken to avoid affecting aerodynamic performance. The candidate engine components are considered to be conventional and reflect the current state-of-the-art in their projected performance.

Acoustic analysis results and attenuation treatment. - The results of the acoustic analysis of the five candidate engines are presented in Table VIII. As indicated, the 85-PNdB goal could not be achieved with full attenuating treatment of the inlet and both walls of the bypass duct. Substantial redesign would be required in all five engines to meet the 85-PNdB goal. Figure 35 was prepared to illustrate the severity of the 152-m (500-foot)/85-PNdB goal versus present and proposed regulations at a 0.25-nautical-mile measuring point. The five candidate engine noise levels in this figure are single, unattenuated, bare-engine predictions, with no allowance made for airplane shielding, flight speed effects, or tone correction. Because these points fall substantially below the proposed 1980 regulation, the engine redesign required to reach the 85-PNdB goal was not attempted.

TABLE VIII. ACOUSTIC ANALYSIS RESULTS OF FIVE CANDIDATE ENGINES [152 M (500 FT) SIDELINE NOISE - TWO ENGINES].

Unattenuated Noise (PNdB)			Bypass Duct Treatment for 95 PNdB		Noise with Full Inlet and Bypass Duct Treatment (PNdB)
Engine	Forward	Rear-Ward	Weight kg (lb)	Length cm (in)	
IA	94.5	97.0	3.86 (8.5)	30.5 (12)	88.0
IC	94.5	99.0	7.26 (16.0)	61.0 (24)	90.0
IIA	95.5	98.0	5.22 (11.5)	43.2 (17)	89.0
IIC	94.5	97.5	5.67 (12.5)	40.6 (16)	88.5
IIC/ 9BPR	95.0	99.0	5.44 (12.0)	30.5 (12)	87.5

In order to meet the 95-PNdB value at 500 feet sideline during takeoff, only the rearward propagation noise needs to be suppressed. This can be achieved by lining the outer wall of the bypass ducts. Low-cost attenuators, using perforated metal (hole-metal) honeycomb absorbers, were designed to meet the noise reduction requirements for each engine. The weights and lengths of the attenuators are given in Table VIII. The thicknesses of the honeycomb absorbers are 9.5 mm (0.375 in.) for engines IA through IIC, and 30.5 mm (1.2 in.) for engine IIC/9BPR.

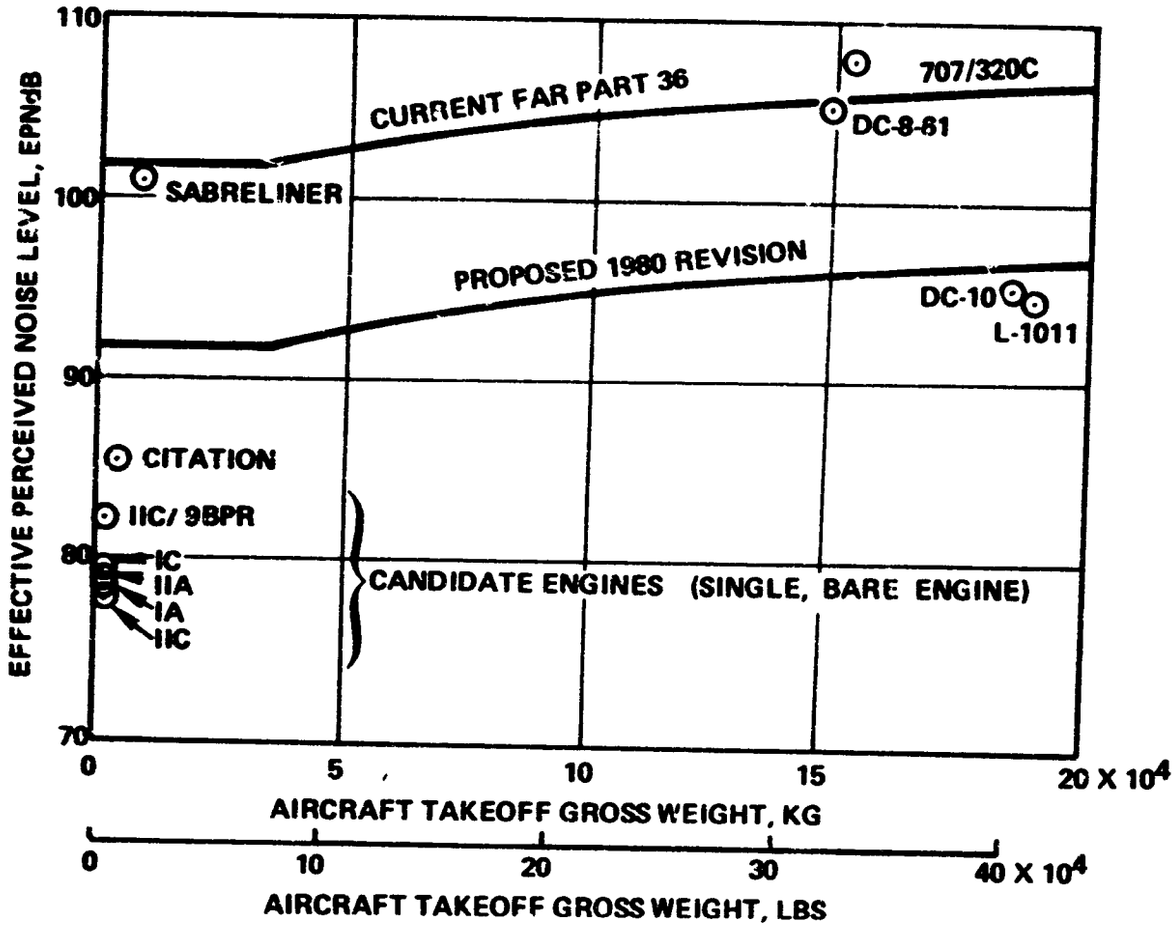

Figure 35. Sideline Noise Comparisons.

Engine Configuration and Weight Analysis

Engine and component configurations.- The basic layouts of the final five candidate engines and their dimensions are presented in Figures 36 through 40. The layouts were prepared in accordance with the engine design principles established in Phase I. The flow paths represent the aerodynamic components and the cycles determined in the candidate engine definitions conducted in Phase II. The configurations shown are supported by a considerable amount of preliminary mechanical design and stress analysis. The layouts also represent the materials and manufacturing methods that were selected as baselines for this study. The layouts are judged to be sufficiently comprehensive to provide a basis for credible weight and cost analyses of the five candidate engines.

One fan was designed and sized for use on the IA, IC, IIA, and IIC engines. This fan has slightly different match points for each engine, because of the small difference in fan airflow required by each engine cycle. The nominal 100-percent speed for this 1.48-pressure ratio fan is 17,000 rpm. A separate fan design and size, producing 1.3 pressure ratio at 11,110 rpm, was required for the IIC/9BPR engine. Both fan baseline designs used Ti6Al-4V titanium blades, with part-span dampers, and aspect ratios of approximately 2.5. The fan blades are attached to high-strength, low-alloy steel hubs and have integral stub shafts. On all engines, the fan outlet stator was divided between the inner and outer flow paths. The inner stator was located close behind the bypass splitter. The outer stator was positioned about 51 mm (2 inches) downstream of the fan, in an effort to achieve a low-noise design. Both stator vane rows are integral with a steel weldment, attached to the engine front frame, and include the inner and outer fan flow-path walls, and the nose section of the bypass splitter.

The front frame of all engines contains the thrust bearings for all rotors, the radial accessory drive shaft, and, in the IIC/9BPR engine, the fan-driving reduction gear. In all engines, the frame is a shell-mold aluminum casting with six integral struts. The accessory gearbox is mounted on the bottom of the frame, with the radial drive shaft, and with the front bearing cavity oil drain passing through the bottom strut, into the gearbox.

The five candidate engines differ primarily in their core compressor configurations.

- Engine IA has a four-stage axial compressor, providing a 4.27 pressure ratio at 37,280 rpm. Each stator stage is an integral-wheel-type investment casting of 17-4PH steel alloy. The individual stages, together with front and rear shafts, are joined by electron-beam welds. The cantilevered, strip-stock stainless steel stator vanes

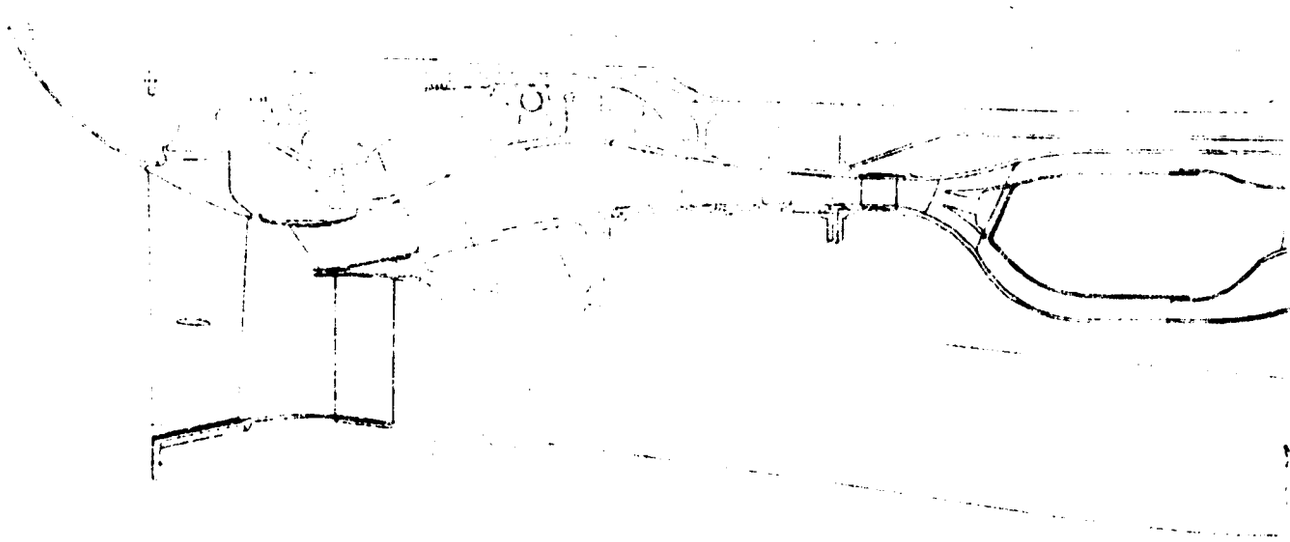

BASIC DIAMETER 53.34 CM (21.0 IN.)
LENGTH FROM INLET FLANGE TO PLANE OR PRIMARY JET NOZ

FOLDOUT FRAME

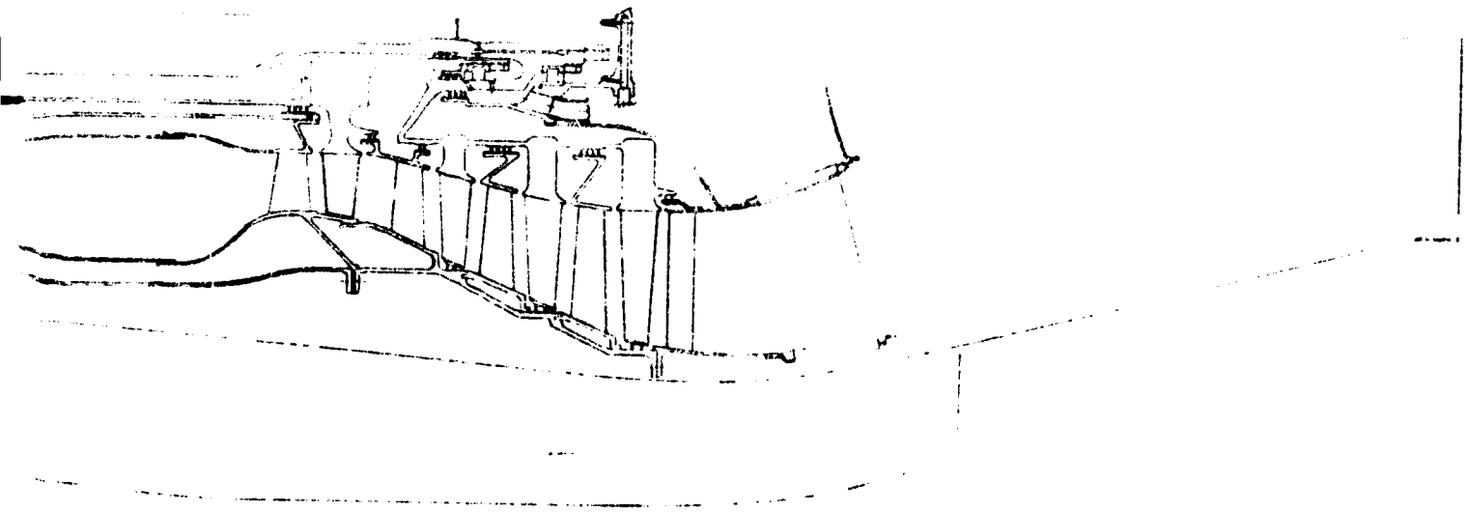

'RIMARY JET NOZZLE 127.76 CM (50.3 IN.)

Figure 36. Candidate Engine Configuration IA.

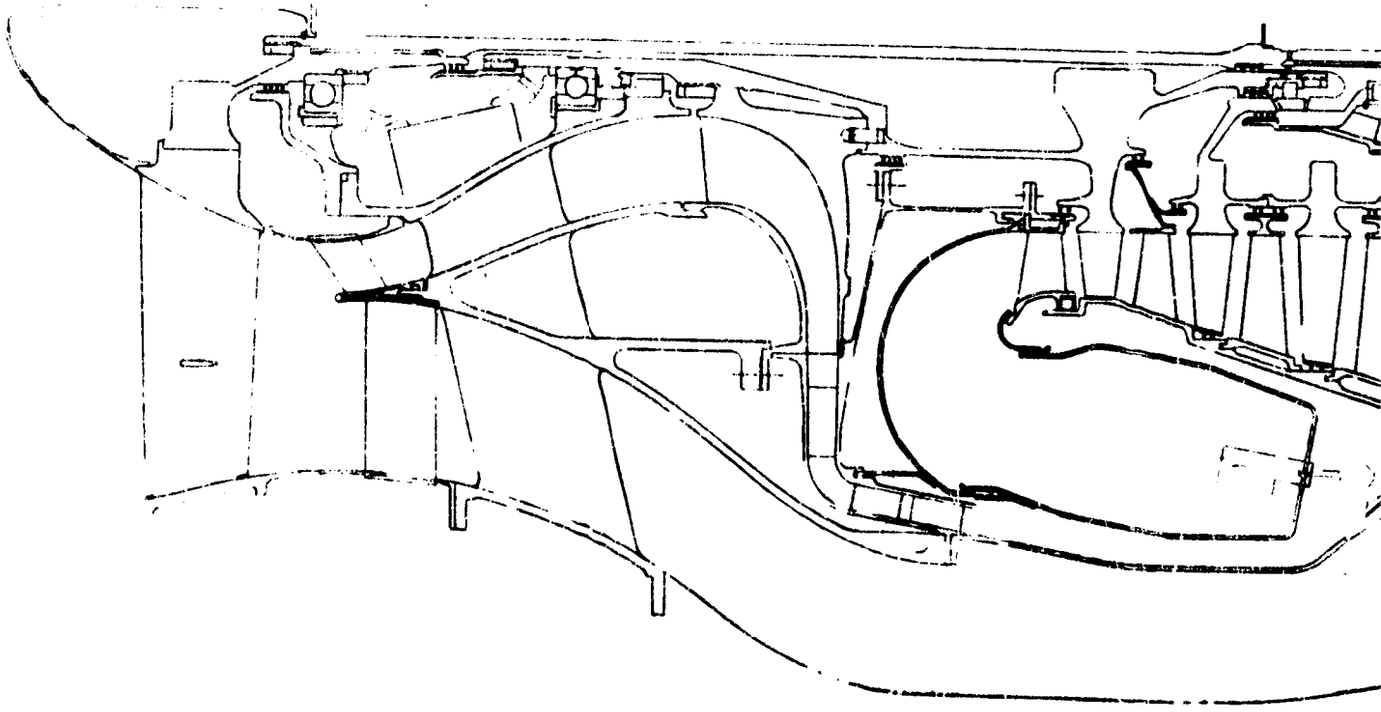

BASIC DIAMETER 62.23 CM (24.5 IN.)

LENGTH FROM INLET FLANGE TO PLANE OF PRIMARY JET NOZ

FOLDOUT FRAME

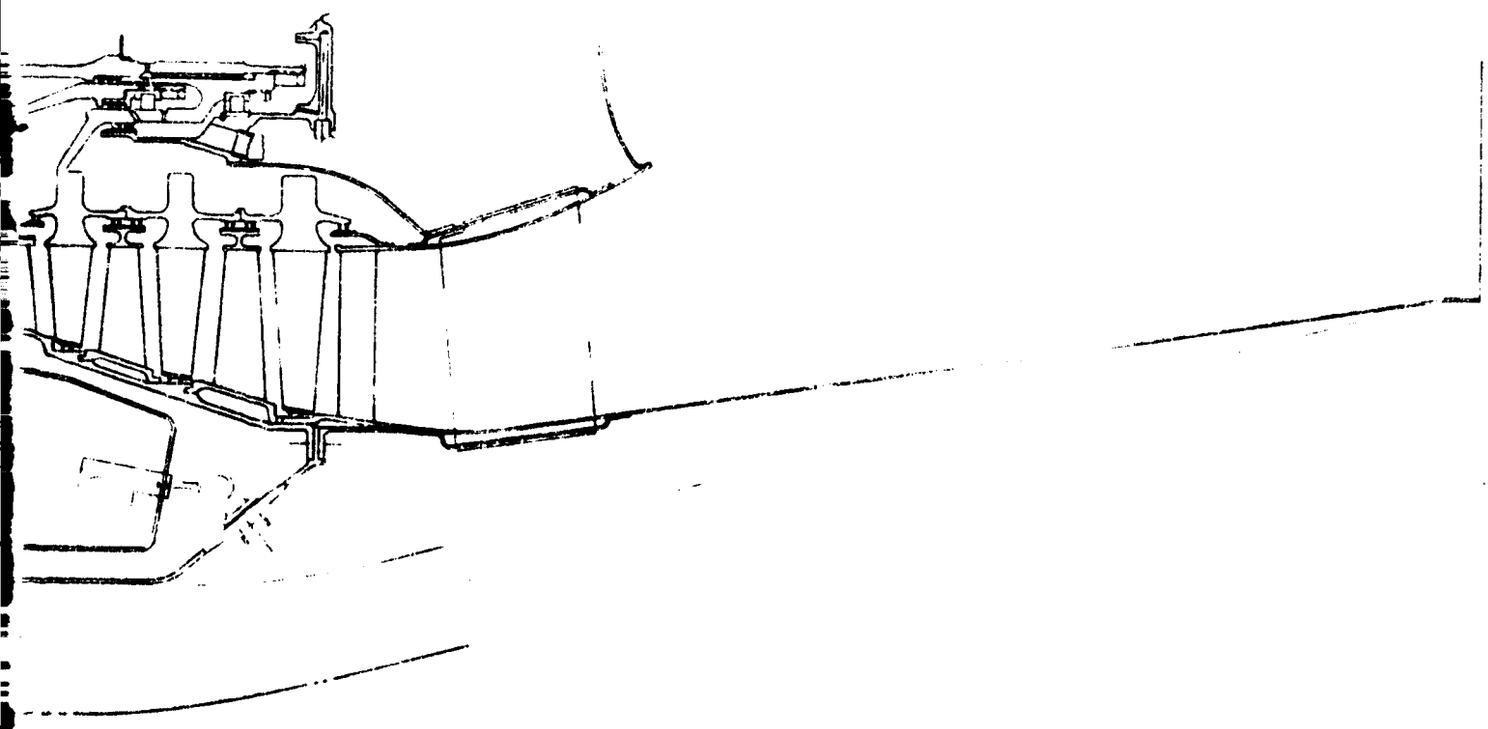

Figure 37. Candidate Engine Configuration IC.

MARY JET NOZZLE 112.77 CM (47.0 IN.)

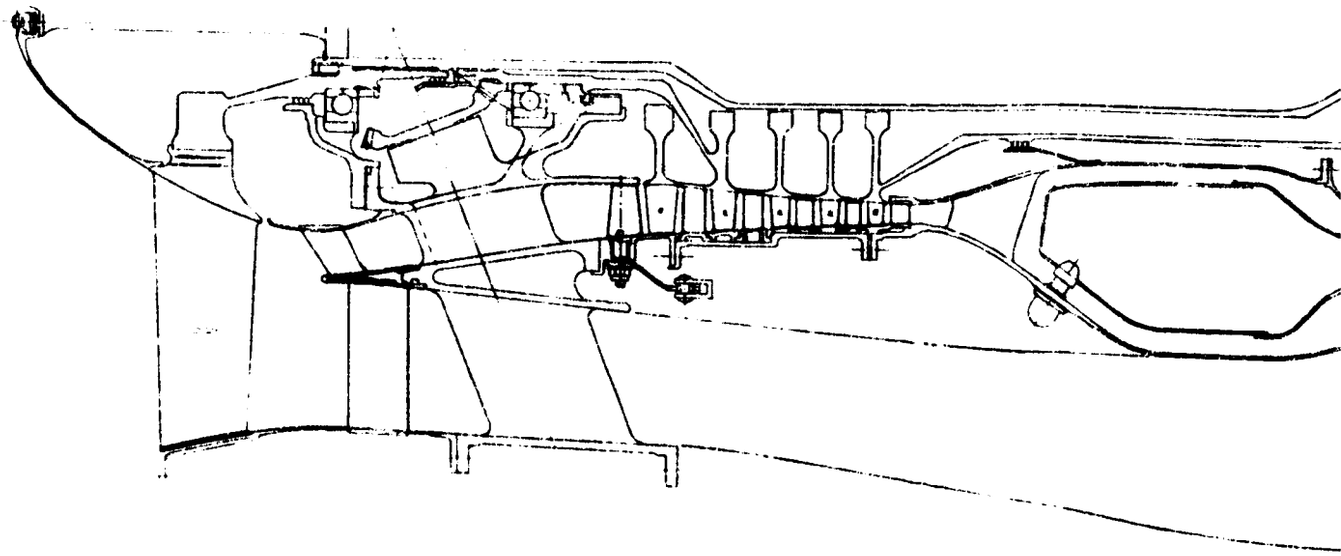

BASIC DIAMETER 53.59 CM (21.1 IN.)
LENGTH FROM INLET FLANGE TO PLANE OF PRIMARY JET N

FOLDOUT FRAME

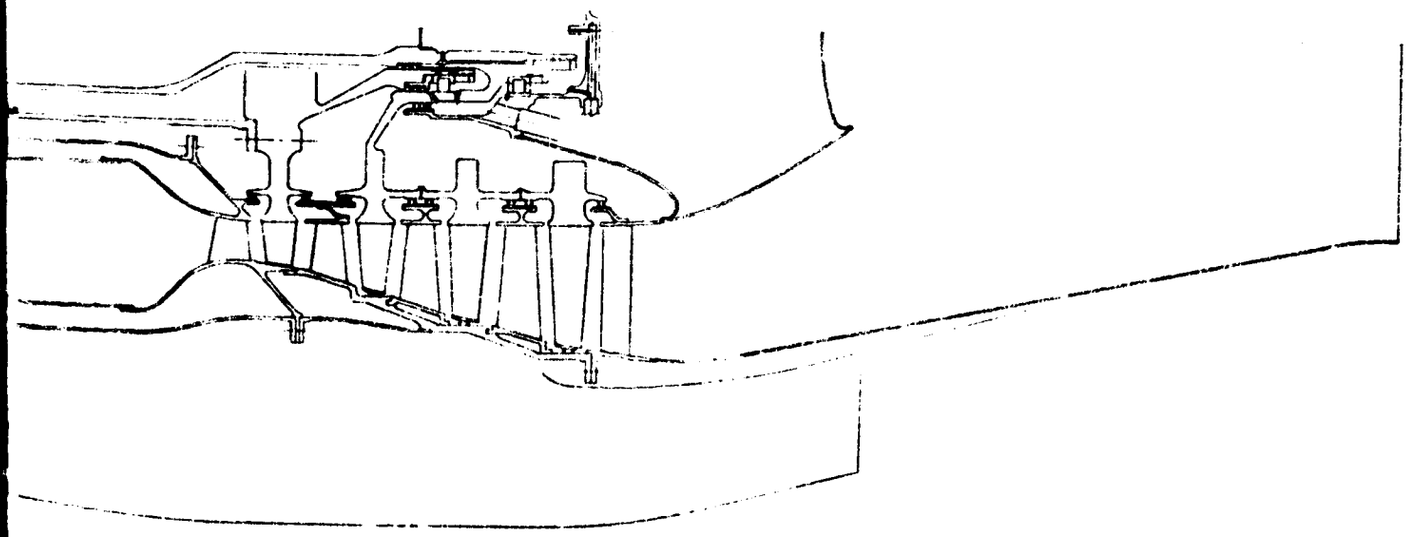

IMARY JET NOZZLE 127.5 CM (50.2 IN.)

Figure 38. Candidate Engine Configuration IIA.

FOLDOUT FRAME

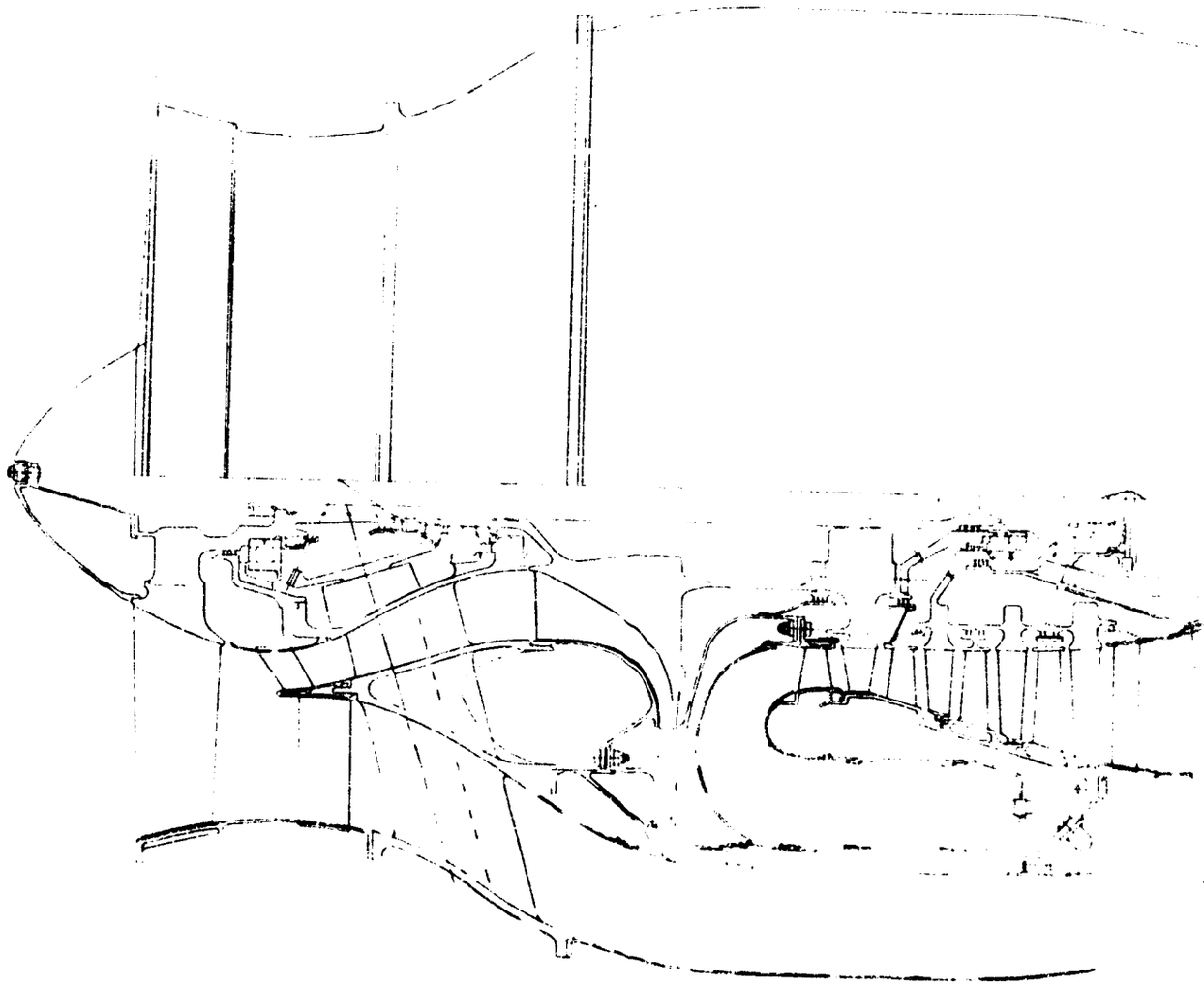

BASIC DIAMETER 60.19 CM (23.7 IN.)
LENGTH FROM INLET FLANGE TO PLANE OF PRIMARY JET

FOLDOUT FRAME

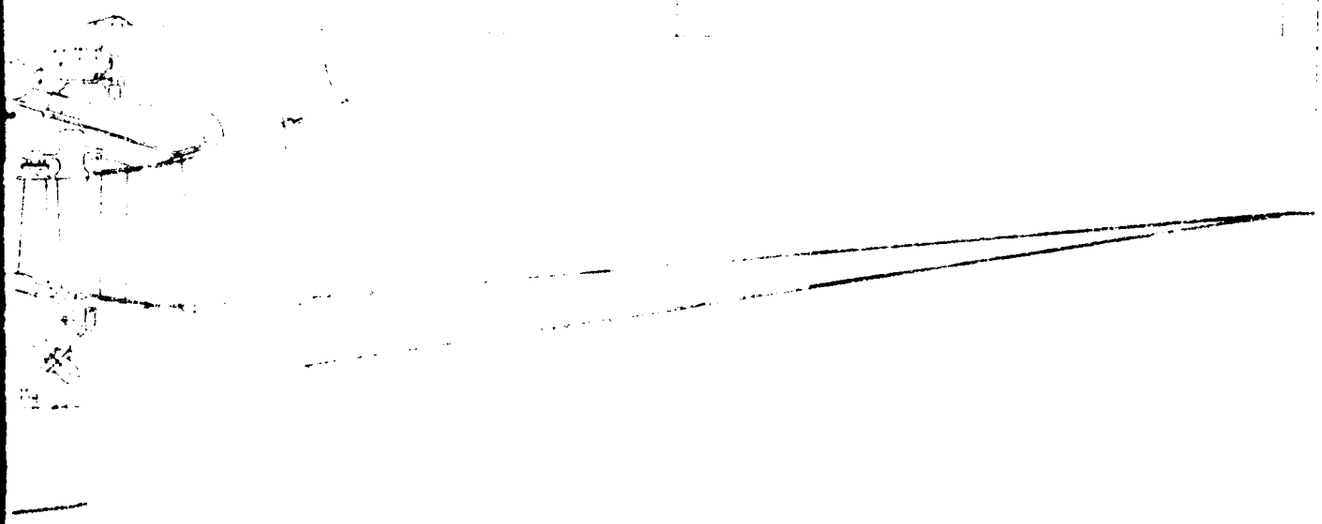

RIMARY JET NOZZLE 134.11 CM (49.2 IN.)

Figure 39. Candidate Engine Configuration IIC.

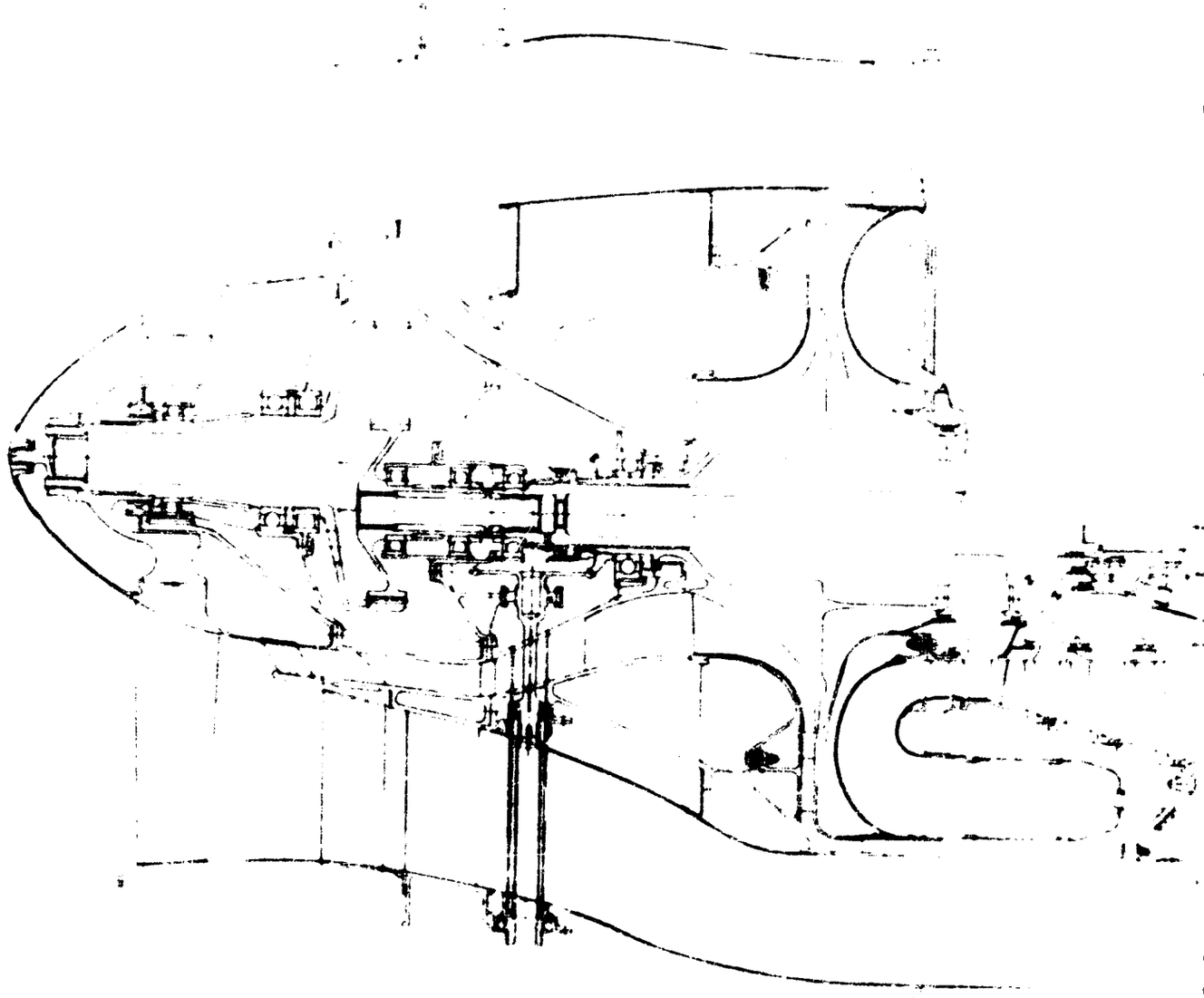

BASIC DIAMETER 68.58 CM (27.0 IN.)
LENGTH FROM INLET FLANGE TO PLANE OF PRIMARY JET NOZ

FOLDOUT FRAME

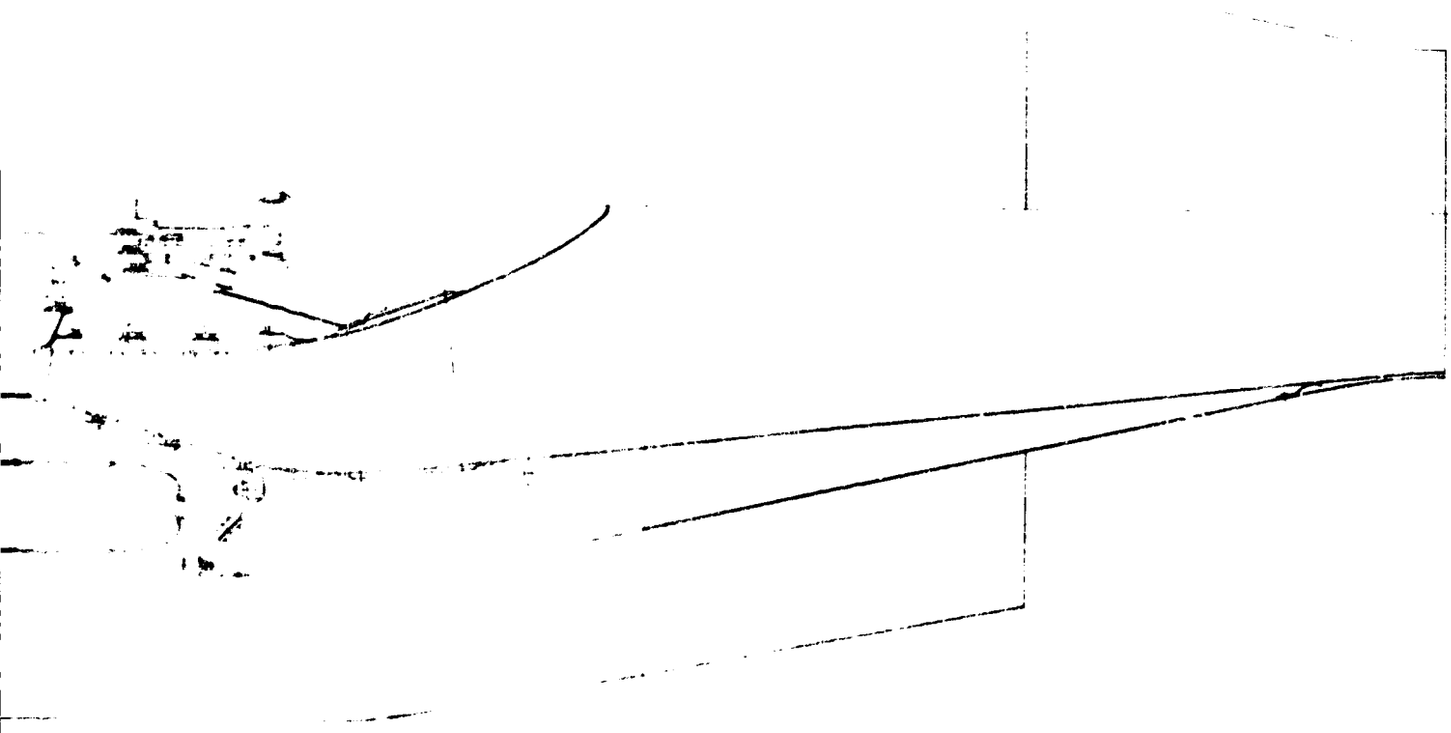

RIMARY JET NOZZLE 150.6 CM (59.3 IN.)

Figure 40. Candidate Engine Configuration IIC/3BPR.

FOLDOUT FRAME 2

are pierced and brazed into a support foot. The stators are carried in a steel casing, split into upper and lower halves by horizontal bolted flanges.

- Engine IC has a single-stage centrifugal compressor, giving 4.28 pressure ratio at 34,680 rpm. The rotor is a precision-machined, Ti6Al-4V titanium forging, mounted on and driven by a shaft that is integral with the turbine wheel. The compressor diffuser is a stainless steel weldment with three vane rows--one radial and two axial.

- Engine IIA has a five-stage axial compressor, giving 6.04 pressure ratio at 33,220 rpm. With the exception of the additional stage and a variable inlet guide vane, this compressor is similar in form and construction to the compressor in engine IA.

- Engine IIC has a centrifugal compressor, giving 5.85 pressure ratio at 36,733 rpm. It is similar in all respects to the IC compressor.

- Engine IIC/9BPR has the same compressor, but has 6.17 pressure ratio at 35,848 rpm, the difference being due to its lower inlet temperature with the lower fan pressure ratio.

All candidate engines have annular combustors, with multiple-vaporizer-pipe fuel injection. The liners are nickel alloy, sheet metal weldments, and the inner and outer housings are stainless steel, sheet metal weldments. The IA and IIA engines have straight-through-flow combustors, while engines IC, IIC, and IIC/9BPR have reverse-flow combustors that wrap around the turbine section.

The compressor-driving turbines of all engines are similar axial-flow, single-stage units. The rotors are integral-wheel type-investment castings of IN-100 nickel-base alloy. The turbine inlet nozzles are investment-cast integral rings of INCO 713C nickel-base alloy.

The fan-driving turbines of all engines are similar axial-flow, three-stage configurations. The rotors are INCO 713C investment castings, with high-aspect-ratio blades and vibration-damping tip shrouds. The first stator is integral with the cast INCO 713C turbine casing. The casing is made of split halves with horizontal flanges. The second- and third-stage stators are multivane segments, also cast of INCO 713C.

The rear frame of all engines contains the rear bearing cavity. This cavity, partly made up of shaft elements, contains an inter-shaft roller bearing, which provides support for the core rotor,

and the fan-turbine roller bearing, which is carried in the rear frame structure. The frame has six structural support struts through the flow path and a row of investment-cast straightening vanes to remove swirl from the gas exiting the last turbine stage. The inner exhaust diffuser cone is integral with the frame. The outer cone, or primary jet nozzle, is attached at a connecting flange. The frame and exhaust cones are N-155 iron-base alloy, sheet metal weldments.

The bypass ducts of all engines are aluminum weldments. The forward duct is of honeycomb construction, with a perforated inner wall providing required acoustic attenuation. The rear duct is of single-wall construction, and at its aft termination, forms the secondary jet nozzle.

The shaft systems of all engines except IIC/9BPR consist of two co-rotating shafts, supported by two bearings on each shaft. Of the four bearings, the core rotor thrust bearing has the largest combination of speed and loading. A 55-mm thrust bearing was chosen for all engines, with resulting bearing DN values between 1.8 and 2.05 million. These DN values are considered to be near the state-of-the-art limit for small aircraft engine bearings and would require considerable development effort to achieve satisfactory bearing life in this application.

The shafting configuration of the IIC/9BPR engine is unique in that a reduction gear is required on the fan rotor to accommodate the design speed difference between the fan and the turbine that drives it. The gear reduces the turbine speed by a ratio of 0.652. This is accomplished by a single internal/external spur-gear arrangement. This differs from customary geared-fan designs that use a planetary reduction gear, with coaxial input and output shafts. In this design, the shaft axes are offset 33.83 mm (1.332 inches). As a result, the fan axis will be offset that amount from the engine core axis. To accommodate this offset, the front frame castings must have carefully designed transition ducts, to match the fan exit flow path to the core and bypass flow paths. With this accomplished by castings, the resulting cost penalty was judged to be minimal. When compared to the usual planetary gear-reduction system with as many as seven individual gears, the internal/external gear-reduction design would effect a considerable reduction in total cost. An additional benefit is the substantial weight savings potential of the simpler design.

Controls.- The fuel-control system selected for the candidate engines utilizes electronic sensing and computing to provide the basic control logic for acceleration and thrust modulation. As shown in the diagram in Figure 41, the fuel-control system is composed of four major sections:

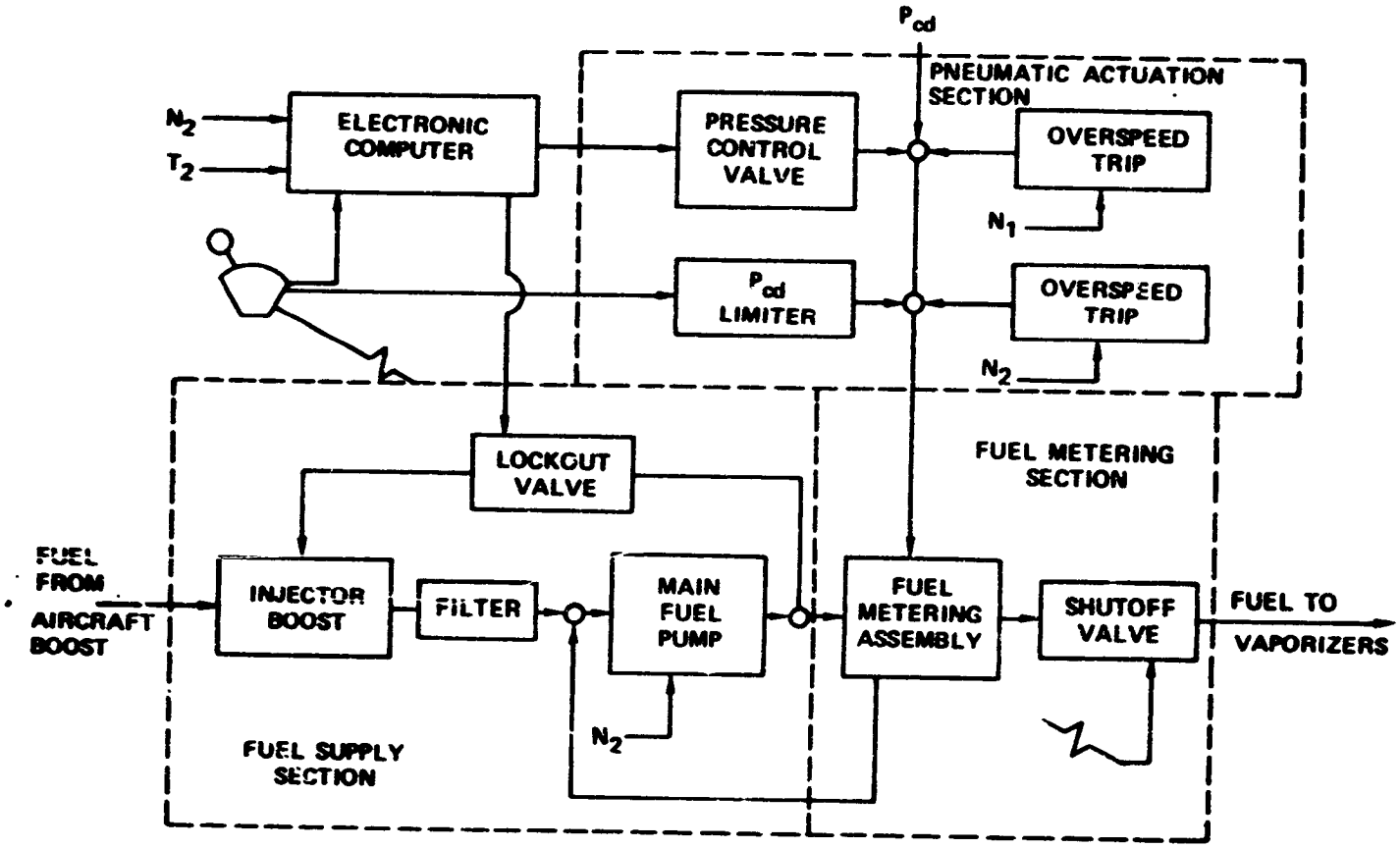

Figure 41. Fuel-Control System Logic Diagram.

- An electronic computing section
- A fuel supply section
- A fuel metering section
- A pneumatic actuation section

The fuel-control schedules consist of a basic maximum (W_f/P_3) ratio to limit acceleration, and a governor function having its set point controlled by an electronic computer. Thrust is modulated by resetting the governor line, which forces the operating point to move along the engine operating line. Should schedule shaping be required, such shaping can be provided by a simple modification to the computer.

Electronic computer.- The electronic control sets the gas generator speed (N_G) by modulating the fuel parameter (W_f/P_3). The power lever generates an electrical signal proportional to the set point gas generator speed (N_G set). The fuel parameter during an engine acceleration is limited by a two-straight-line-function generator. Each line is adjusted by an inlet total temperature signal. During a deceleration, the fuel flow is similarly limited. The output signal modulates the control signal to the fuel metering section by bleeding off the compressor discharge pressure signal (P_3) to a value (P_X) the ratio of which is proportional to the electrical signal. At zero current (an electrical system failure), the pressure-control valve (P_{CV}) bleeds off the P_3 pressure to provide a reduced but safe engine operating point. A diagram of the electronic control logic is presented in Figure 42.

Fuel supply.- This section receives fuel from the aircraft fuel system, filters it, and delivers it to the fuel metering section at the required pressure level. An electrically operated lockout valve is used to shut off motive flow during the engine starting process. It is proposed to use a gear pump operating at 15,000 rpm as the main fuel pump and an injector pump as the boost element. Based on an estimated total pump flow of 680 kg/hr (1500 pounds per hour), and a maximum discharge pressure of 165 N/cm^2 (240 psia), the pump would have a displacement of 1.43 cm^3 (0.10 cubic inch) per revolution.

Fuel metering.- This section is composed of a conventional bellows-operated metering valve and a bypass valve to maintain a constant head across the metering valve. A manually operated shutoff valve is controlled by the power lever

Pneumatic actuation.- This section contains elements that control the pressure entering the metering valve actuation bellows. These elements are:

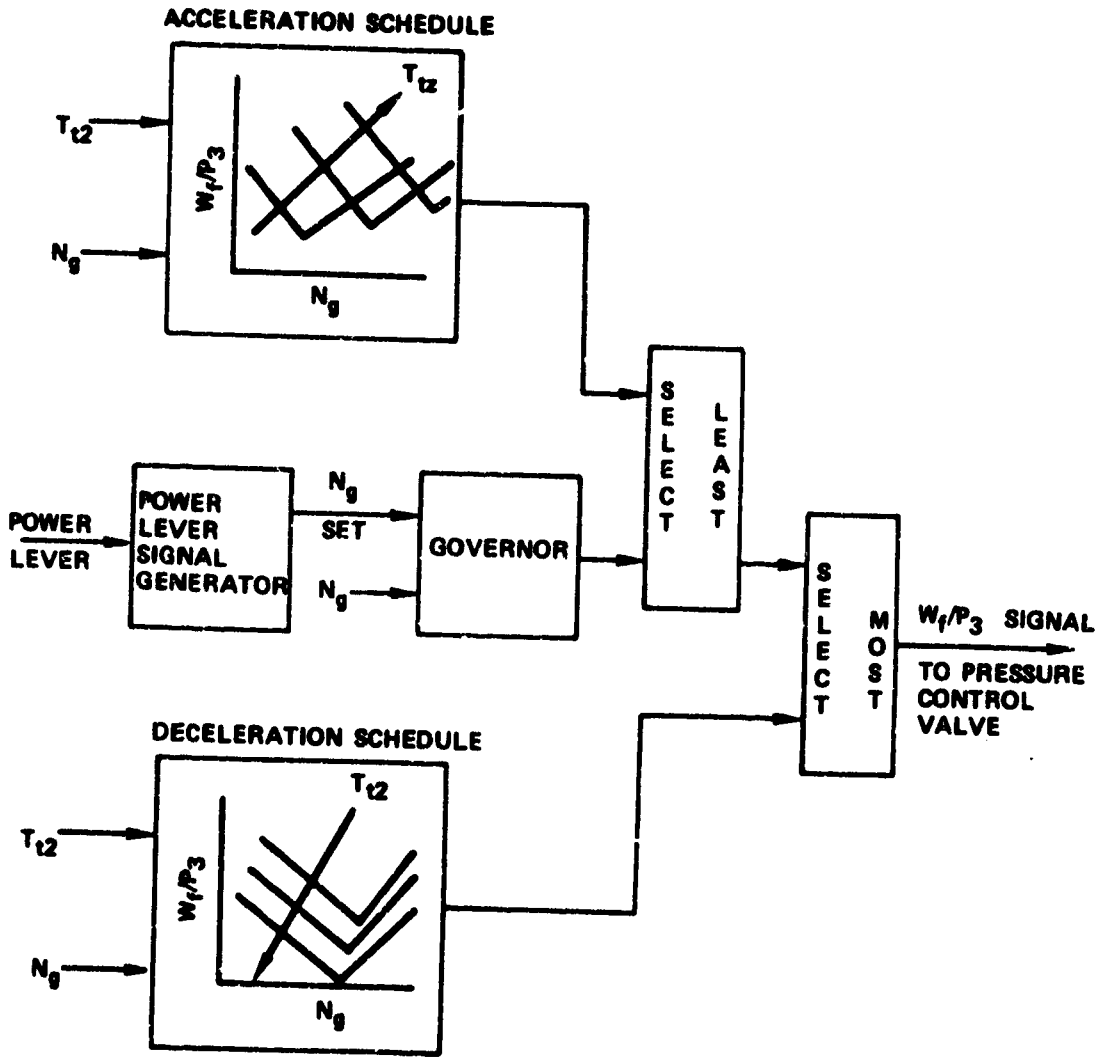

Figure 42. Electronic Computer Logic Diagram.

(a) Two overspeed trip mechanisms--one for the gas generator section and one for the free turbine section of the engine--to protect against an overspeed failure mode.

(b) A P_{cd} limiter element to provide manual control in the event of an electrical power failure.

(c) A pressure control valve that is used in normal operation as the interface between the computer and the fuel metering section. This unit receives electrical signals from the computer and provides a pneumatic pressure to the metering valve actuation bellows to properly position the metering valve to provide the desired fuel flow.

To further evaluate suitable control system approaches, the applicability of the fuel control concept described in NASA Technical Note TN D-5871 (Reference 12) was studied. This control concept was demonstrated on a turbojet engine and the evaluation report of this activity is contained in Appendix B of this study report.

Accessories.- Accessories prescribed for the candidate engines include a starter generator, oil cooler, speed sensors, ignition exciter, ignition lead, ignition plugs, hydraulic pump drive, and an oil pump.

Starter generator.- A 28-volt, 200-ampere starter generator is recommended for the candidate engines. This size was selected as much for generating capacity as it was for starting capacity. A generator of this capacity will provide sufficient power to support the electrical needs of the airplane in one-engine-out situations. However, the pad should be capable of handling generators of larger capacity in case an airplane is provided with extensive electrical anti-ice equipment.

Oil tank.- An oil flow of 9.5 l/min (2.5 gpm) was derived by scaling from the TFE731 oil system. With a dwell time similar to that of the TFE731, the tank capacity could be as small as 1/2 gallon. Based on this capacity, it was determined that an oil-supply cavity could be integrated into the accessory gearbox case design. This would provide advantages such as reduced plumbing, better inlet conditions for the oil pump, less air to remove from the oil, and the elimination of a separate stainless steel tank.

Oil cooler.- The oil cooler proposed for the candidate engines is an aluminum unit 12.5 cm (5 in.) long with a barrel diameter of 5.1 cm (2 in.). Based on a flow of 9.5 l/min (2.5 gpm), and 317°K (110°F) fuel, oil flowing into the cooler at 422°K (300°F) would exist at 400°K (260°F). Satisfactory engine lubrication will be ensured by maintaining the oil at this temperature.

Fuel heater.- A fuel heater is not recommended for the candidate engines. Fuel is presently available that contains an anti-ice additive. It is anticipated that it will soon be available in all jet fuel.

N_1 speed sensor.- This sensor would provide a speed signal to the cockpit indicator. Magnetic screws would be inserted in the tips of two or more fan blades. Speed would be sensed by an inexpensive monopole pickup aligned with the magnetic screws.

N_2 speed sensor.- This sensor would sense the speed of the high-pressure (HP) rotor. It would provide a signal to the electronic fuel-control computer. Normally, the signal would be generated by a monopole speed pickup positioned opposite a toothed wheel driven by the HP rotor. However, ripple voltage from the starter generator may be used to provide the N_2 speed indication if the signal characteristics are satisfactory for the computer.

Ignition exciter, lead, and plugs.- A dual ignition system is proposed for the candidate engines. The exciter will be capable of operating for long periods of continuous ignition. The ignition lead will be furnished with the engine. Straight ignition plugs with lead elbows are provided. These plugs are very reliable and cost about one-half the price of 90-degree plugs.

Hydraulic pump drive.- A pad and drive system that is capable of supplying 10 horsepower for driving customer accessories will be provided. The drive speed at 100 percent engine speed will be 12,000 rpm.

Oil pump.- The oil pump will furnish lubricant to the bearing cavities and the accessory gearing. Since the forward cavity will drain into the accessory gearbox, only two spots must be scavenged. The pump pressure stage will take oil directly from the accessory gearbox; therefore, only the rear bearing cavity will require the use of a scavenge section.

The proposed pump will be small and light. It will be driven at 12,000 rpm and will utilize Gerotor pumping elements with side porting. The pressure element will pump 95 l/min (2.5 gpm) at 100 percent speed. With an altitude limit of 9144 m (30,000 ft) there will be no significant decrease of flow. Therefore, the system can operate without pressure regulation, employing only a simple overpressure relief to limit pressure buildup during cold starts.

The IIC/9BPR engine having a gear-driven fan has additional bearings to be lubricated. Oil must also be provided to lubricate and cool the reduction gears. The pressure pump section must pump 19 l/min (5 gpm) at rated speed.

Nacelle configuration.- A nacelle design study was conducted in order to distinguish the design and configuration criteria peculiar to these small engines. No attempt was made to define optimum aerodynamic shapes, or to provide the total internal/external flow-field matching that would be required to accomplish

optimum installed-engine/nacelle performance. However, nacelle design criteria were addressed to the extent that a credible overall nacelle configuration could be achieved that would be applicable to the five candidate engines and would reflect the installed-performance increments resulting from engine configuration differences.

The nacelle/engine installation study layout for the IIA engine is presented in Figure 43. This figure illustrates the engine mounting, accessory location, and general nacelle configuration characteristics. It is representative of all the candidate engine nacelles. The only characteristic that appears to distinguish the small-engine installations from those of larger engines is the relatively larger space and nacelle dimensions required to accommodate the engine accessories. In the axial-flow engines particularly, the accessories dimensions were found to affect the nacelle length as well as the diameter. With limits on nacelle contour angles and rates of curvature established by aerodynamic drag criteria, the radial projection of the accessory envelope determines both the length of the inlet and the rearward distance to the plane of both jet nozzles. For example, Figure 43 shows an arbitrary 15-degree maximum boattail angle and approximately 154 cm (60 inches) radius of curvature. With the outer wall of the primary nozzle also limited to a 15-degree angle, the drawing shows the shortest possible nozzles that will clear the accessory envelope and meet these nacelle contour limits.

The total nacelle length of the shorter engines having centrifugal compressors and reverse-flow combustors is about equal to the engines with axial-flow compressors. With the larger combustor diameter occurring at the rear of the engine, and the outer wall of the primary nozzle limited to the same angle, the primary exhaust duct is longer, and offsets the basic-engine length advantage.

It was found that the shortest inlet that would provide conventional nacelle contours, which would clear the accessories, was about one fan diameter in length. To establish the minimum length quantitatively would require an extensive drag trade-off analysis of the nacelle forebody.

The nacelle inlet duct was sized as a cylinder equal in diameter to the fan tip. At the maximum fan corrected flow, the fan face axial Mach number is 0.60, and the inlet duct Mach number is about 0.50, thus providing the opportunity for desirable acceleration of the flow immediately ahead of the fan. At maximum cruise velocity, the Mach number is 0.577, and external isentropic diffusion to the 0.50 duct Mach number occurs. It should be possible to offset the drag effect of this small amount of diffusion by properly contouring the inlet lip for maximum lip suction. The low speed performance of the nondiffusing duct should be adequate to eliminate the need for flow-augmenting suck-in doors.

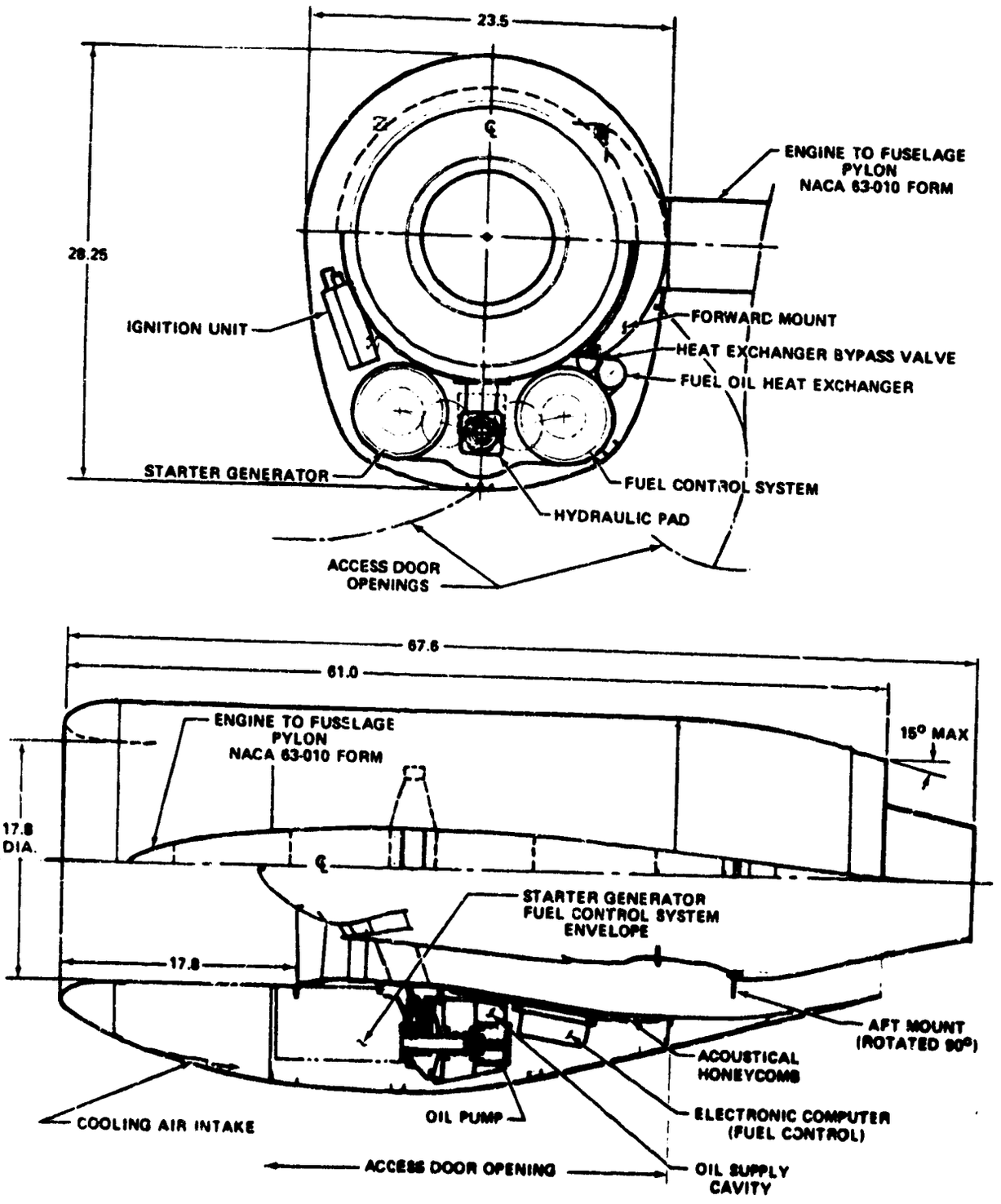

Figure 43. Installation of Engine IIA.

Table IX presents the overall dimensions of the candidate engine nacelles, as well as the characteristic engine dimensions that establish the nacelle boundaries.

The nacelle study included accessibility and maintainability. It was shown that all accessories requiring frequent maintenance and servicing can be grouped at the bottom of the engine, with access through large hinged door panels. Engine mounting can be accomplished in a manner that facilitates rapid installation and removal of the engine. The simple-three point mounting system (two fixed mounts and one stabilizing link) was achieved in the design study, with no compromise to the engine design.

Neither the small size nor the configurations of the candidate engines were found to have either a detrimental or advantageous effect on the nacelle configurations. Conventional nacelle design and engine installation practice should be applicable to the candidate engines.

Propulsion system weight analysis.- Engine weight calculations were based on the basic layout drawings of the five candidate engines. Each engine component weight was calculated separately, with each part being resolved into simple geometric shapes to facilitate analysis. By this method, the engine weight estimates should be accurate to within 5 percent.

The nacelle weight was calculated for each engine by scaling components of a nacelle produced for the AiResearch TFE731-2 turbofan engine. The component weights separately evaluated were: pylon; engine mounting structure; cowls and skins; fuel, pneumatic, hydraulic, and lubrication lines and fittings, including trapped fluids; fire detection and extinguishing systems; instrumentation and controls. In addition, pylon and nacelle structural weights were calculated for the nacelle design study shown in Figure 43, confirming the weights derived by scaling.

Table X lists the estimated basic engine weight, the total engine weight with accessories, bypass duct, and jet nozzles, estimated nacelle plus pylon weight, and the total installed pod weight. In addition, the weight of engine IA with a steel fan and engine IC with a steel compressor are given to show the effect of substituting steel for titanium. Finally the engine specific weight (weight-to-thrust ratio) is given, as it was input to the aircraft synthesis computer program.

TABLE IX. NACELLE DIMENSIONS AND CHARACTERISTIC ENGINE DIMENSIONS.

Engine		IA	IC	IIA	IIC	IIC/9BPR
Fan Diameter	cm in.	45.21 17.8	45.21 17.8	45.21 17.8	45.21 17.8	57.40 22.6
Engine Diameter	cm in.	53.34 21.0	62.23 24.5	53.59 21.10	60.19 23.7	68.58 27.0
Engine Length to Primary Nozzle	cm in.	127.76 50.3	119.38 47.0	127.50 50.2	124.97 49.2	150.60 59.3
Nacelle Width	cm in.	59.44 23.4	68.33 26.90	59.69 23.5	66.29 26.1	74.68 29.4
Nacelle Height	cm in.	71.63 28.2	76.07 29.95	71.76 28.25	75.06 29.55	88.39 34.8
Nacelle Length to Secondary Nozzle	cm in.	146.56 57.7	118.11 46.5	154.94 61.0	14.21 55.2	181.48 71.45
Nacelle Length to Primary Nozzle	cm in.	172.97 68.1	164.59 64.8	171.71 67.6	170.18 67.0	208.03 81.9

TABLE X. ESTIMATED WEIGHTS OF CANDIDATE ENGINES.

Engine		IA	IC	IIA	IIC	II C/ 9BPR	IA with Steel Fan	IC with Steel Compressor
Basic Engine Wt.	kg	98	112.5	104.8	122.9	143.3	113.4	123.8
	lb	216	248	231	271	316	250	273
Total Engine Wt.*	kg	136	149.7	145.2	163.3	192.3	151.5	161
	lb	300	330	320	360	424	334	355
Nacelle Wt.	kg	43.5	43.5	43.5	43.5	50.8	43.5	43.5
	lb	96	96	96	96	112	96	96
Total Pod Wt.	kg	179.5	193.2	188.7	206.8	242.1	195	204.5
	lb	396	426	416	456	536	430	451
Specific Wt. (Total Engine Wt./SLS Thrust)	kg/kg or lb/lb	0.231	0.253	0.233	0.283	0.280	0.257	0.272

* Includes starter-generator, bypass duct, and primary and secondary jet nozzles.

Airplane Definition and Analysis

Initial engine/airplane performance analysis.- The airplane defined for the initial analysis was termed a "conversion." Turbofan engines were substituted for the piston engines used on the Cessna Model 340 with minimum change to the configuration. Figure 44 is a three-view study drawing, showing the forward-extension wing-mounted engines, which preserves the original center of gravity location and minimizes configuration changes.

Unlike turbojets that have essentially flat thrust decrements with increasing flight speed, turbofan engine cycles may be tailored to have thrust decrements of any amount desired. By manipulating engine fan pressure ratios and bypass ratio, the thrust requirements throughout the desired airplane performance envelope may be met by an engine that is sized for cruise. Based on this assumption, the drag characteristics of the Model 340 "conversion" were defined for use in a separate exercise, directed to the identification of engine thrust-decrement characteristics that would establish a best airplane/engine performance match. The takeoff, second-segment climb, and single-engine climb performance of the airplane was tested with four turbofan cycles sized for cruise, each having significantly different thrust decrements. The cycle with the best performance match was thereby identified. As a result of this exercise, the fan pressure ratio variable was eliminated from the parametric engine work conducted in Phase II.

An airplane performance ground rule suggested by NASA was incorporated into the study. This ground rule stipulated that the performance requirements of FAR Part 25 be applied to the study. One of the regulations in Part 25 states that twin-turbofan-powered aircraft must be capable of maintaining a 2.4-percent climb gradient to an altitude of 122 m (400 ft) above runway level with one engine out. This criterion defines a minimum (thrust-drag)/weight value for climb capability. Since 1.2 V_s must be maintained, the attitude of the aircraft during the second-segment climb phase is approximately constant. With the requirement that $\tan \gamma = 0.024$, where γ is the angle between the flight path and the horizon, the applicable equation, $\sin \gamma = \frac{F_N \cos\alpha}{W} - \frac{C_D}{C_L}$, may be solved for net thrust (F_N)-- that is, the minimum thrust to meet the 2.4-percent gradient. This solution assumes a constant W_g (aircraft gross weight), α (angle of attack), and $\frac{C_D}{C_L}$. By determing 1.2 V_s for various altitudes and ambient temperatures, a general mapping of minimum thrust requirements is possible. The single-engine second-segment climb thrust requirement for the "conversion" airplane is 2722 N (612 lb). Second segment-climb profiles for the minimum 2.4 percent climb gradient are shown in Figure 45, for standard and hot day atmospheres.

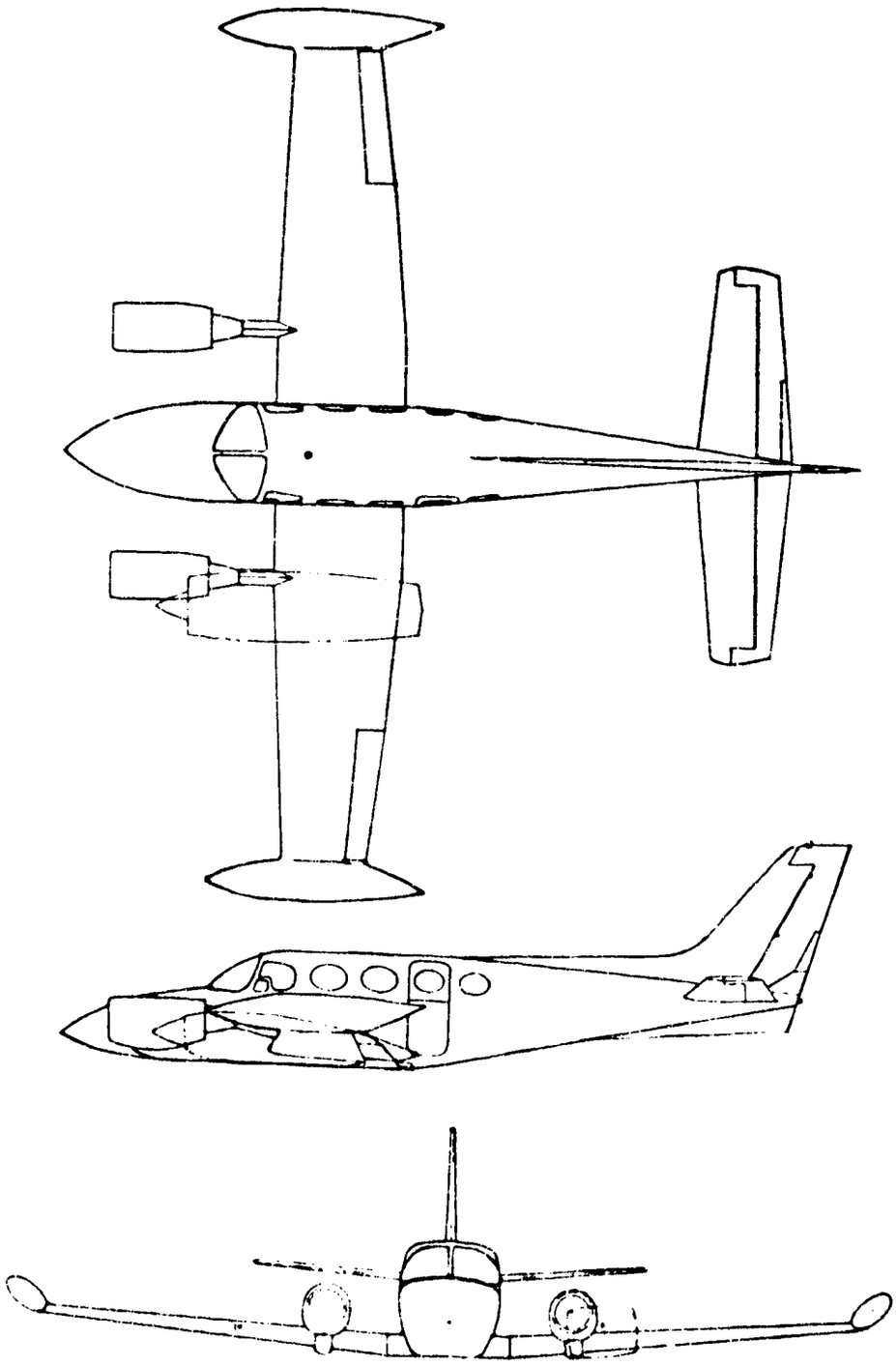

Figure 44. Three-View Study of Cessna Model 340 "Conversion."

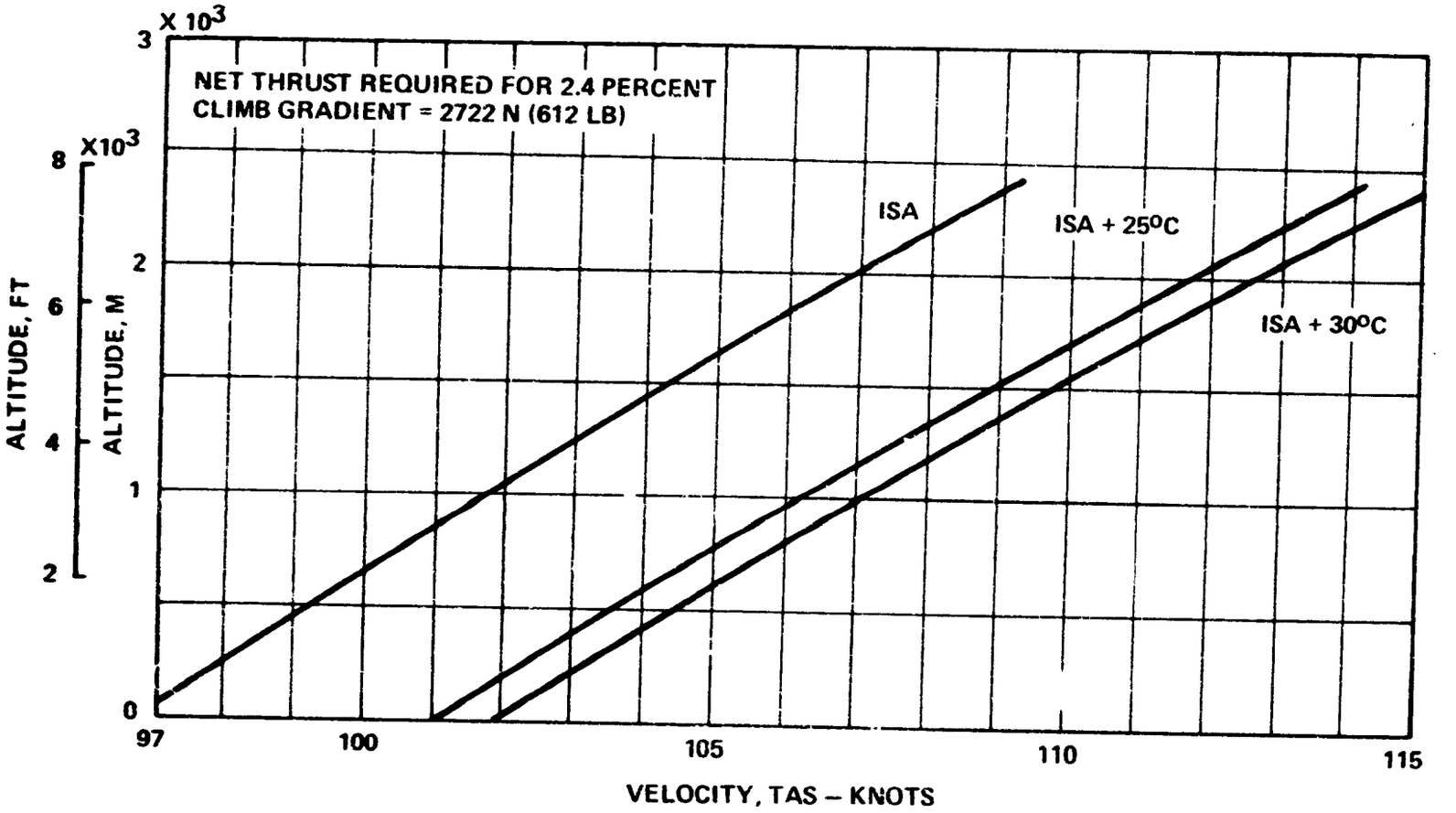

Figure 45. Second-Segment Climb Profiles at Standard Hot Day Atmospheres Model 340 "Conversion" at Gross Weight of 2722 kg (6000 lb).

Calculations were made to show the capabilities of the Cessna Model 340 "conversion" having a decreased wing area with similar basic aerodynamic characteristics. Initial studies compared a common-core turbofan with different bypass ratios at various values of range and takeoff distance. The aircraft gross weight was assumed to be 2676 kg (5900 lb), the cruise altitude 7315 m (24,000 ft) and the cruise speed 648 km/hr (350 kts) TAS. Installed engine weight differences affected the available fuel load, and differences in nacelle drag affected the cruise lift-drag ratio (L/D). The effect of bypass ratio (BPR) on range is shown in Figure 46. Range is maximized with the BPR = 5 engine cycle due to the tradeoff between L/D and thrust specific fuel consumption (TSFC).

By increasing the Model 340 wing-loading from 156 to 269 kg/m^2 (32 to 55 lbs per sq ft), the L/D ratio at start of cruise with the nacelle sized for 5:1 bypass ratio increased from 6.13 to 7.24. The weight difference between the turbofan and reciprocating engines yielded 243 kg (535 lb) for additional fuel capacity. While maintaining a 344-kg (1200-lb) payload, the higher wing-loading and extra fuel resulted in a cruise-range increase of 367 to 727 nautical miles with a 5:1-BPR engine. The initial cruise thrust requirement decreased from 2140 to 1810 N (481 to 407 lb) per engine.

It was determined during the study that takeoff and landing speeds close to those of the Model 340 could be achieved with the use of full-span leading-edge devices and slotted Fowler flaps. With the adoption of spoilers for roll control, it is possible to use full-span trailing-edge 100 percent Fowler-action flaps. As shown by Raisbeck (Reference 11), a maximum lift coefficient of 3.0 in the landing configuration should be attainable. While maintaining the gross weight and stall velocities of the Model 340, the wing-loading could be increased to 317 kg/m^2 (65 lbs per sq ft). As the aircraft configuration was refined, engine sizing and wing-loading was traded and adjusted so that the takeoff and landing characteristics of the Model 340 could be retained.

In the initial takeoff analyses, a reasonable takeoff performance resulted from the assumption of a maximum lift coefficient of 1.97 in the takeoff configuration. With 5:1-BPR turbofan engines the normal takeoff distance to 15 m (50 feet) altitude at a gross weight of 2722 kg (6000 lb) was calculated to be 727 m (2384 ft) on a standard sea-level day. This is slightly better than the Model 340 with reciprocating engines, which requires a normal takeoff distance of 741 m (2430 ft). With turbofan engines, the balanced-field length was calculated to be 1027 m (3368 ft), with 268 kg per m^2 (55 lbs per sq ft) wing-loading and an engine failure occurring at 174 km per hr (108.1 mph) TAS. The accelerate-stop distance for the reciprocating-engined Model 340 is 942 m (3090 ft). Although these distances (balanced field length and

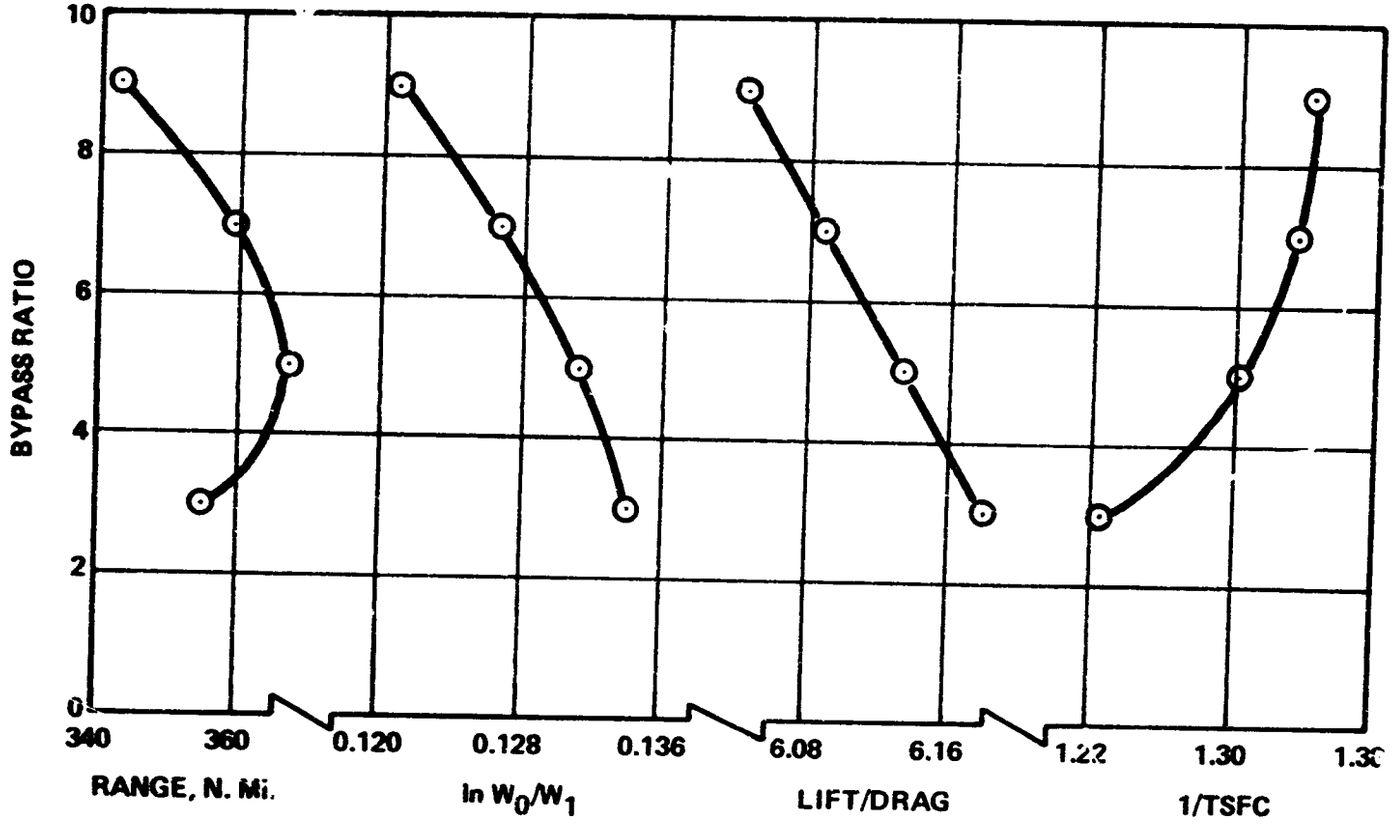

ln = LOG TO BASE e

W_0 = GROSS WEIGHT

W_1 = WEIGHT AT END OF CRUISE

Figure 46. Bypass Ratio Versus Components of Brequet Range Equation.

accelerate-stop distance) are not directly comparable, the two aircraft display similar takeoff performance. The second-segment climb gradient limit for the turbofan-engined derivative occurred at 1753 m (5750 ft) on an international standard altitude (ISA) + 27.1°C day. With Fowler flaps on the high-wing-loaded airplane and 5:1 bypass-ratio engines, low-speed performance could be significantly better than that of the Model 340.

The analyses indicated that turbofans having bypass ratios greater than 5:1 were not required to meet the 914 m (3000 ft) field length requirements specified for the study, with a configuration having a higher wing-loading than the Model 340. Furthermore, based on the results shown in Figure 46, it was determined that the high nacelle drag and greater weight of the higher bypass ratio engines would penalize cruise performance and for a fixed range would result in a larger, more expensive airplane.

The preliminary airplane modeling and sizing studies were especially useful in the early definition of viable candidate engine cycles and configurations. Even though the results indicated that high-bypass-ratio engines would not be required, a 9:1-bypass-ratio candidate was defined for use in subsequent in-depth synthesis and sensitivity analyses. As described in Phase III, these early results were confirmed quantitatively with respect to both airplane size and operating economics.

Aircraft synthesis computer program. - A computer program (Reference 7), developed by NASA/Ames, was used to evaluate the effects of five candidate engines on the basic purchase price and total operating cost of a baseline airplane having constant mission and performance characteristics. A systemized total design process was used to rapidly identify and evaluate the influence of various design parameters on airplane sizing, aerodynamics, performance, structural weight and balance, economics, and propulsion sizing. This approach is similar to that used to analyze current and future civil transports. The synthesis model was based on previous NASA experience and study programs in related technology areas. The economic correlations used in the program were primarily based on the techniques discussed in the "Technology Assessment of Advanced General Aviation Aircraft," developed for NASA at Lockheed Georgia (Reference 8).

Checkout and initial modeling for the program was completed with use of Gates Learjet airplane data. The results of this checkout confirmed the ability of the program to duplicate the performance, size, and cost characteristics of an airplane. The checkout established the feasibility of the modeling approach for deriving the conceptual design characteristics of small turbofan-powered general-aviation aircraft.

The operational procedure and usage of the NASA synthesis program was initiated by defining a representative turbofan engine cycle as a substitute for the reciprocating engines used on the Cessna Model 340. Drag polars were defined for the turbofan model with the use of polars supplied by Cessna, and modified to reflect the removal of the reciprocating engines and nacelles. Airplane weight and sizing determinations were based on the group weight statement and on the general arrangement of the Model 340 shown in Figure 47.

Basic airplane performance requirements recommended for adoption included:

- Cruise altitude of 7315 m (24,000 ft) at 648 km/hr (350 knots) TAS
- Six-seat capacity
- Takeoff and landing distance not greater than 914 m (3000 ft)
- A 2.4-percent climb gradient to 122 m (400 ft) above the runway elevation specified in FAR 25

FAR 25 specifies a minimum thrust-to-weight ratio for climb. Since a stall velocity of 1.2 must be maintained as closely as possible, the attitude of the aircraft during the climb segment above 122 m (400 ft) runway elevation is approximately constant. Therefore, the net thrust required to meet the climb gradient established one of the engine sizing requirements. The other engine sizing criterion was determined by the net-thrust requirement at the start of cruise.

The synthesis program consists of several modules that perform various tasks in the design of general aviation airplanes. The fundamental modules that form the basis for the synthesis program consist of an airplane geometry module, an aerodynamics module, a propulsion-system module, a weight and balance module, a mission performance module, and an economics module. Input for each module consists of quantities generated internally by other modules, or design variables that are input directly, or both. The integrated approach established in the program methodology ensures that the multiple effects of design variables are continuously accounted for in the aircraft sizing procedure.

The calculations performed in the airplane geometry module include the sizing of the wing, fuselage, empennage, and engine nacelles. The wing geometry is characterized by parameters such as aspect ratio, taper ratio, airfoil thickness, quarter-chord sweep, etc. The fuselage shape and volume are related to the number of passengers, seating arrangement, and fuselage configuration. Typical output of the geometry module is shown in Figure 48.

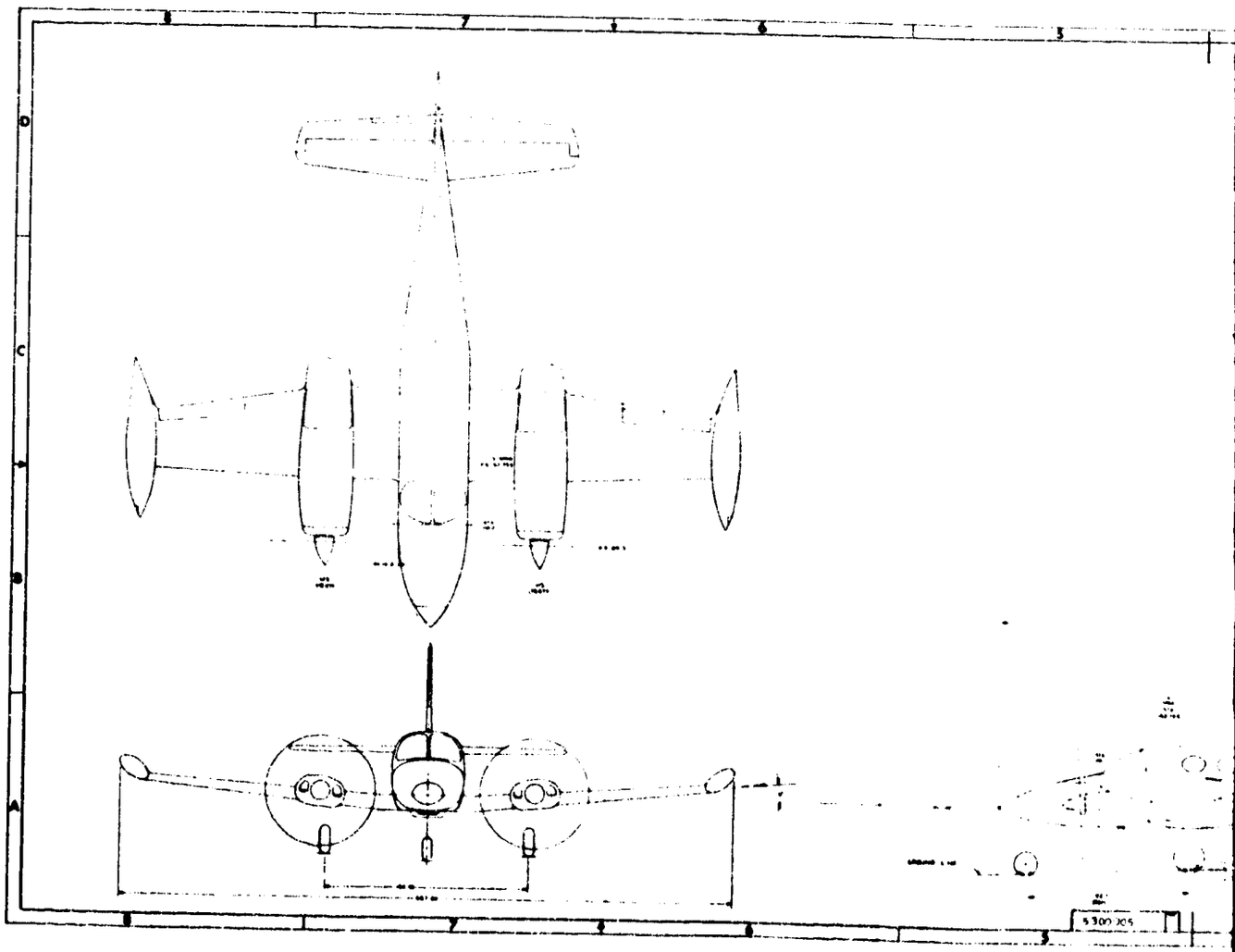

PRECEDING PAGE BLANK NOT FILMED

FOLDOUT FRAME

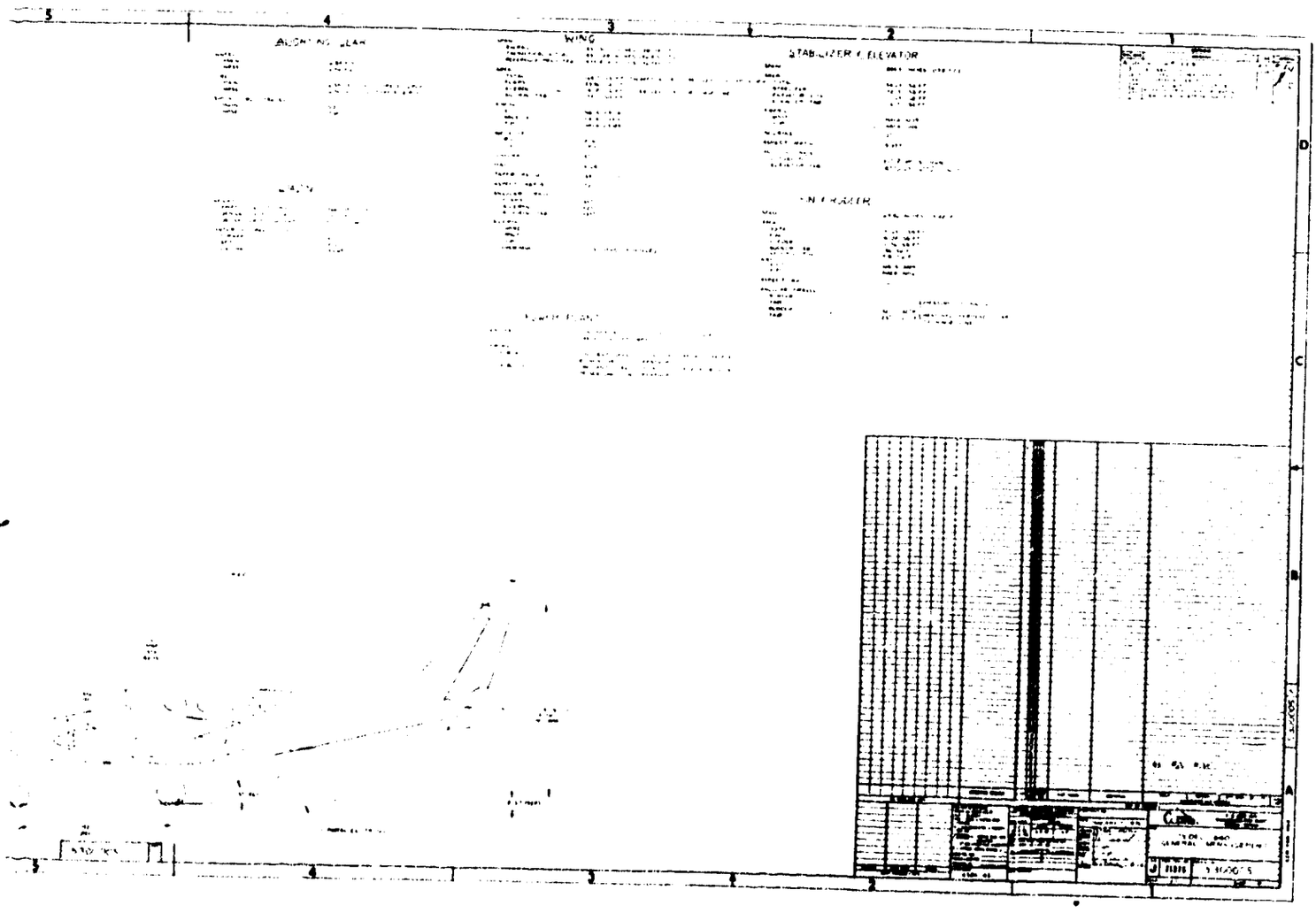

Figure 47. Cessna Model 340 General Arrangement Drawing.

FOLDOUT FRAME 2

GROSS WEIGHT = 6230. PASSENGERS = 5. PLUS CREW OF 1

FUSELAGE	LENGTH	(ELF)	32.13	FT
	WIDTH	(SWF)	4.67	FT
	WETTED AREA	(SF)	371.	SQFT
	DELTA P	(DELP)	5.21	PSI
WING	ASPECT RATIO	(AR)	7.86	
	AREA	(SW)	100.5	SQFT
	SPAN	(B)	28.1	FT
	GEOM. MEAN CHORD	(CBARW)	3.64	FT
	QUARTER CHORD SWEEP	(DLMC4)	0.0	DEG
	TAPER RATIO	(SLM)	.615	
	ROOT THICKNESS	(TCR)	.180	
	TIP THICKNESS	(TCT)	.090	
	WING LOADING	(WGS)	62.0	PSF
	WING FUEL VOLUME	(VFW)	15.9	CUFT
HOR. TAIL	ASPECT RATIO	(ARHT)	5.32	
	AREA	(SHT)	44.8	SQFT
	SPAN	(BHT)	15.43	FT
	MEAN CHORD	(CBARHT)	2.96	FT
	THICKNESS/CHORD	(TCHT)	.075	
	MOMENT ARM	(ELTH)	16.0	FT
	VOLUME COEFF.	(VBARH)	1.960	
VERT. TAIL	ASPECT RATIO	(ARVT)	1.71	
	AREA	(SVT)	23.7	SQFT
	SPAN	(BVT)	6.36	FT
	MEAN CHORD	(CBARVT)	3.80	FT
	THICKNESS/CHORD	(TCVT)	.075	
	MOMENT ARM	(ELTV)	17.0	FT
	VOLUME COEFF.	(VBARV)	.142	
ENG.NACELLES	LENGTH	(ELN)	3.58	FT
	MEAN DIAMETER	(DBARN)	1.46	FT
	NUMBER ENGINES	(ENP)	2.0	
	WETTED AREA	(SN)	32.87	SQFT
TIP TANKS	VOLUME	(VFTP)	6.46	CUFT
	DIAMETER	(BXIS)	1.32	FT
	LENGTH	(AXIS)	8.90	FT
	WETTED AREA	(STIP)	56.10	SQFT

Figure 48. Summary Output for Sizing.

The aerodynamic module computes the airplane lift and drag characteristics on a point-by-point basis during takeoff, climb, cruise, and landing. The cruise drag is determined for each aircraft component based on Reynolds number and Mach number. Form factors are used to account for body shaping component interference, or for duplicating the drag of an existing aircraft. Cruise lift is based on an input value of angle of attack for zero lift and a semi-empirical method for computing the lift curve slope. The increments in lift and drag due to high-life devices are based on methodology discussed in Reference 9. Plain, split, slotted, and Fowler-type trailing-edge flaps are simulated. The methodology accounts for flap deflection, span and chord, wing sweep, thickness, and aspect ratio. A sample output of the aerodynamic module is presented in Figure 49. Nacelle drag is accounted for as either an aircraft drag or as a propulsion system drag reflected as an increase in the TSFC. Note that Figure 49 shows the latter option with the drag of the nacelles being set to zero.

```
CRUISE MACH =  .577          CRUISE ALTITUDE =  24000.

CRUISE RE.NUM. PER FT.   = 2.011E+06    FLATPLATE CF AT RE=10**7 IS  .00281

AERODYNAMICS DATA
    TOTAL EFFECTIVE FLATPLATE AREA    (FE)      3.028   SQFT
    TOTAL WETTED AREA                 (SWET)    744.1   SQFT
    MEAN SKIN FRICTION COEFF.         (CHARF)   .00365
  (NACELLE DRAG INCLUDED IN INSTALLED ENGINE PERFORMANCE)
       (DOES NOT APPEAR IN FLATEPLATE OR WETTED AREAS)

DRAG BREAKDOWN IN SQFT
    WING                              (FEW)      .892
    FUSELAGE                          (FEF)     1.336
    VERT. TAIL                        (FEVT)     .222
    HOR. TAIL                         (FEHT)     .411
    ENGINE NACELLES                   (FEN)     0.000
    TIP TANKS                         (FETP)     .127
    INCREMENTAL FE                    (DLTAFE)   .040

AERODYNAMIC COEFF.
    A1                                           .7335
    A2                                          -.1158
    A3                                           .0534
    A4=.75*(T/C)                                 .1015
    A5=CDO--                                     .0213
    A6                                          3.1575
    A7=1/(PI*SEE*AR)                             .0484
    3-D LIFT SLOPE AT CRUISE MACH     (CLALPH)  5.6610   PER RADIAN
    OSWALD FACTOR                     (SEE)      .8171

CRUISE  CD =  .0301 +   .0484 CL**2
LANDING GEAR CD INCREMENT= .03457
```

Figure 49. Summary Output for Aerodynamics.

The propulsion-system module provides data relative to the size and performance of the engine. The propulsion-system is initially sized to match the cruise drag and a rate of climb requirement at the end of climb. Program options are included that a specified takeoff distance can be met and the climb requirements of FAR Part 25 satisfied. Engine diameter and weight were calculated as a function of engine front-face design-point Mach number, the hub-tip diameter ratio, and the specific weight.

The engine nacelle dimensions were determined from the ratios of engine length to diameter. The length-to-diameter ratio for this study was 2.45. This ratio was established from a survey of existing turbofan installations. The program option to account for nacelle drag in terms of engine net-thrust decrement was selected for the study.

The unscaled generalized-engine-performance-data input to the program was provided in terms of corrected values of net thrust, fuel flow, and airflow. The engine power setting was the ratio of either corrected rotor speed or turbine exhaust to the compressor inlet temperature. Resizing of the engine was completed on the basis of specific thrust and airflow. Inlet total pressure recovery was accounted for directly.

A weight and balance analysis was completed on the airplane after the configuration geometry was defined and the engine size and weight were calculated. Weights for the various airplane subsystems were estimated from trend equations based on the correlation included in Reference 10 adjusted for the general-aviation class of airplane. Available fuel was determined from the empty airplane weight, which was computed by summarizing the subsystem weights, and the input gross weight and payload. An option for specifying tip tanks is included in the program. If tip tanks are required, the synthesis program will automatically recompute the aerodynamics, engine size, and airplane structural weight. Airplane weight and balance summary outputs provided by the synthesis are shown in Figures 50 and 51.

The airplane mission module provides computations of the airplane performance during taxi, takeoff, climb, cruise, and landing. Options are available in this module for calculating engine-out and accelerate/stop distance, best rate of climb, best cruise lift-to-drag ratio, and additional airplane and engine operating characteristics. The effects of gear and flap retraction and ground effect are accounted for during the takeoff segment. In the climb segment, speed is restricted to 463 km/hr (250 knots) equivalent airspeed or less at altitudes below 3048 m (10,000 ft). Fuel reserve inputs are accounted for in the cruise segment. Range is accounted for during the climb and cruise segment. When a specific range definition is required, a program option is utilized that iterates on the airplane gross weight until the calculated range is within a specific tolerance of the required range.

VDIVE = 333. KTS VMO = 283. KTS MMO = .753
ULT. LF = 5.70 MAN. LF = 3.80 GUST LF = 2.61

PROPULSION GROUP			
PRIMARY ENGINES	(WEP)	632.	
PRIMARY ENGINE INSTL.	(WPEI)	209.	
FUEL SYSTEM	(WFSS)	34.	
PROPULSOR WEIGHT	(WPROP)	0.	
TOTAL PROP.GROUP WT.	(WP)	875.	
STRUCTURES GROUP			
WING	(WW)	455.	
HOR. TAIL	(WHT)	83.	
VERT. TAIL	(WVT)	46.	
FUSELAGE	(WB)	646.	
LANDING GEAR	(WLG)	279.	
PRIMARY ENG. SECTION	(WPES)	170.	
TIP TANKS	(WTIP)	85.	
GROUP WEIGHT INC.	(DELWST)	0.	
TOTAL STRUC.GROUP WT.	(WST)	1763.	
FLIGHT CONTROLS GROP			
COCPIT CONTROLS	(WCC)	21.	
FIXED WING CONTROLS	(WCFW)	63.	
SAS	(WSAS)	0.	
GROUP WEIGHT INC.	(DELWFC)	0.	
TOTAL CONTROL WT.	(WFC)	83.	
WT. OF FIXED EQUIPMENT	(WFE)	641.	
WEIGHT EMPTY	(WE)	3363.	
FIXED USEFUL LOAD	(WFUL)	537.	(INC. CREW OF 1)
OPERATING WEIGHT EMPTY	(OWE)	3900.	
PAYLOAD	(WPL)	400.	(PAX= 5.)
FUEL	(WFA)	1931.	(WFW= 794.) (WFTP= 646.)
GROSS WEIGHT	(WG)	6230.	

Figure 50. Summary Output for Weights.

WING LOCATION INFO.

FUSELAGE LENGTH	= 32.13	H-TAIL VOL. ARM	= 16.02
WING 1/4C LOC.ON C.L.	= 13.99	H-TAIL C.G.LOCATION	= 30.21
MAC 1/4C LOCATION	= 13.89	H-TAIL MAC FROM C.L.	= 3.56
MAC DIST.FROM C.L.	= 6.47	H-TAIL LOCAT ON VERT.	= .25
WING C.G.LOCATION	= 14.25	V-TAIL VOL. ARM	= 17.01
TIP TANKS C.G.LOCATE	= 13.99	V-TAIL C.G.LOCATION	= 31.20

AIRCRAFT C.G. LOCATION = 13.81 FT. OR .230 OF MAC

C.G.LOCATION OF PROPULSION= 20.89
C.G.OF REMAINING WEIGHT = 10.60

Figure 51. Summary Output for Airplane Balance.

The economics module calculates airplane first cost and total operating cost for a converged airplane design based on the results obtained from weights, size, engine, mission, etc. First cost is determined by estimating the labor hours, material costs, purchased equipment costs, and the appropriate markups for overhead, tooling sales, and manufacturer's and dealer's profit.

Total operating cost is broken into variable and fixed costs. Variable costs consist of fuel and oil cost, inspection and maintenance cost, and reserve for overhaul cost. Variable costs are calculated in terms of dollars per hour of operation. Fixed cost is independent of annual utilization rate and is computed on an annual basis. This includes storage, insurance, depreciation, crew salary, and taxes.

The variable and fixed costs were combined to determine total operating costs for annual utilization rates from 100 to 800 hours per year. Summaries of the airplane first cost and the total operating cost breakdown as determined in the synthesis are shown in Figures 52 and 53.

```
          *** COST DATA ***
ENGINES       NUMBER =      2.  TYPE=      7

EMPTY WEIGHT=     3363. LBS                  MAX.CRUISE SPEED=    349. KNOTS

CONSUMER PRICE= 306158. DOL.          BASIC PRICE= 306158. DOL.
                                      ADD. EQUIPMENT COST=       0. DOL.

DIRECT LABOR ( 4086.MHRS.)              13893.
LABOR OVERHEAD(140.PCT)                 19513.
AIRFRAME MATERIALS                       4995.
PURCHASED EQUIP.                       115218.
   (ENGINE= 45289.)
   (PROP. =     0.)
   (OTHER = 24640.)

                                       153620.  SUB-TOTAL
ENG.TL.SALES.G-A( 34.PCT)               52180.
                                       205799.  MANUFACTURING COST
FACTORY PROFIT( 14.PCT)                 29707.
                                       235506.  DEALER COST
DEALER-DIST. MARKUP( 30.PCT)            70652.
                                       306158.  BASIC PRICE
```

Figure 52. Summary Output for Basic Airplane Cost.

```
RANGE=     999. N.M.    BLOCK FUEL=    1553. LBS    BLOCK TIME=  2.963 HRS.

FUEL RATE= 78.3 GPH.    TBO= 2000. HRS.    HOURS/INSP.=  100. HRS.

VARIABLE COST     (DOL/HR)          FIXED COST      (DOL/YR)
   FUEL.OIL         37.05             STORAGE        3000.
   INSP.+MAIN.      26.20             INSURANCE      6338. (HULL 2.0PCT)
   OVERHAUL RES.    18.95             DEPRECIATION  30616. ( 8.YR-20.PCT)
   OTHER             0.00             OTHER             0.
                                      CREW              0.(OVERHEAD 50.PCT)
                                      FAA TAX         243.
                    82.20 TOTAL                      40197. TOTAL

UTILIZATION(HRS/YR)          100.     200.     300.     400.     500.     800.
TOTAL OPR.COST(DOL/HR)     484.17   283.19   216.19   182.69   162.60   132.45
```

Figure 53. Summary Output of Total Operating Cost.

PHASE III - EVALUATION OF CANDIDATE TURBOFAN ENGINES THROUGH AIRCRAFT SYNTHESIS AND SENSITIVITY ANALYSES

Updated Aircraft Synthesis Computer Program

A general review of the synthesis program was completed prior to the parametric analyses of the candidate turbofan engines with the base-line airplane. It was concluded during the review that updates to the hourly operating cost portion of the economics module were required to account for inspection and maintenance costs and a reserve for overhaul cost. The updates were considered significant, since these costs can vary widely according to airplane size and complexity, and were not adequately defined for turbofan configurations in the original synthesis program.

Maintenance costs (labor and parts) include upkeep and repair of the airframe, engine, electrical equipment, and other accessories. A generalized inspection and maintenance-cost correlation based on airplane empty weight and total power is described in Reference 8. The correlation was compared to the inspection and maintenance costs of the turbofan powered Cessna Citation provided in the Citation sales brochure. The generated correlation compared very well with these published inspection and maintenance costs; therefore, the generalized correlation provided in the reference was adapted to the synthesis program. The inspection and maintenance cost-per-flight-hour trend correlation used for the parametric study of the candidate engines is shown in Figure 54.

Periodically, some of the major equipment or parts of an airplane will require replacement or overhaul. A reserve for overhaul cost must consequently be considered in determining the operating cost of an airplane. Since this cost will vary widely with airplane size, the generalized correlation discussed in Reference 8 was developed to include overhaul reserve funds as a function of total engine thrust. A test case conducted with the JT15D Engine used on the Citation indicated that the referenced correlation cost was $37 per hour compared to $23 per hour as listed in the Citation sales brochure. As a consequence, the revised correlation was inserted in the synthesis model. The revised correlation is shown in Figure 55.

Initial results obtained with the synthesis program indicated that airplane aerodynamic quality was a significant factor affecting airplane size and resultant cost for the specified mission. It was found that the design parameter that affected the aerodynamic quality most significantly was wing loading. For maximum cruise lift-drag ratio, wing loading must be such that the induced drag (drag due to lift) is equal to total parasitic drag. If cruise speed is low and cruise altitude high, wing loading will be low. If cruise speed is high at low to medium altitude, then the smallest possible airplane will have a high wing loading.

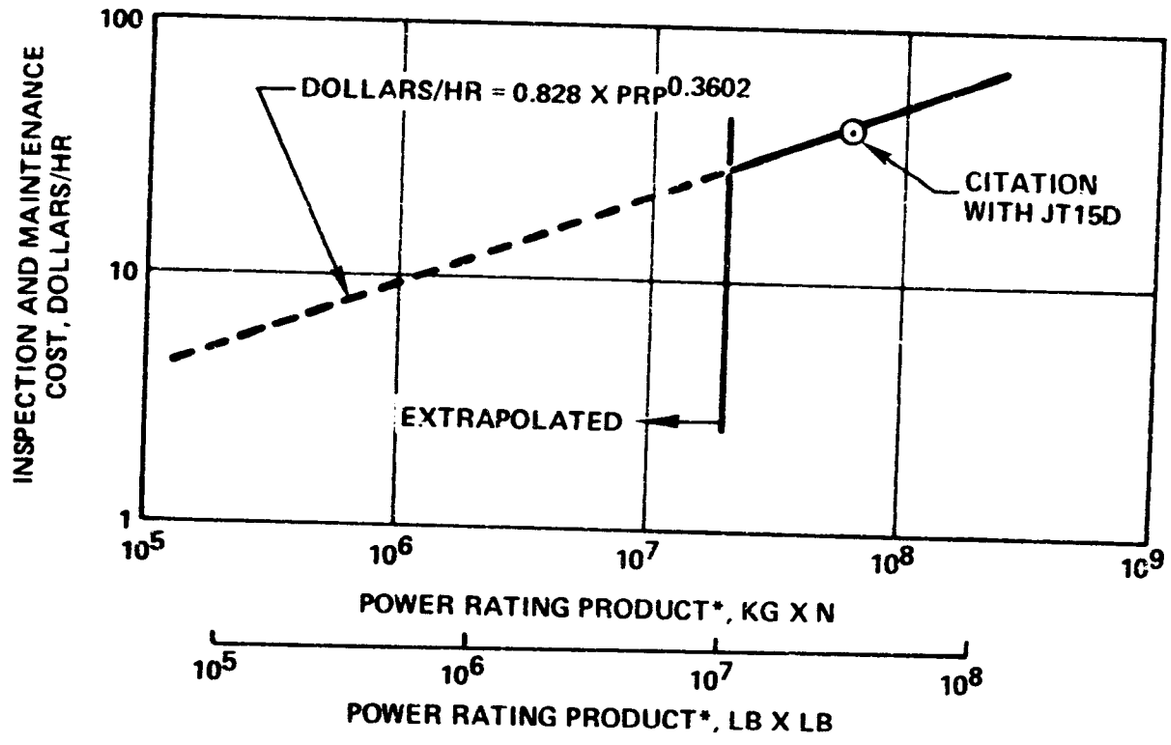

Figure 54. Inspection and Maintenance Cost per Flight-Hour Trend (Ref. NASA CR-114339).

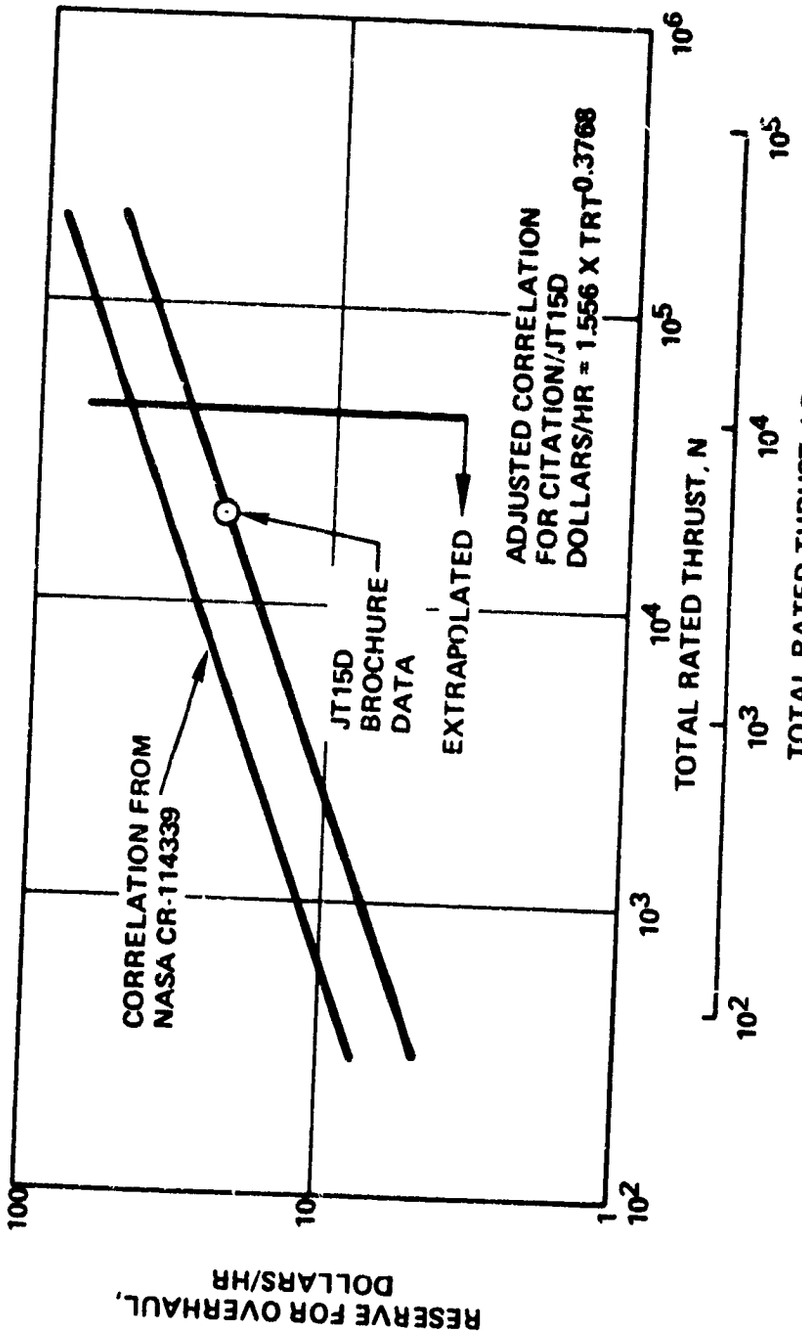

Figure 55. Reserve for Overhaul Cost Trend per Hour.

Wing loading studies were undertaken in order to determine a best baseline airplane wing loading for the parametric analyses of the candidate engines. Wing loadings between 156 and 342 kg/m^2 (32 and 70 lb per sq ft) were investigated. Other variables such as the mission payload and range, airplane configuration, and the engine performance were held constant. Figures 56 and 57 show the results of this study for the airplane first cost and total operating cost. As shown in Figure 56, the airplane first cost was reduced approximately 40 percent as the wing loading increased from 156 to 303 kg/m^2 (32 to 62 lb per sq ft). Similarly, as shown in Figure 57, the total operating cost was reduced approximately 32 percent as the wing loading was increased from 156 to 303 kg/m^2 (32 to 62 lb per sq ft). This is attributed to the reduced drag, lower airplane gross weight and the smaller engines permitted by the increased wing loading, as shown in Figures 58 and 59. Aside from the aerodynamic and economic advantages of the higher wing loading and the reduced wing weight, there is a definite advantage in the gust-load factor and passenger comfort.

A parameter used to evaluate cruise ride quality is the inverse function of wing gust response. This parameter increases with wing loading and decreases with aspect ratio. With the wing aspect ratio of the reference airplane, an improvement in cruise ride quality of approximately 40 percent can be obtained by increasing the wing loading from 156 to 303 kg/m^2 (from 32 to 62 lb per sq ft). This was confirmed with the use of data provided in Reference 11.

On the basis of the economic advantages shown in the wing loading study, a survey of existing light twin airplanes was completed to establish a reasonable stall speed for the reference airplane. The gross weights and stall speeds are listed in Table XI. This data was obtained from Reference 2. The results of this survey showed that a stall speed of approximately 145 km/hr (90 miles per hour) was average for an airplane of the type under consideration for this study.

Once the desired stall speed had been selected and the wing loading determined, a trailing-edge flap analysis was conducted to establish the maximum lift coefficient. Three flap configurations were selected and their maximum lift coefficients were calculated for stall speeds ranging from 129 to 161 km/hr (80 to 100 miles per hour). The results of this study are illustrated in Figure 60. By selecting a stall speed of 146 km/hr (91 miles per hour) and a flap similar to that described in Reference 11 (full-span, single-action Fowler), a wing loading of 303 kg/m^2 (62 lb per sq ft) was established for the baseline airplane. After selecting the flap configuration it was concluded that the airplane design options that would tend to minimize the size and cost had been reasonably exercised, establishing the reference airplane model for conducting the investigation of cost interrelationships with the candidate engines.

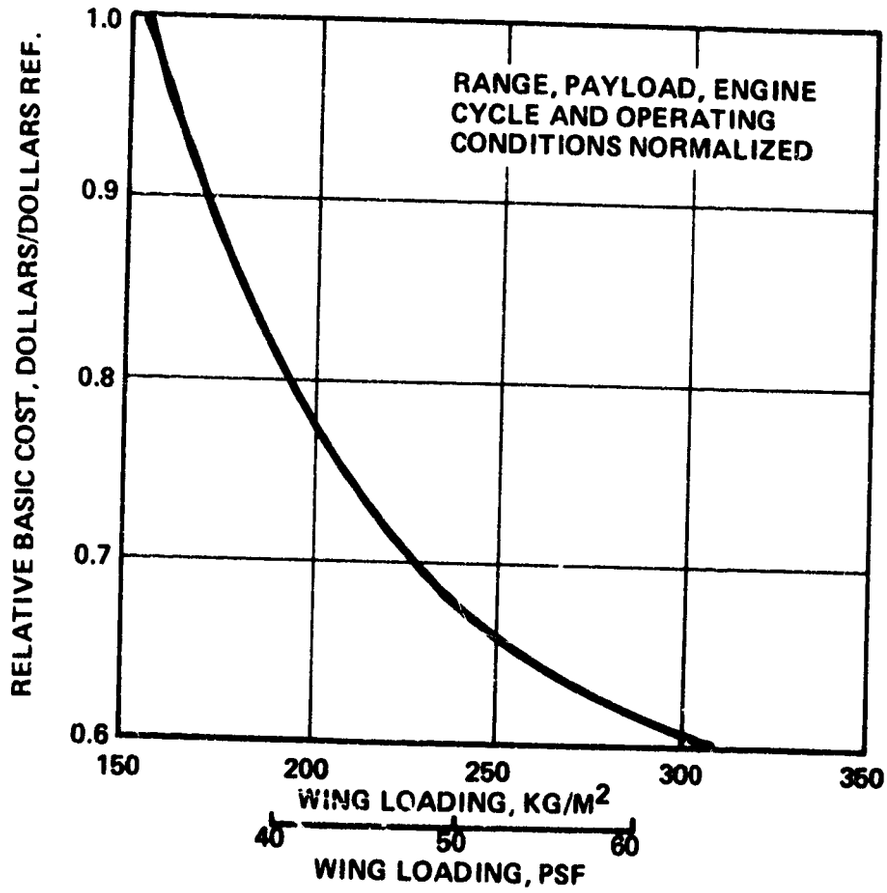

Figure 56. Effect of Wing Loading on Basic Airplane Cost.

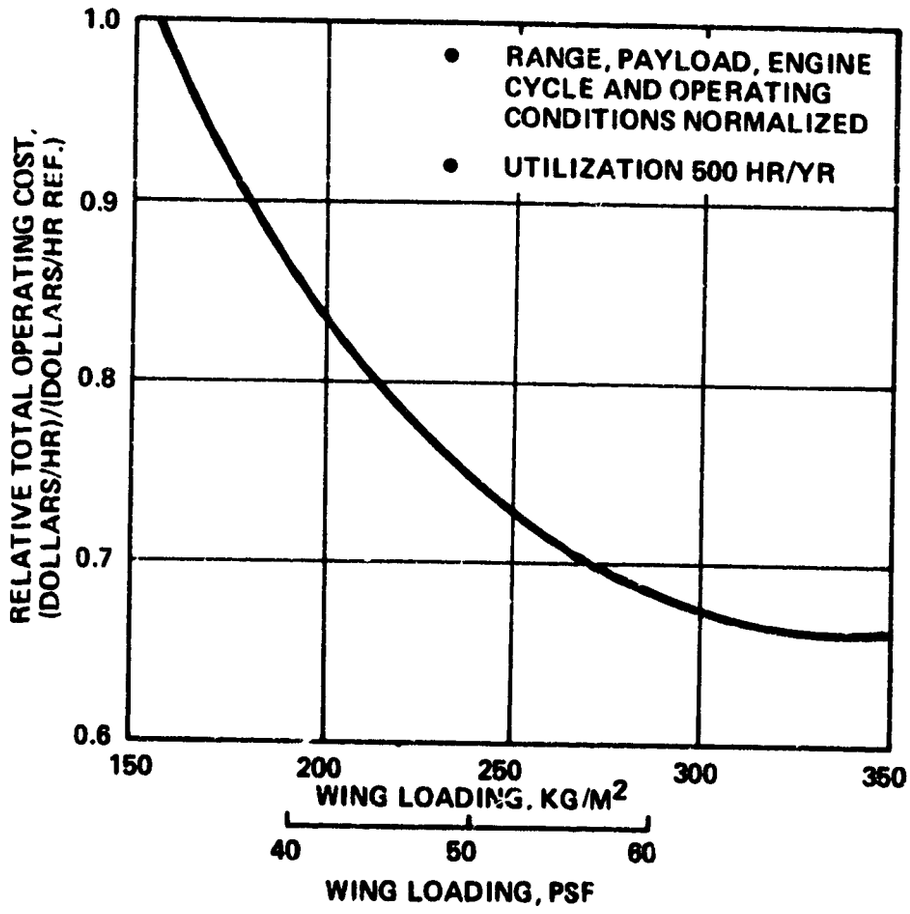

Figure 57. Effect of Wing Loading on Total Operating Cost.

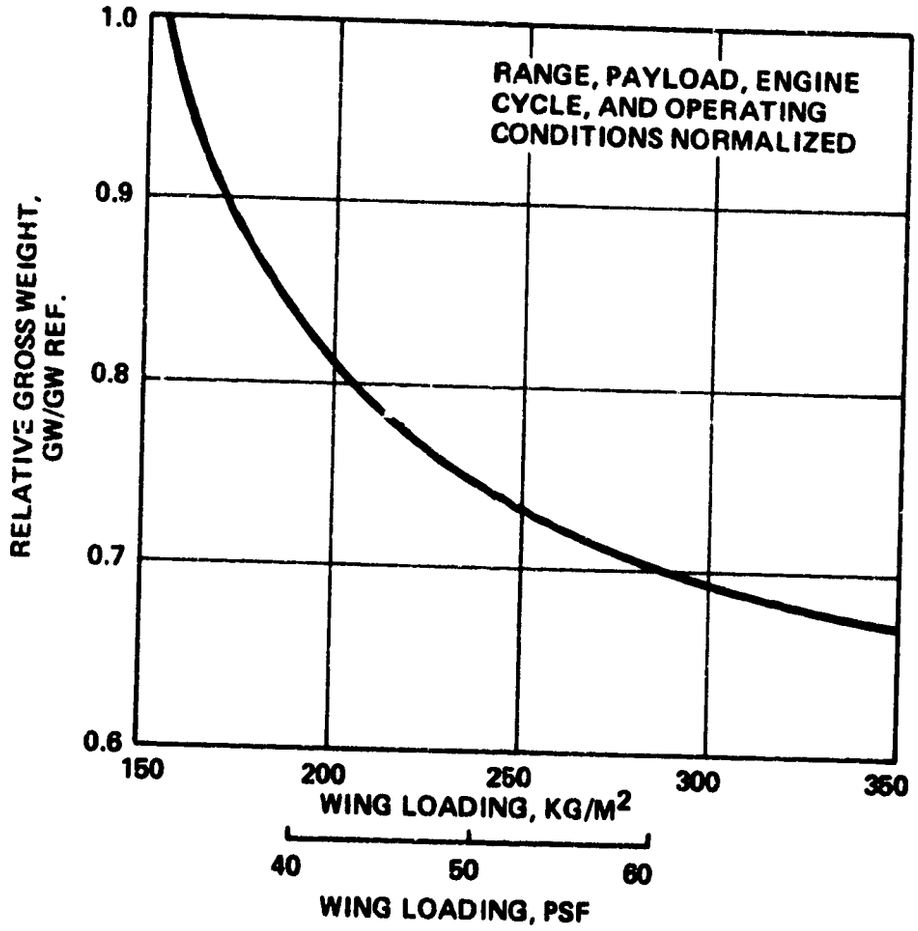

Figure 58. Effect of Wing Loading on Airplane Gross Weight.

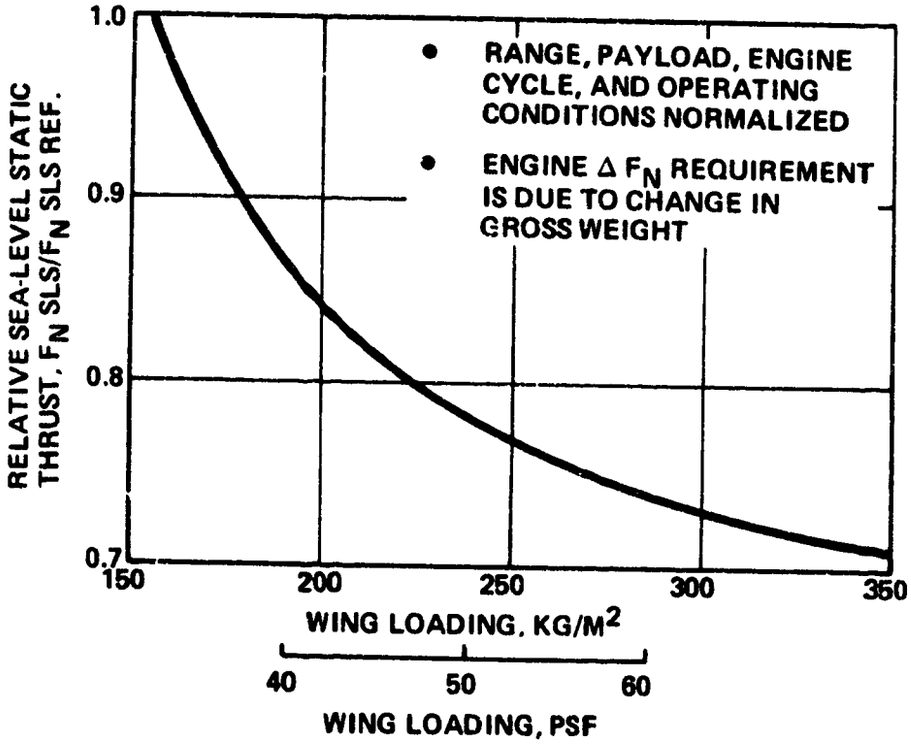

Figure 59. Effect of Wing Loading on Sea-Level Static Thrust.

TABLE XI. SUMMARY OF EXISTING AIRPLANE STALL SPEEDS

TYPE	MODEL	GROSS WEIGHT (KG)	GROSS WEIGHT (LB)	V_{STALL} (KM/HR)	V_{STALL} (MPH)
Cessna	Citation	4921	10,850	156	97
Cessna	340	2710	5,975	132	82
Cessna	421B	3379	7,450	138	86
Beechcraft	E90	9117	20,100	143	89
Beechcraft	A100	5216	11,500	138	86
Beechcraft	A60	3073	6,775	140	87
Piper	Nav. Chieftan	3175	7,000	137	85
Piper	Nav. B	2948	6,500	117	73
Mitsubishi	MU-2J	4899	10,800	135	84
Mitsubishi	MU-2K	4500	9,920	132	82
Swearingen	Merlin III	5670	12,500	154	96
Swearingen	Merlin IV	5670	12,500	159	99
North American Rockwell	685	4105	9,050	138	86
North American Rockwell	690	4672	10,300	143	89
North American Rockwell	Sabre 60	9072	20,000	156	97
Gates Learjet	25C	6804	15,000	193	120
Gates Learjet	24D	6123	13,500	159	99

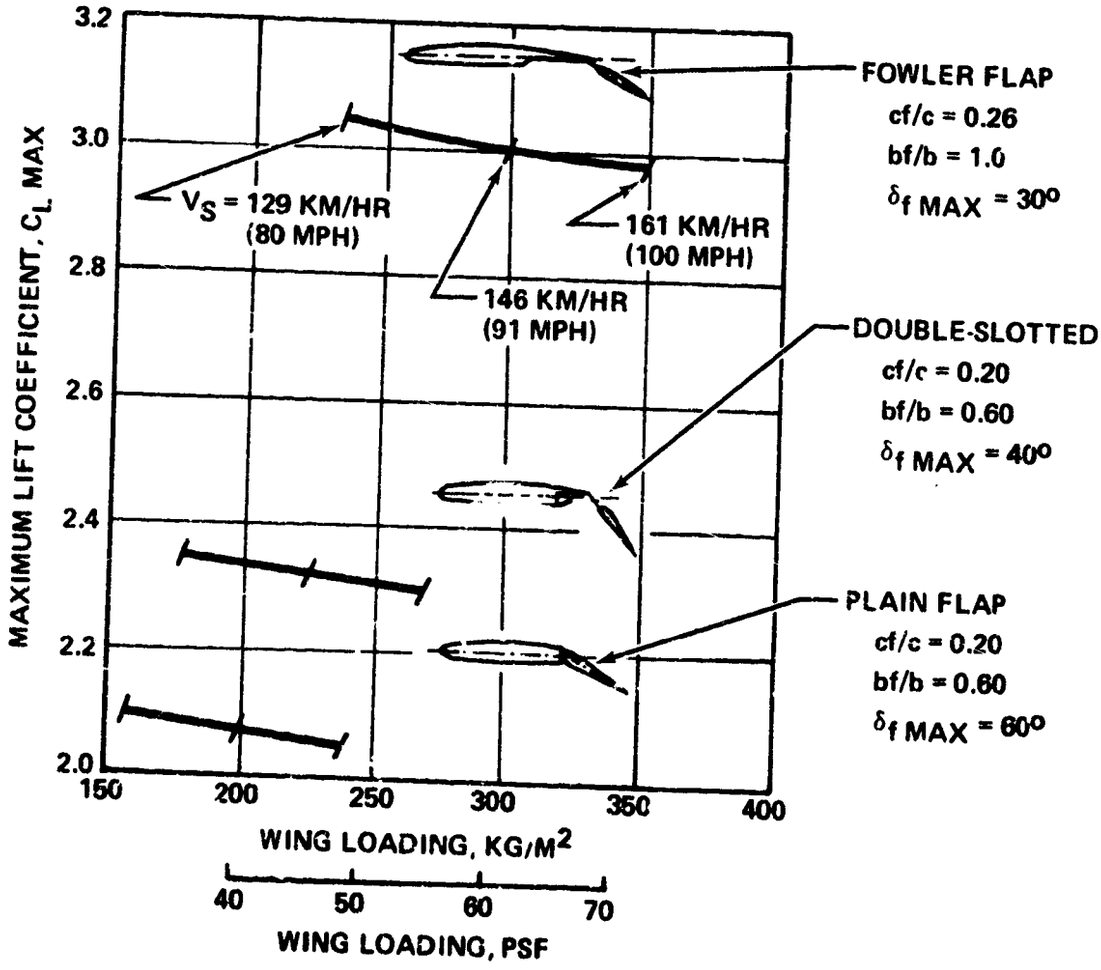

Figure 60. Maximum Lift Coefficient Versus Wing Loading Estimated from Synthesis Program.

In order to maintain consistency in the parametric engine analyses, a common mission and engine sizing procedure was established as follows:

- Base-line mission
  - Cruise altitude = 7315 m (24,000 ft)
  - Cruise velocity = 648 km/hr (350 knots)
  - Design payload = 181 kg (400 lb)
  - Fixed useful load = 244 kg (537 lb)
  - Range = 1000 n. mi.
  - Reserve = 45 minutes

- Engine sizing requirements
  - Start of cruise thrust
  - One-engine-out rate of climb

The design payload exludes the pilot and his baggage. This weight is included in the fixed useful load.

Engine Cost Analyses and Price Estimates

Basic engine price.- Production cost analyses of the candidate engines were done in a manner that would ensure credible comparative prices for the candidate engines. The engine basic layouts were the basis for estimating and summing the production cost of all engine parts and assemblies. The analyses were made on the basis of a production rate of 1000 engines per year and the additional assumption that the candidate engine would be produced concurrently with other engines in an established facility.

Several factors make the prediction of engine production cost difficult. Important examples of these are:

(a) Production rate is a fundamental driver of cost; and if the production rate prediction is substantially wrong, the same will be true of cost. Similarly, the cost of a new engine will be affected by a varying production rate of other engines produced concurrently in the same facility.

(b) Initial cost estimates are prepared from conceptual engine layouts that can be expected to change in ensuing detail design and development phases. The accuracy of initial cost estimates depends upon the quality of the conceptual designs and upon the extent to which the conceptual designs are adhered to in later phases.

(c) The cost of materials and special manufacturing processes can be expected to change at much greater rates than the general economic trends that affect the engine manufacturer's labor costs.

Despite these prediction difficulties, the candidate engine production cost analyses were not hedged in anticipation of cost-altering possibilities. A consistent and reasonable set of costing ground rules were established which would ensure that the comparative prices for the five candidate engines were accurate. The most important ground rule was that the engines were analyzed as drawn.

In order to accomplish the overall purpose of this study--that is, to establish performance, weight, size, and cost interrelationships between the engine and the airplane--not only must the relative price of the candidate engine be accurate, but also the actual prices must be fairly and accurately predicted if the engine/airplane interrelationships are to be correct and meaningful.

In the conceptual phase of a new engine program, the prediction of O.E.M. (original equipment manufacturer) sales price is hazardous, as well as difficult. Since large sums of money can be committed on the basis of preliminary engine price predictions, the

consequences of substantial error in the predictions greatly distress the engine manufacturer and his airplane-producing customers.

Factors affecting commercial engine pricing are many and complex. Considerations such as government sponsorship of engine development for a military application and concurrent production of the military version can substantially affect the commercial engine price. The manufacturer's general pricing policies, the effects of competition, and the status of the airplane market are, of course, fundamental operators on the price of engines. These factors can effect a large variance in the engine price. For this study, a reasonable set of pricing ground rules were established, which reflect the considerations listed above, but which do not necessarily represent a future pricing posture that would be taken by AiResearch with respect to future products like the candidate engines of this study. The first ground rule was that a candidate engine would be a commercial development, with no government sponsorship. Second, the cost of engineering, development, and production tooling would be amortized over a 5-year production run. Third, the total markup, including warranty cost, after-sale service, general and administrative expenses, and profit would total 54 percent of the engine production cost. The prices and the specific prices (dollars per pound of thrust) given for the candidate engines in Table XII are based on the preceding considerations. While the prices are individually subject to further examination, the comparative prices of the engines are sufficiently credible that the most cost-effective candidate engine can be identified in airplane synthesis and sensitivity analysis.

TABLE XII. CANDIDATE ENGINE PRICE ESTIMATES.

	Engine				
	IA	IC	IIA	IIC	IIC/9BPR
O.E.M. Price (Dollars)	45,007	46,646	47,756	47,521	53,185
Specific Price (Dollars per pound of thrust)	34.65	35.80	34.83	37.42	35.18

Price increment for acoustic attenuation treatment.- Results of the acoustic analyses of the five candidate engines showed that the engines could not meet the 85 PNdB noise-limit criteria of the study. Additional analysis showed that the 95-PNdB goal could be met by suppressing rearward-propagated fan noise with suitable

acoustic treatment of the fan bypass duct. The required treatment was defined for each candidate engine, and a cost estimate was made for incorporation of the treatment into each engine design. The resulting O.E.M. price increase increment for each candidate engine is given in Table XIII.

TABLE XIII. PRICE INCREASE INCREMENT FOR ENGINE ACOUSTIC TREATMENT.

Engine	IA	IC	IIA	IIC	IIC/9BPR
Price increase increment ($)	770	1540	1078	924	2772

Synthesis Evaluation of Candidate Engines

Following the definition of the reference airplane and mission, a parametric synthesis analysis was conducted with the five candidate turbofan engines. The same basic geometrical, weight, and aerodynamic characteristics of the airplane were held constant while the airplane synthesis design was completed with each of the five candidate engines. The engine parameters which varied were those associated with specific engine characteristics such as weight, thrust, fuel flow, airflow, front-face Mach number, hub-to-tip-diameter ratio, and engine specific cost (sale price to thrust ratio). The reference airplane was appropriately resized with each engine to provide the specified mission requirements in terms of range, fuel reserves, etc.

The initial airplane synthesis was completed for each candidate engine, with engine specific prices varying from $4.50 to $9.00 per N ($20 to $40 per lb) of sea-level static thrust. The effects of engine specific price, for each engine, on airplane purchase price and on total operating cost, are presented in Figure 61 and Figure 62. As indicated in Figure 61, the effect of engine specific cost on the basic airplane price is approximately 1.7 percent per specific dollar engine sale price for the four BPR-5 engines and 2.0 percent per specific dollar for the BPR-9 engine. Of the five candidate engines evaluated on a constant specific engine price basis, the No. IA (axial) engine resulted in the lowest airplane price. The price of the airplane with the BPR-9 engine was significantly greater than the airplanes equipped with the lower BPR engines. Similarly, in Figure 62, the total operating cost of the airplane with Engine IIA is least, and with Engine IIC/9BPR, the total operating cost is highest by a wide margin.

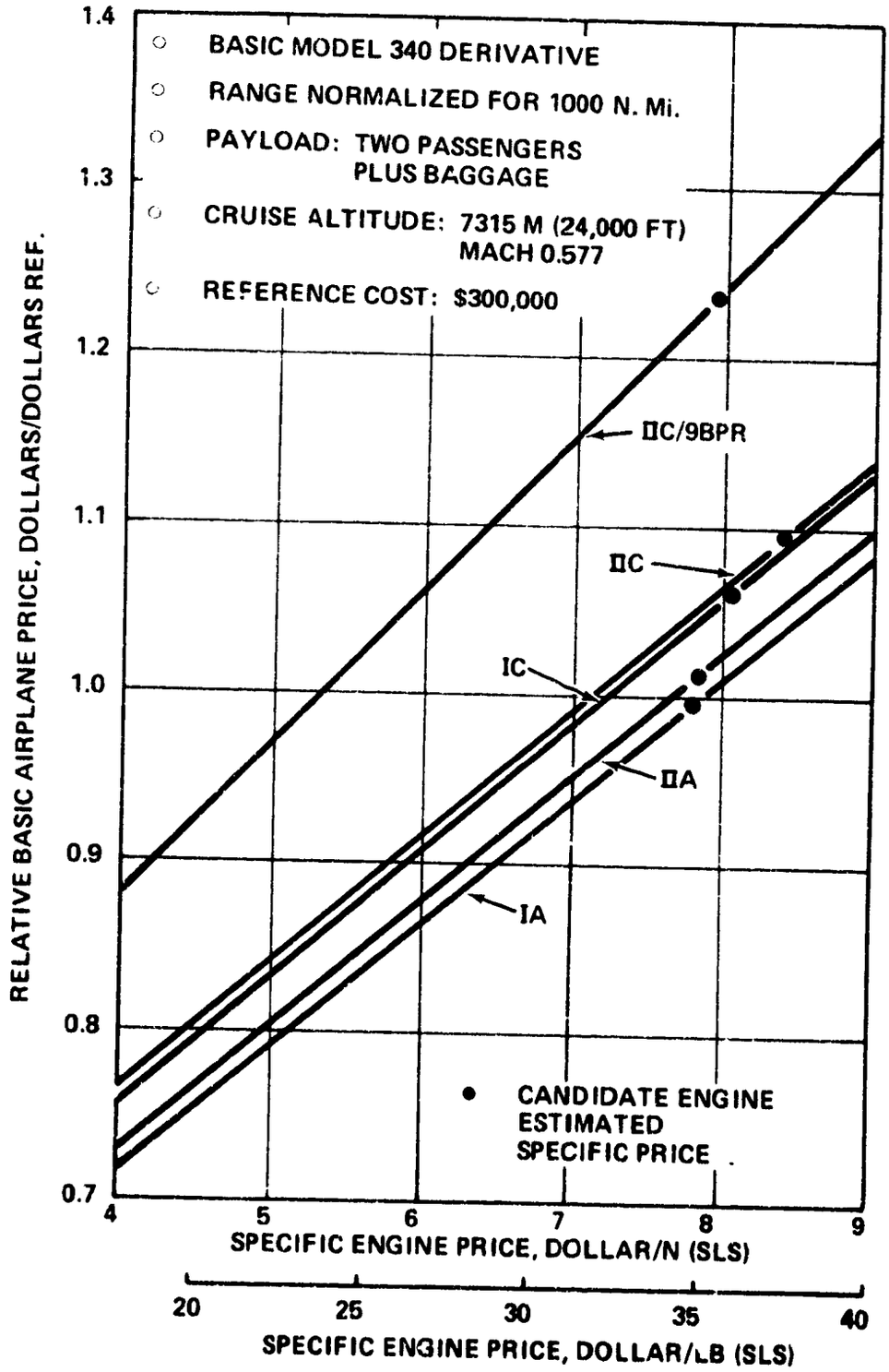

Figure 61. Effect of Engine Price on Basic Airplane Price.

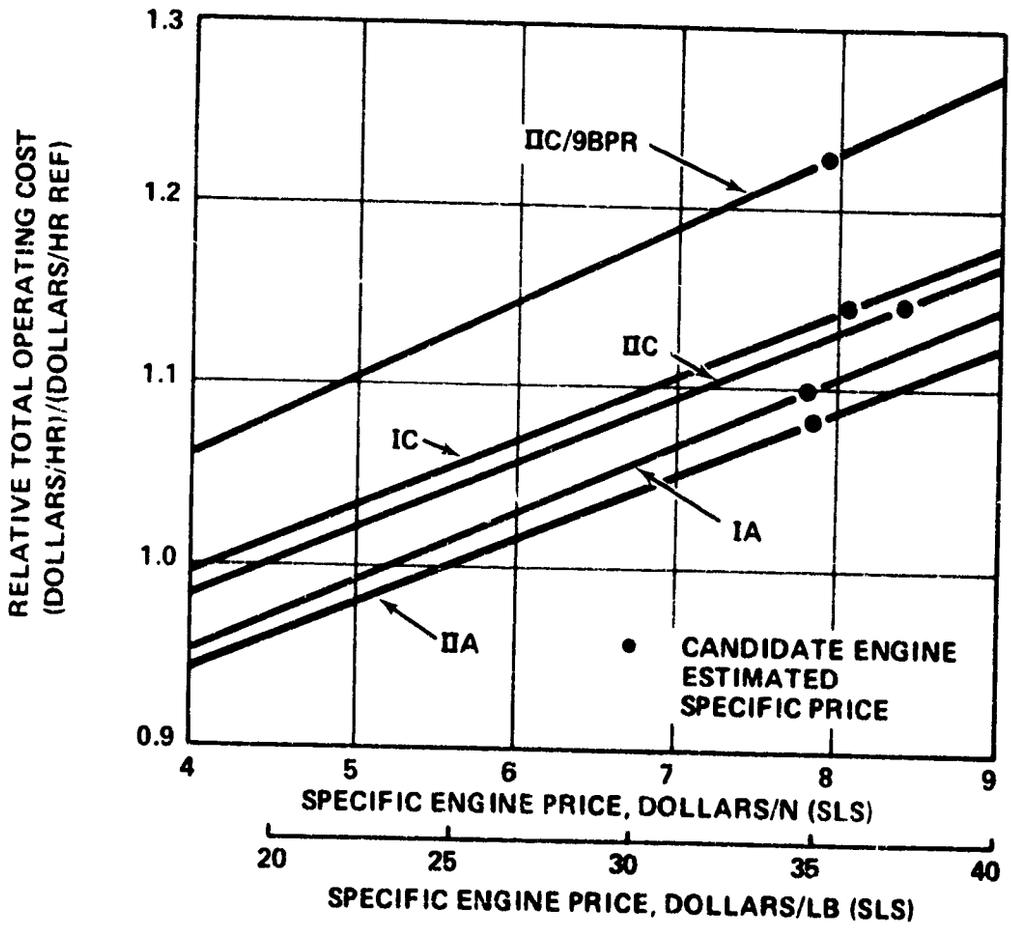

- BASIC MODEL 340 DERIVATIVE
- RANGE NORMALIZED FOR 1000 NM
- PAYLOAD: TWO PASSENGERS PLUS BAGGAGE
- CRUISE ALTITUDE: 7315 M (24,000 FT)
  MACH 0.577
- DOLLARS/HR REFERENCE: $150.00
- UTILIZATION RATE: 500 HR/YEAR

Figure 62. Effect of Engine Price on Total Operating Cost for Utilization of 500 Hours per Year.

In addition to the effects of engine specific price, the effects of the varying candidate engine performance qualities can be determined from Figures 61 and 62. By comparing the results, at any constant specific price, the combined effects of engine weight, specific fuel consumption, and nacelle drag are apparent. It is notable that Engine IA, with the highest thrust-to-weight ratio, resulted in the lowest price airplane.

Estimated specific engine prices for the five engines, as shown in Figures 61 and 62, range between approximately $7.75 and $8.40 per N ($34.50 and $37.50 per lb) of sea-level static thrust. Tradeoffs in terms of specific engine price versus airplane price can be examined. For example, in order for the price of the airplane with Engine IIC/9BPR to equal that of the IIA-engined airplane, a reduction in engine specific price of $2.60 per N ($11.70 per lb) of sea-level static thrust would be required. This would require a net reduction of approximately 30 percent of the estimated price of that engine.

The effect of engine TSFC on total operating cost is illustrated in Figure 62. Engines IIA and IIC are slightly heavier, but have lower TSFC than Engines IA and IC, respectively. Although they result in heavier, higher-priced airplanes, the TSFC advantage of Engines IIA and IIC results in their providing lower airplane total operating cost. This effect of TSFC advantage clearly does not extend to Engine IIC/9BPR. This engine has marginally the best uninstalled TSFC, but an offsetting higher nacelle drag, and is substantially heavier.

Engine specific price versus total operating cost tradeoffs can be examined. For example, at the reference operating cost of $150 per hour, a difference in total operating costs between Engines IIA and IA of approximately $2 per hour is shown. Consequently, for the 500-hour-per-year utilization rate on which the estimate was based, a cost difference of $1500 per year will result between the IIA- and IA-engined airplanes. This can be compared to the basic price difference of approximately $4500 between these two airplanes. In order to reduce the specific price of Engine IA to obtain the same relative airplane operating cost as with Engine IIA, a reduction of $0.45 per N ($2 per lb) of thrust would be required. Similarly, the reduction in Engine IIA specific price required to provide an airplane price equal to that with Engine IA would be approximately $0.22 per N ($1 per lb) of thrust.

Based on the evaluations of the economics of the two most cost-effective candidate engine/airplane systems, Engine IIA is shown to be the most cost-effective. A summary of the airplane characteristics obtained with each of the candidate engines is presented in Table XIV. As shown in Table XIV, the airplane gross weights range from 2826 kg to 3131 kg (6230 lb to 6903 lb) with

TABLE XIV(SI)*. SUMMARY OF AIRPLANE CHARACTERISTICS WITH EACH CANDIDATE ENGINE

Airplane Parameter	Candidate Engines				
	IA	IC	IIA	IIC	IIC/9BPR
Gross weight (kg)	2961	3044	2826	3039	3131
Empty weight (kg)	1531	1604	1525	1640	1768
Structure group weight (kg)	819	840	800	842	895
Propulsion group weight (kg)	382	433	397	466	540
Wing area (sq m)	9.78	10.05	9.34	10.04	10.34
Block fuel (kg)	1005	1015	876	974	938
Payload (kg)	181	181	181	181	181
Range (n. mi.)	1000	1000	1000	1000	1000
Takeoff over 15-m obstacle (m)	827	828	779	835	771
Landing over 15-m obstacle (m)	661	661	661	661	661
Average rate of climb (m/min)	346	343	353	341	393
Net thrust of cruise (N)	3029	3078	2971	3083	3154

*Systeme International

TABLE XIV(CU)*. SUMMARY OF AIRPLANE CHARACTERISTICS WITH EACH CANDIDATE ENGINE

Airplane Parameter	Candidate Engines				
	IA	IC	IIA	IIC	IIC/9BPR
Gross weight, (lb)	6527	6711	6230	6700	6903
Empty weight (lb)	3375	3536	3363	3615	3897
Structure group weight (lb)	1205	1851	1763	1857	1974
Propulsion group weight (lb)	843	954	875	1028	1190
wing area (sq ft)	105.3	108.2	100.5	108.1	111.3
Block fuel (lb)	2215	2238	1931	2148	2069
Payload (lb)	400	400	400	400	400
Range (n. mi.)	1000	1000	1000	1000	1000
Takeoff over 50-ft obstacle (ft)	2715	2718	2556	2741	2528
Landing over 50-ft obstacle (ft)	2170	2170	2170	2170	2170
Average rate of climb (ft/min)	1134	1126	1159	1120	1290
Net thrust at cruise (lb)	681	692	668	693	709

*Customary Units.

Engines IIA and IIC/9BPR. All engines provided more than adequate performance in terms of thrust to meet the 914-m (3000-ft) takeoff and landing distance criteria. The average rate of climb from sea level to 7315 m (24,000 ft) for Engines IIA and IIC/9BPR were 353 and 393 m per minute (1159 and 1290 ft per minute), respectively. This is an indication of the only discernable performance advantage inherent in the higher bypass ratio engine.

Engine IIA provided the best rate of climb and general performance characteristics were the best of the four BPR-5 candidate engines. The FAR Part 25 climb requirements for each of the engines are summarized in Table XV. As indiciated, all engines exceeded the climb requirements.

Total operating costs versus the utilization rate for each of the candidate engines are shown in Figures 63 through 67. Examination of these figures shows that Engine IIA provides the lowest total operating cost for utilization rates greater than 200 hours per year. However, as the utilization rate decreases below 200 hours per year, the difference in total operating costs between Engines IIA and IA becomes insignificant.

In order to establish the two-engine service ceiling and rate-of-climb characteristics, a rate of climb at maximum allowable speed [463 km/hr to 3048 m (250 knots to 10,000 ft)] and best rate-of-climb analysis was conducted for the IA- and IIA-engined airplanes. The results of this analysis are shown in Figure 68. As indicated, the two-engine service ceiling for both engine/airplane systems is approximately 10.97 km (36,000 ft), confirming that both engines have sufficient margin for climb requirements. A rate-of-climb schedule at maximum allowable speed was used for the synthesis analyses done in airplane sizing. The best rate-of-climb schedule was derived during these rate-of-climb studies. Both climb schedules are viable flight plan options: the first for minimizing block time on a short flight; the second for maximizing range. As shown in Figure 68, the climb characteristics of Engine IIA are superior to those of Engine IA in all cases.

A payload-versus-range analysis for the IIA-engined airplane is provided in Figure 69. Range at the specified engine/airplane sizing condition is 1000 nautical miles. The maximum zero payload range provided by this airplane is 1035 nautical miles. Available mission fuel was the same at this condition as at the sizing condition; however, the gross weight of the airplane was 181 kg (400 lb) less. As fuel was off-loaded to accommodate the maximum payload of 454 kg (1000 lb) (five passengers and baggage) the range decreased to 565 nautical miles.

On the basis of airplane cost effectiveness and performance, Engine IIA emerged as the best of the five candidate engines evaluated during the study. However, it should be noted that both

TABLE XV. SUMMARY OF FAA PART 25 CLIMB REQUIREMENTS FOR CANDIDATE ENGINES SIZED FOR BASIC MISSION.

Condition	Rate of Climb					
	Reqd.	IA	IC	IIA	IIC	IIC/9BPR
Takeoff flaps, (m/min) one engine out, (ft/min) gear down	0 0	282.2 925.9	283.2 929.1	324.4 1064.4	275.9 905.1	330.8 1058.2
Takeoff flaps, (m/min) one engine out (ft/min)	94.9 311.4	385.1 1263.4	386.8 1268.9	434.2 1424.6	378.2 1240.7	435.9 1430.1
Cruise flaps, (m/min) one engine out (ft/min)	47.5 155.7	247.9 813.4	248.0 813.5	293.6 963.1	241.6 792.8	296.5 972.8
Landing flaps, (m/min) one engine out (ft/min)	75.8 248.8	178.4 585.4	180.3 591.5	224.8 737.4	171.9 564.0	229.8 753.8
Landing flaps, (m/min) all engines (ft/min)	100.2 328.6	250.7 822.4	251.6 825.6	292.9 961.1	244.3 801.5	299.3 981.9

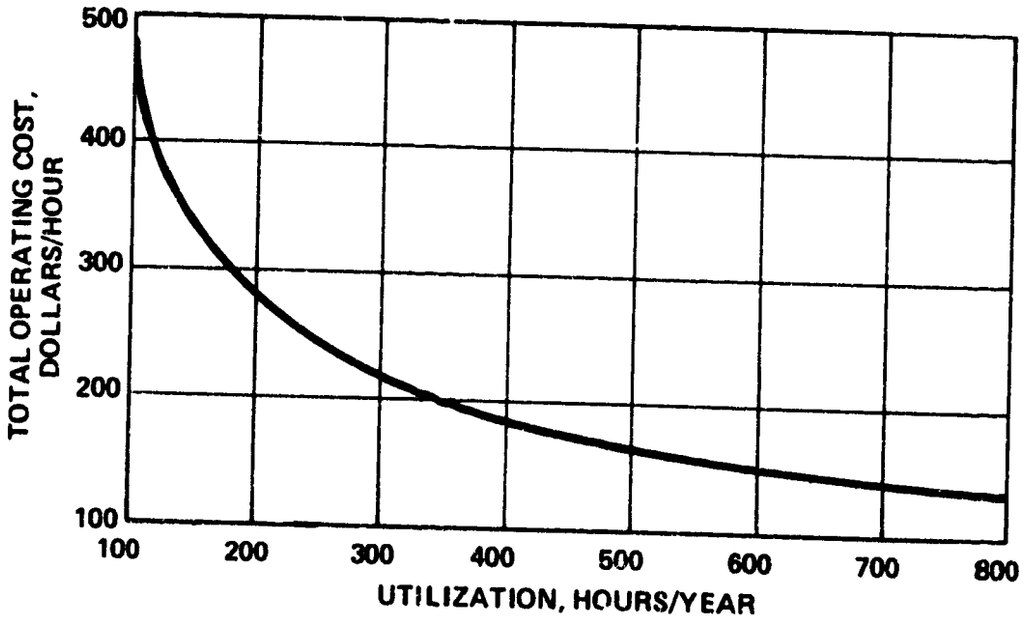

- BASIC MODEL 340 DERIVATIVE
- RANGE NORMALIZED FOR 1000 N. Mi.
- PAYLOAD: TWO PASSENGERS PLUS BAGGAGE
- CRUISE ALTITUDE: 7315 M (24,000 FT)
  MACH 0.577
- GROSS WEIGHT: 2961 KG (6527 LB)
- ENGINE COST/N (SLS) $7.79, [LB F_N (SLS) $34.65]

Figure 63. Total Airplane Operating Cost Versus Utilization Rate, Engine IA.

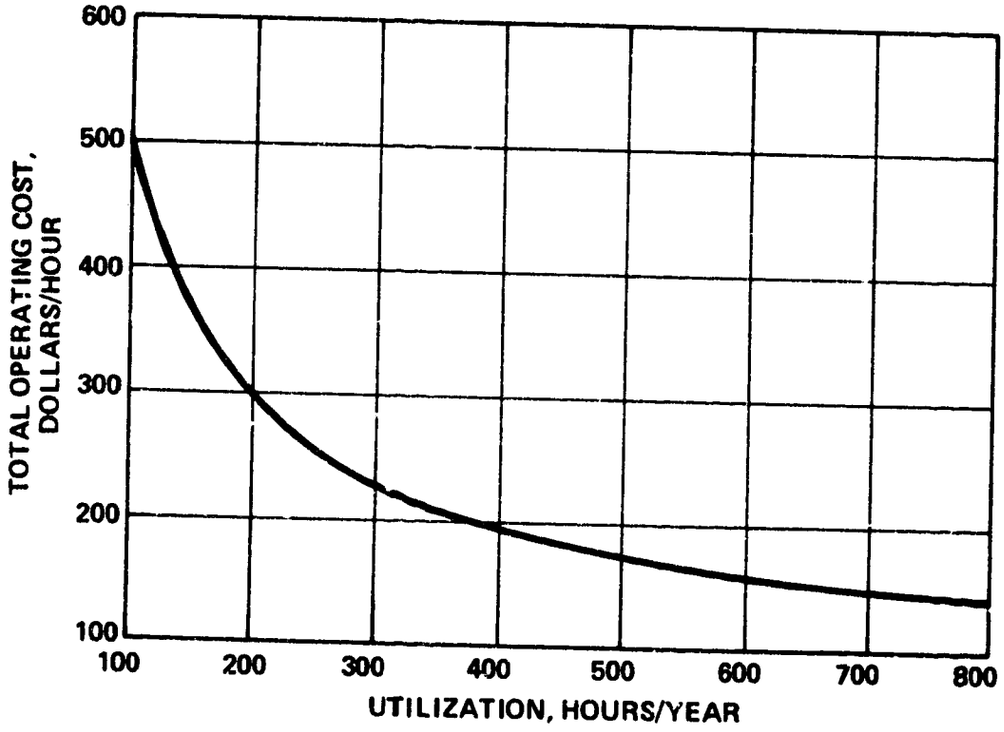

- BASIC MODEL 340 DERIVATIVE
- RANGE NORMALIZED FOR 1000 N. Mi.
- PAYLOAD: TWO PASSENGERS PLUS BAGGAGE
- CRUISE ALTITUDE: 7315 M (24,000 FT)
  MACH 0.577
- GROSS WEIGHT: 3044 KG (6711 LB)
- ENGINE COST/N (SLS) $8.05, [LB F_N (SLS) $35.80]

Figure 64. Total Airplane Operating Cost Versus Utilization Rate, Engine IC.

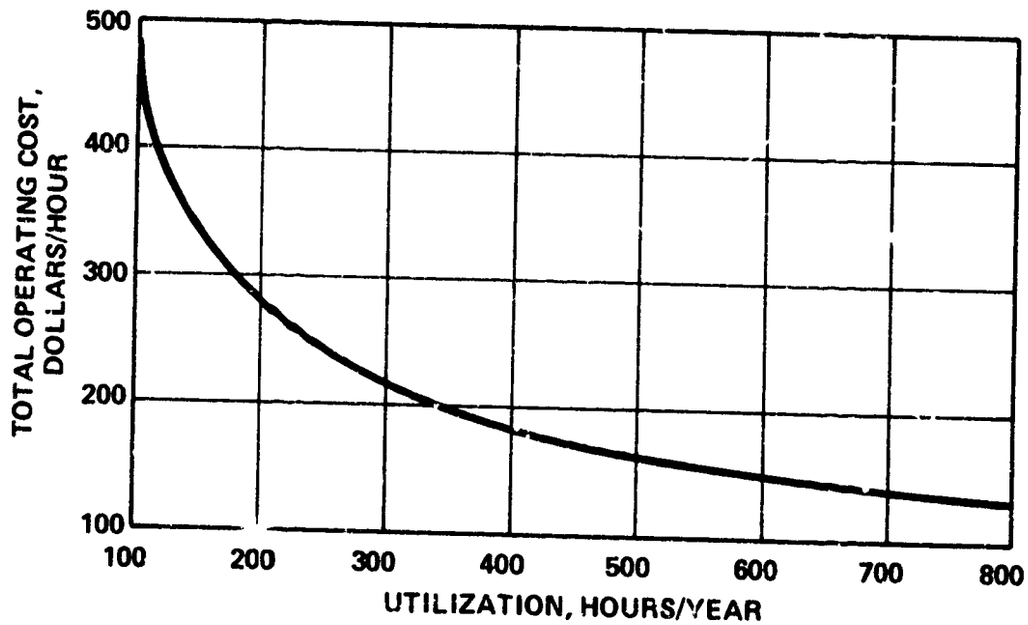

- BASIC MODEL 340 DERIVATIVE
- RANGE NORMALIZED FOR 1000 N. Mi.
- PAYLOAD: TWO PASSENGERS PLUS BAGGAGE
- CRUISE ALTITUDE: 7315 M (24,000 FT)
  MACH 0.577
- GROSS WEIGHT: 2826 KG (6230 LB)
- ENGINE COST/N (SLS) $7.83, [LB F_N (SLS) $34.83]

Figure 63. Total Airplane Operating Cost Versus Utilization Rate, Engine IIA.

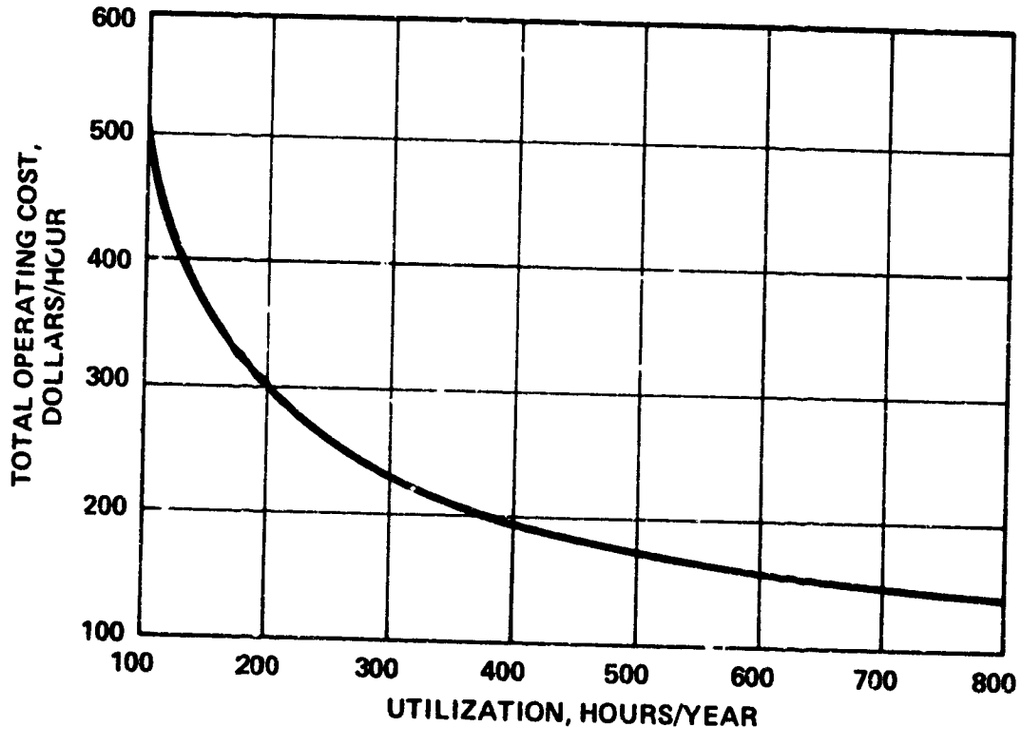

- BASIC MODEL 340 DERIVATIVE
- RANGE NORMALIZED FOR 1000 N. Mi.
- PAYLOAD: TWO PASSENGERS PLUS BAGGAGE
- CRUISE ALTITUDE: 7315 M (24,000 FT)
  MACH 0.577
- GROSS WEIGHT: 3039 KG (6700 LB)
- ENGINE COST/N (SLS) $8.41, [LB F_N (SLS) $36.42]

Figure 66. Total Airplane Operating Cost Versus Utilization Rate, Engine IIC.

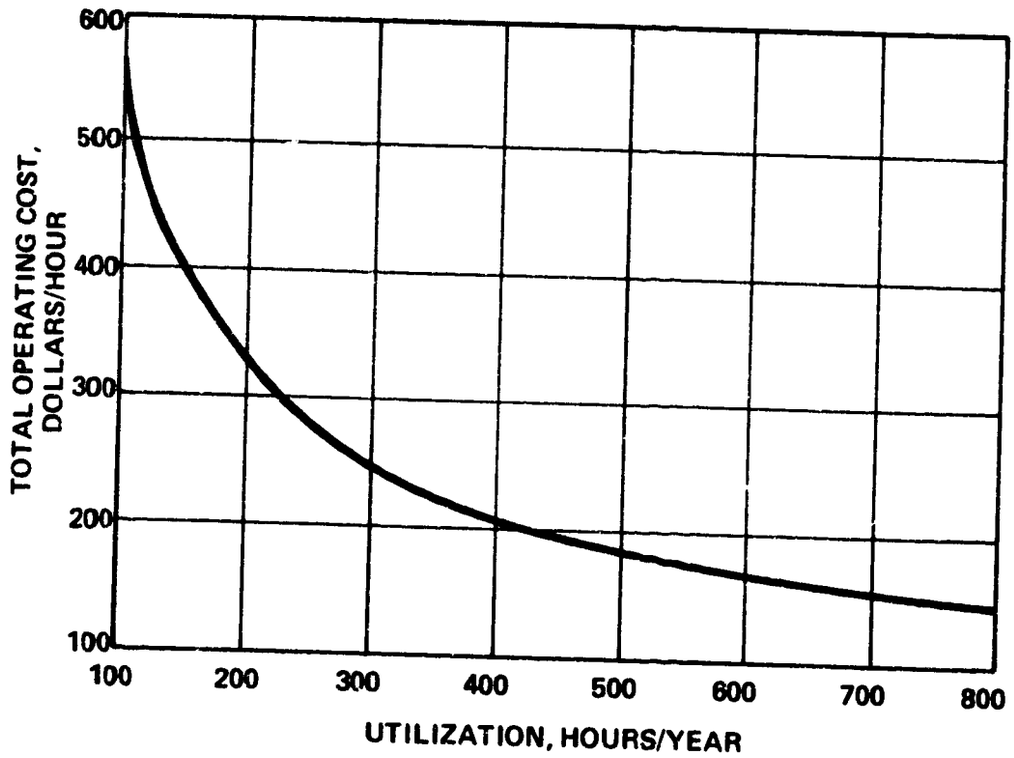

- BASIC MODEL 340 DERIVATIVE
- RANGE NORMALIZED FOR 1000 N. MI.
- PAYLOAD: TWO PASSENGERS PLUS BAGGAGE
- CRUISE ALTITUDE: 7315 M (24,000 FT)
  MACH 0.577
- GROSS WEIGHT: 3131 KG (6903 LB)
- ENGINE COST/N (SLS) $7.91, [LB F_N (SLS) $35.18]

Figure 67. Total Airplane Operating Cost Versus Utilization Rate, Engine IIC/9BPR.

MAX ROC SCHEDULE				
ENGINE	TIME TO ALT 7315 M (24K FT) (MINUTES)	FUEL KG	FUEL LB	DISTANCE (N. Mi.)
IA	8.8	60	133	32
IIA	8.3	50	110	31

MAX SPEED ROC SCHEDULE				
ENGINE	TIME TO ALT 7315 M (24K FT) (MINUTES)	FUEL KG	FUEL LB	DISTANCE (N. Mi.)
IA	20.0	141	310	112
IIA	19.5	120	265	110

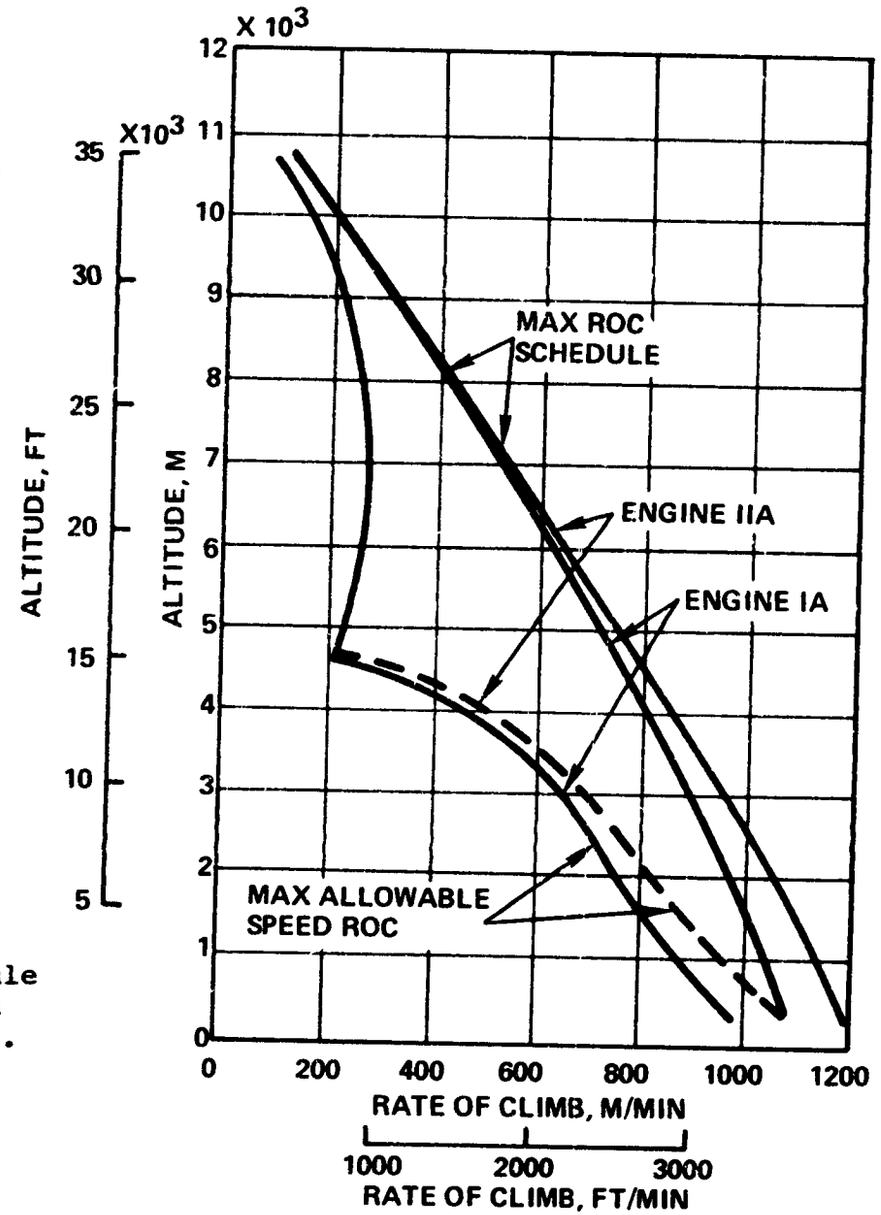

Figure 68. Rate of Climb (ROC) Schedule Versus Altitude Comparison Between Engines IA and IIA.

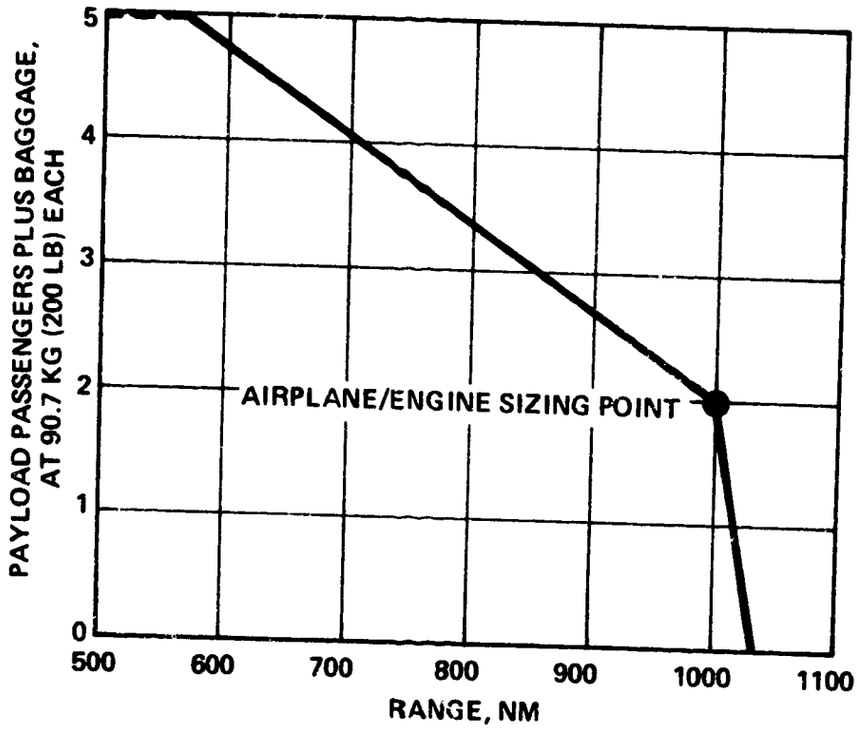

- CRUISE AT 350 KTS, 7315 M (24,000 FT)
- RESERVE OF 45 MINUTES AT CRUISE
- ONE CREW MEMBER PLUS 244 KG (537 LB) OF EQUIPMENT

Figure 69. Payload Versus Range of the Baseline Airplane with Engine IIA.

Engine IA and Engine IIA are considered to be near optimum within the constraints of this analysis and that the small differences obtained in first cost and total cost should not constitute a rigid basis for selecting one engine over the other. While questions of that nature require more extensive analysis for solution than is provided in a program of this scope, the analysis and synthesis program will provide Management and Engineering with some valuable insight during the conceptual phase of airplane design. Airplane characteristics and a three-view drawing derived from the synthesis analysis are shown in Figure 70.

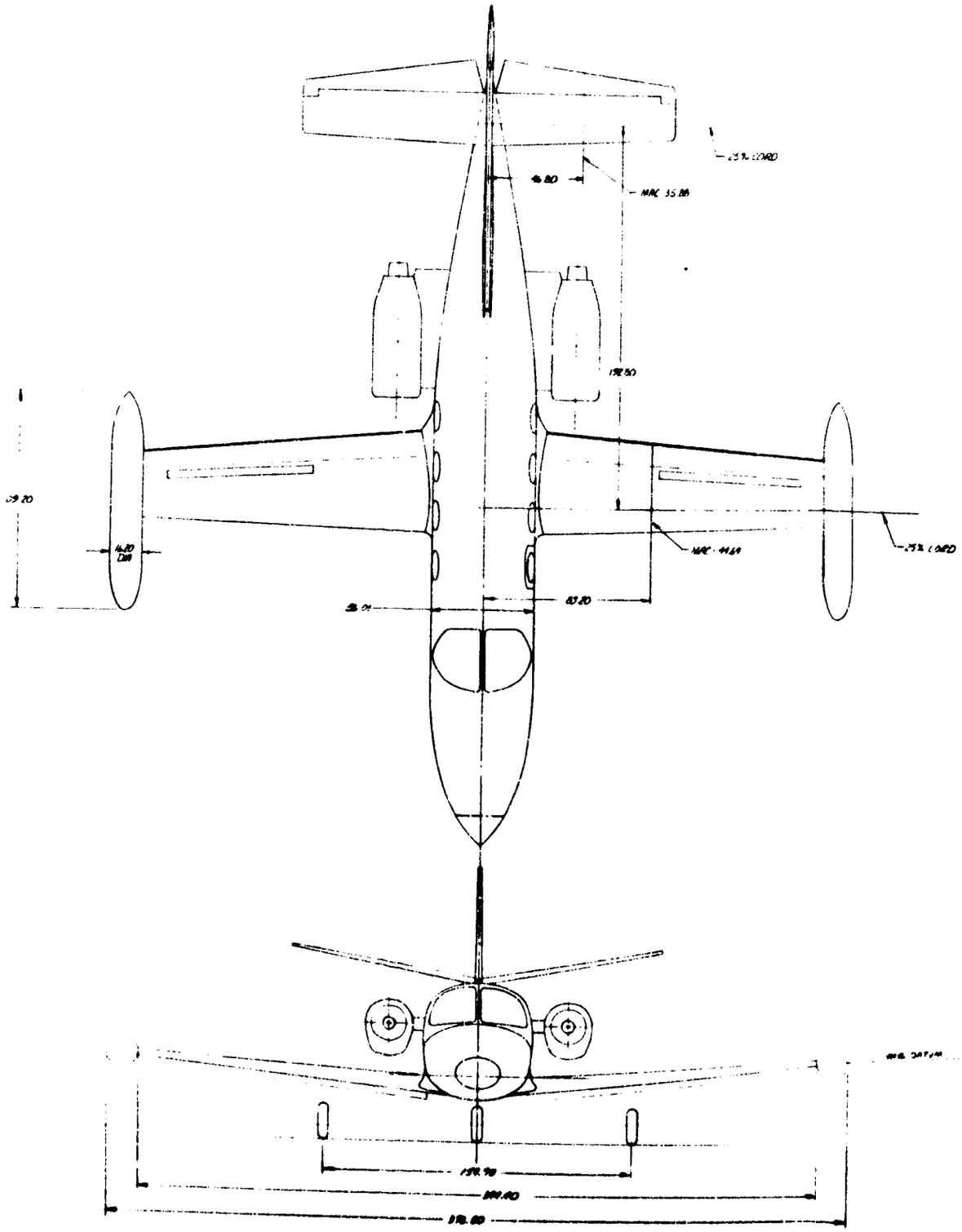

PRECEDING PAGE BLANK NOT FILMED

FOLDOUT FRAME

ALIGHTING GEAR

TIRES
- MAIN--18x5.5, 10 PLY, TYPE VII
- NOSE--18x5.5, 10 PLY, TYPE VII

SHOCK STRUT TRAVEL
- MAIN----------9.00 IN.
- NOSE----------7.00 IN.

LOADING

WEIGHT
- EMPTY (DRY)----------3484 LBS
- DESIGN USEFUL LOAD----3024 LBS

POWER PLANT

ENGINE----------TURBOFAN, STATIC THRUST AT SEA LEVEL = 1373.3 LBS

WING

SPAN
- OVERALL---376.80 IN. (31.4 FT)
- THEORETICAL (ACTUAL WING)----------344.40 IN. (28.7 FT)

AREA
- TOTAL----------105.00 SQ FT
- FLAPS----------27.30 SQ FT

AIRFOIL
- ℄----------NACA 23018
- TIP----------NACA 23009

INCIDENCE
- ROOT----------0°
- TIP----------0°

DIHEDRAL----------5°
MAC----------44.64 IN.
TAPER RATIO----------0.615
ASPECT RATIO----------7.86

STABILIZER

SPAN--186.96 IN. (15.58 FT)
AREA
- TOTAL---------45.60 SQ FT

AIRFOIL
- ROOT----------NACA 0009
- TIP----------NACA 0006

INCIDENCE----------0°
DIHEDRAL----------10°
MAC----------35.88 IN.
ASPECT RATIO----------5.32

FIN

SPAN-----77.64 IN. (6.47 FT)
AREA TOTAL-------24.40 SQ FT
AIRFOIL
- ROOT----------NACA 0009
- TIP----------NACA 0006

MAC----------46.32 IN.
ASPECT RATIO----------1.71

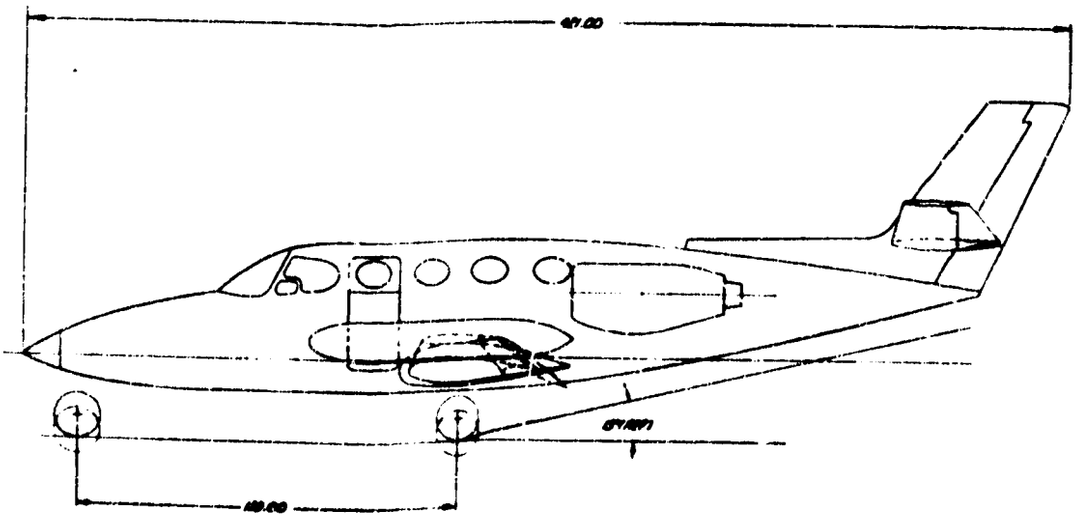

Figure 70. Baseline Airplane.

Cost-Sensitivity Analysis

Engine characteristics such as weight, performance, and cost have a major effect on airplane size and resultant cost. In order to evaluate the impact of some of these characteristics, the IIA-engined airplane was subjected to a sensitivity analysis. The primary engine characteristics investigated were weight, thrust, specific fuel consumption, specific engine cost, and cycle temperature. In addition, a brief investigation was conducted on the cost impact imposed by the location of the engines on the airframe. The reference airplane, shown in Figure 70, had an estimated first cost of $306,158 and a total operating cost of $162.60 per hour based on a utilization rate of 500 hours per year. The total weight (basic weight plus acoustic treatment) of the unscaled IIA engine is 150 kg (331.5 lb). The TSFC at design point is 0.075 kg/N-hr (0.738 lb/hr/lb).

The sensitivity analysis was implemented to provide a means of assessing the effect of engine weight and fuel consumption on the airplane cost characteristics. The reference engine weight was varied ±23 kg (±50 lb) with respect to nominal weight, and new synthesis designs were established for each weight change. Similarly, the engine specific fuel consumption was varied ±10 percent. For each synthesis design, the parameter under investigation was the only one changed. Other characteristics of the reference airplane and engine such as engine cost, thrust, and basic mission were held constant.

The sensitivity of the airplane basic price to changes in engine weight and specific fuel consumption is shown in Figure 71. At the airplane price and related engine sizes derived from the analyses, the airplane basic price changes $864 per kg ($392 per pound) of engine weight change and $1228 per point [0.001 kg/N-hr (0.01 lb/hr/lb) of TSFC change. It is apparent when examining Figure 71 that one point of engine TSFC change has the same effect on airplane basic price as 1.4 kg (3.1 lb) of engine weight change. For example, by adding a compressor stage to reduce TSFC one would realize a net decrease in airplane basic price if the compressor weight increase were less than 1.4 kg (3.1 lb) for each point of improvement in TSFC.

The sensitivity of total operating cost (500-hour/year utilization) to engine weight and specific fuel consumption is shown in Figure 72. As indicated, 0.45 kg (1 lb) of engine weight will change the total operating cost $0.29 ($0.13) per hour on the reference IIA-engined airplane. Since each point of TSFC change will have the same effect on total operating costs as 3.42 kg (7.54 lb) of engine weight change, the change in total operating costs will be $0.98 per hour. Given an improvement of 5 points in TSFC, the total operating cost of the airplane would be reduced by $2450 per year.

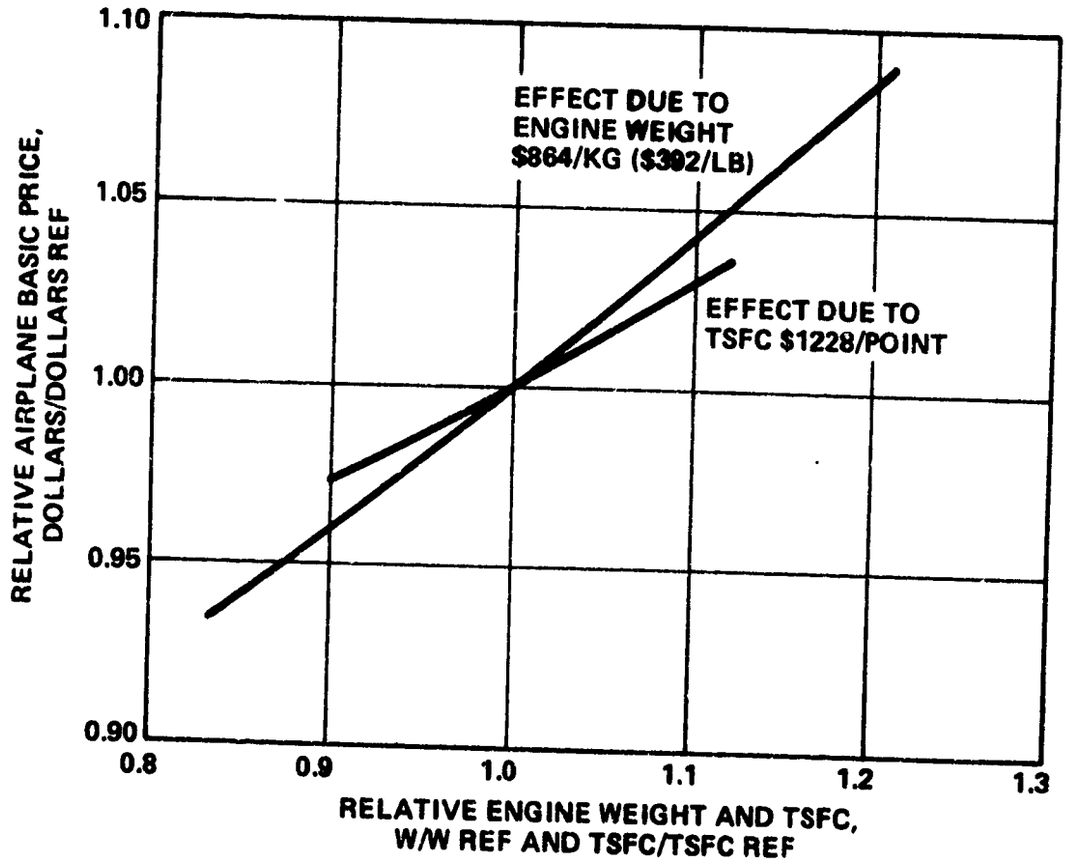

- RANGE 1000 N. Mi.
- CYCLE IIA CONSTANT
- REFERENCE WEIGHT 150 KG (331.5 LB)
- REFERENCE TSFC 0.074 KG/N-HR (0.738 LB/HR/LB)
- REFERENCE COST $306,158

Figure 71. Effect of Weight and Thrust Specific Fuel Consumption on Airplane Basic Price.

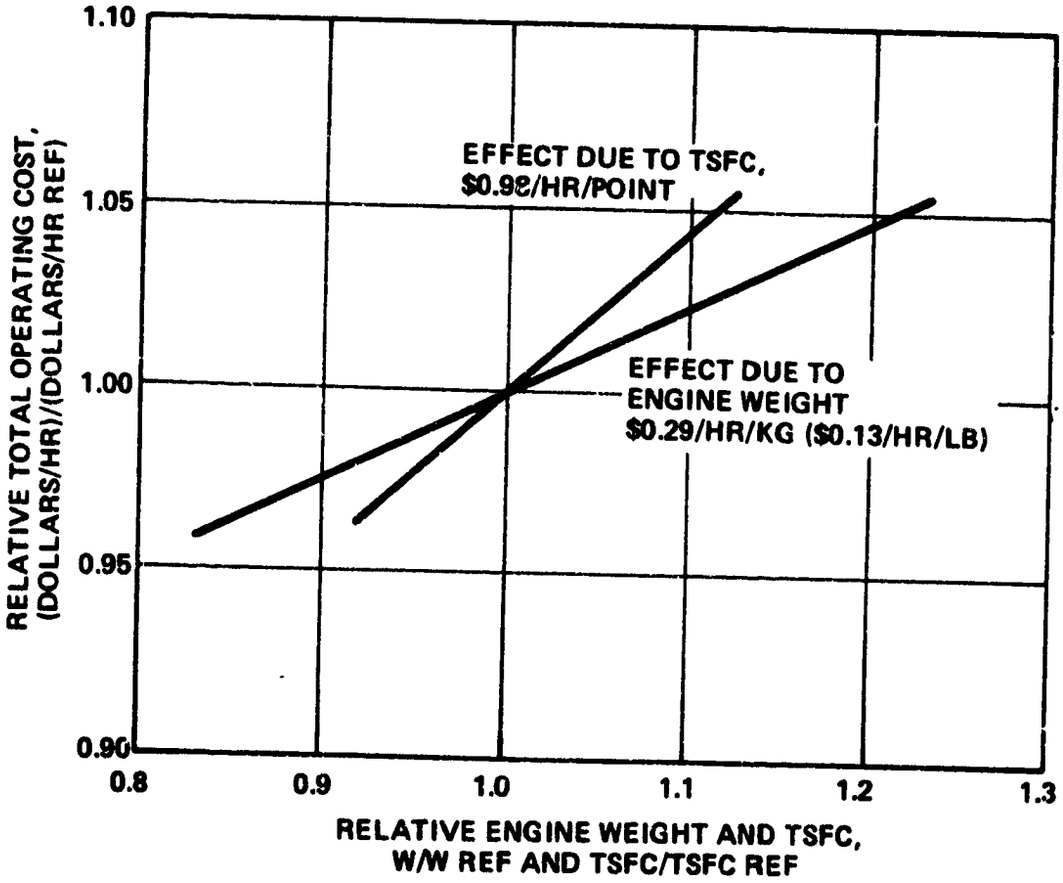

- RANGE 1000 N. Mi.
- CYCLE IIA CONSTANT
- REFERENCE WEIGHT 150 KG (331.5 LB)
- REFERENCE TSFC 0.074 KG/N-HR (0.738 LB/HR/LB)
- REFERENCE COST $162.20/HR

Figure 72. Effect of Engine Weight and Thrust Specific Fuel Consumption on Total Operating Cost.

During the conceptual phase, when the engine cycle studies are conducted, the selection of cycle temperature should be considered in terms of material selection and engine life. Therefore, a study was completed to evaluate the effects of cycle temperature on Engine IIA. The reference-design cycle temperature for that engine was 1167°K (2100°R) at cruise power. The cycle temperature was reduced to 1083°K (1950°R) in three steps, with the design thrust maintained at the design cruise conditions. The results of this rematching on the specific fuel consumption are presented in Figure 34. The change in TSFC on the reference IIA engine at the optimum bypass ratio versus turbine inlet temperature is illustrated in Figure 73. As shown in Figure 73, a 2-percent increase in TSFC will result when the turbine inlet temperature is reduced 84°K (150°R) for the same fan and compressor pressure ratios at 648 km/hr (350 knots), 7315 m (24,000 ft), standard-day operating conditions. The estimated increase in engine weight caused by decreasing the cycle temperature is shown in Figure 74. The weight increase resulted from the increased core airflow and dimensions required to provide the design cruise thrust.

Overall effects on total operating cost and airplane basic price due to an 84°K (150°R) turbine inlet temperature reduction was estimated as an approximate 6.1-percent increase in the basic price of the reference IIA airplane, and a 4.5-percent increase in total operating cost. For this example, the specific engine cost, time between overhaul, and all other characteristics of the airplane were held constant.

The effect of the turbine inlet temperature reduction on engine price was evaluated. The effect was determined to be negligible. The lower cost of the engine hot section due to materials changes was found to be offset by the increased cost of all core components due to their slightly increased size. It was on this basis that engine specific price was held constant in the cycle temperature sensitivity analysis.

During the sensitivity analysis, studies were conducted to determine the additional weight required to meet FAA noise criteria and the effect of that weight on cost. The weight of acoustic material required for the IIA engine was 5.2 kg (11.5 lb). With the use of the sensitivity analysis, the estimated increase in basic airplane price due to acoustic material weight was calculated as 1.5 percent. Additional total operating cost attributable to acoustic material weight is approximately 1 percent. This example assumes no performance changes caused by the acoustic lining in the engine bypass duct.

The reference airplane used to conduct the synthesis analysis has aft fuselage-mounted engines. An analysis was completed to evaluate the effect of this location as opposed to a wing-mounted engine installation. Over-the-wing mounting was used in the

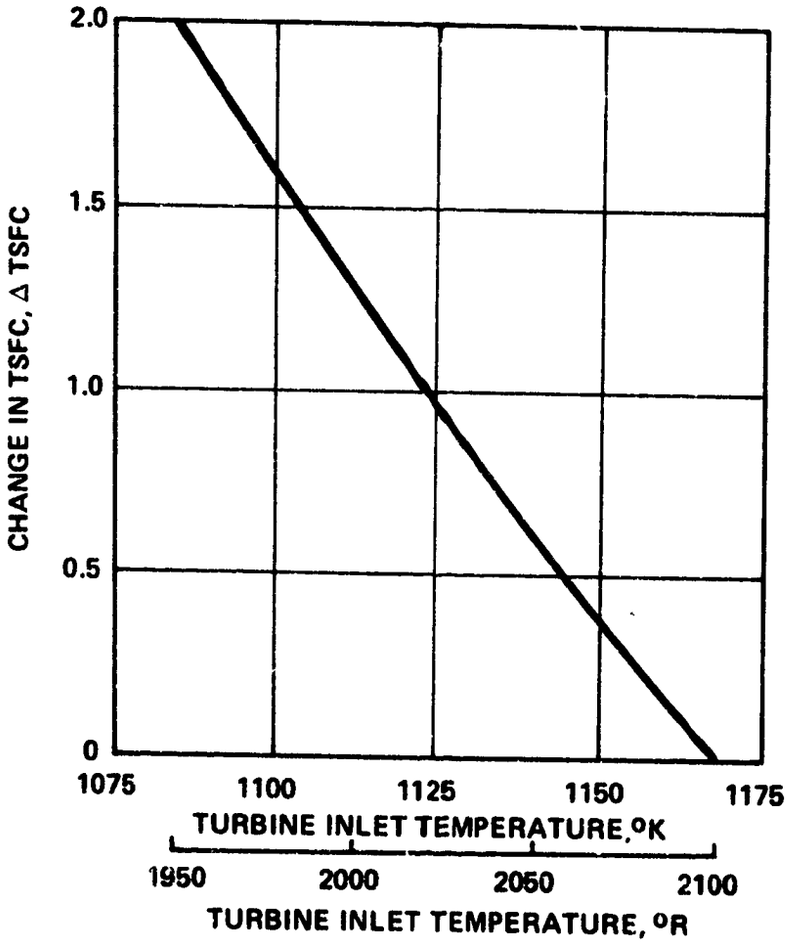

- CRUISE 350 KTS AT 7315 M (24,000 FT)
- FAN PRESSURE RATIO = 1.48
- CORE PRESSURE RATIO = 6.00
- OPTIMUM BYPASS RATIO

Figure 73. Effect of Cycle Temperature on TSFC for Engine IIA.

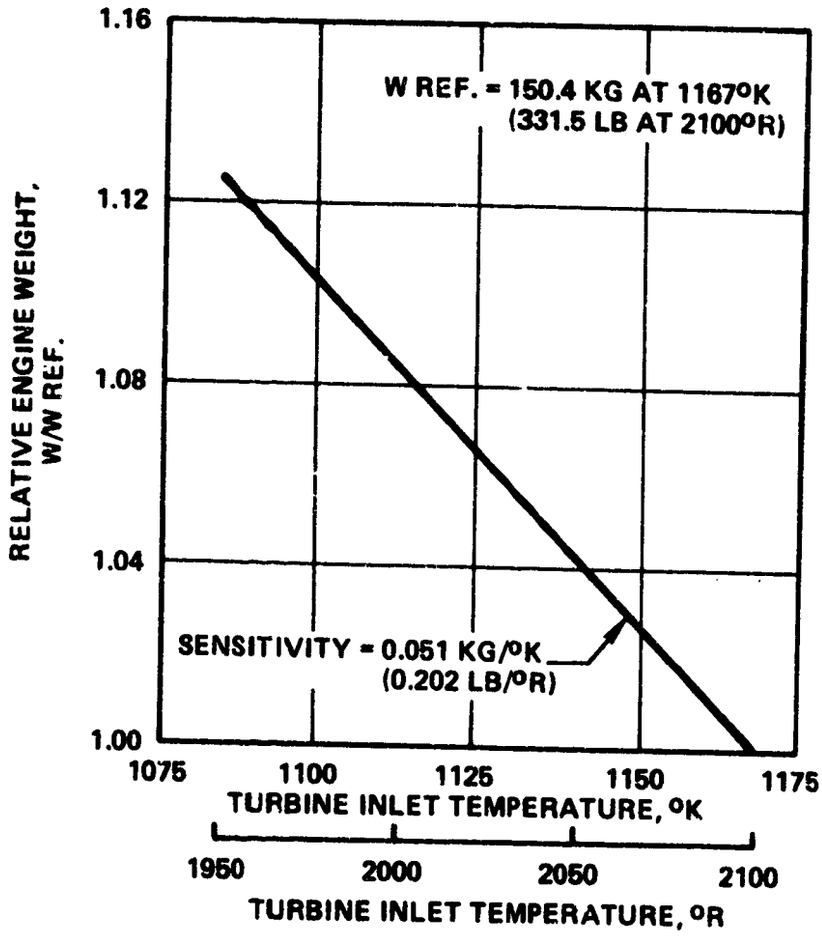

Figure 74. Effect of Cycle Temperature on Engine Weight.

analysis. This concept is favored in several future high-performance civil transport configurations. As reported in the February 1973 edition of Flying International, wind tunnel tests on future wide-body transports showed that a properly contoured over-wing nacelle can reduce drag-rise Mach number. In addition, installations of this type could provide advantages in terms of noise attenuation, and in reducing engine foreign object damage incurred in unimproved field operations. A model similar to the one shown in Figure 75 was used to determine the cost effects on the reference IIA-engined airplane. A reduction of 4.5 percent in airplane purchase price was obtained with the wing-mounted engines. The reduction in total operating cost was 3.1 percent below that obtained with the IIA aft fuselage-mounted engine. This indicates that the cost savings on the basic price and operation are sufficient to warrant further consideration of installations of that type. The primary design factors affected by the engine mounting location are the wing structure and interrelated components due to the relief load characteristics of the wing and the engine pylon structure.

A tradeoff analysis was conducted to determine the effect on airplane basic price of a lower-cost, but heavier steel fan replacing the titanium fan on the baseline engine design. The engine cost savings was estimated based on the use of investment-cast steel fan blades, a heavier fan disc, shaft, and front frame structure. The total savings for two engines, including both engine and airframe manufacturers' mark-ups, was $10,280. The engine weight increase was calculated to be 15.4 kg (34 lb). From the engine weight sensitivity analysis, at $864/kg ($392/lb), the resulting airplane price would increase $13,328, if the specific price of the engine were constant. This airplane price increase due to increased size exceeds, by over $3000, the price reduction potential of the steel-fan engine. Again, all airplane sizing, performance, and mission parameters are held constant in this tradeoff analysis.

The results of aircraft synthesis and sensitivity analyses, evaluation of candidate engines, and cost-versus-performance tradeoff studies conducted in Phase III are summarized as follows:

- On the basis of the constraints defined for this study and a survey of existing light twin airplanes, the Cessna Model 340 offers the most adaptable configuration for conversion to turbofan engines.

- The study shows that airplane size, engine thrust requirements, airplane basic price, total operating costs, and cruise ride quality are strongly dependent on the selection of initial design options such as wing loading, aspect ratio, stall speed, and flap configuration.

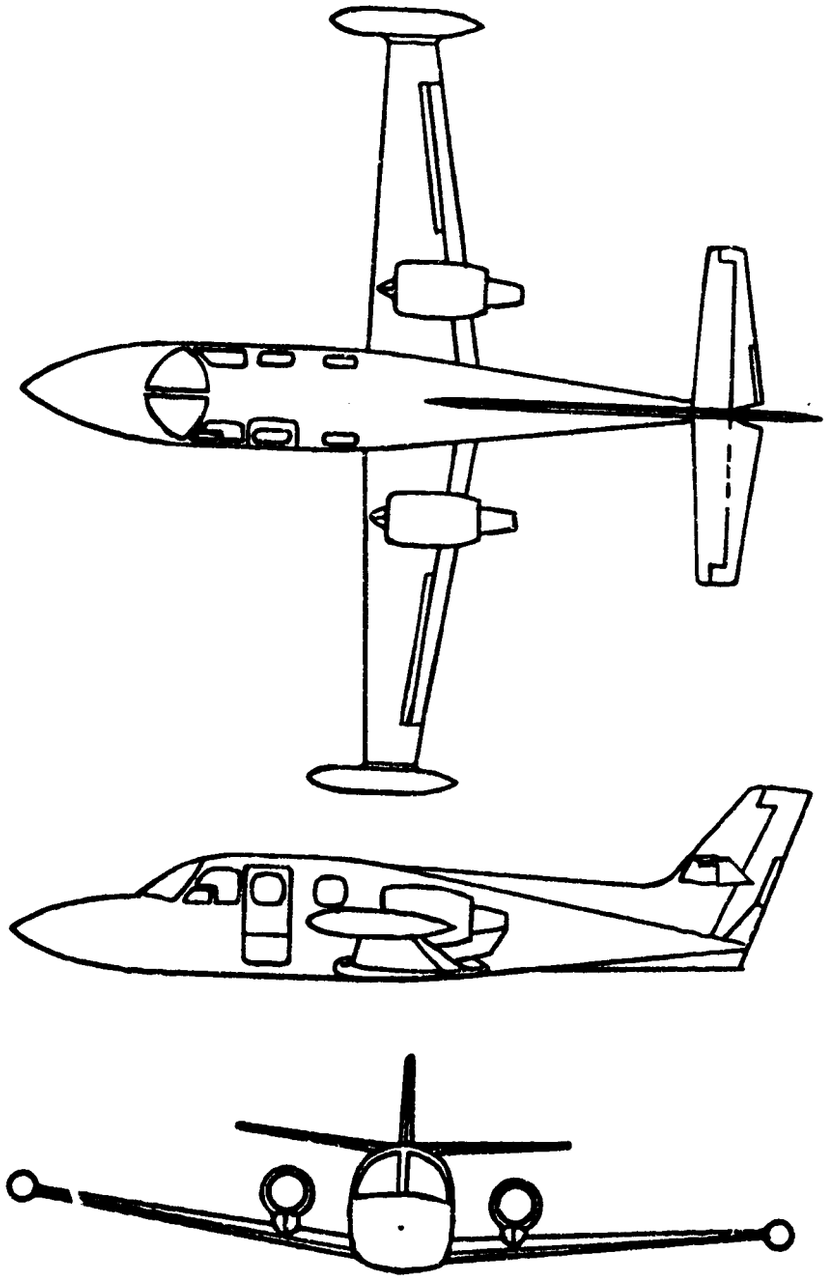

Figure 75. Baseline Airplane with Wing-Mounted Engines.

- The reference airplane basic price and total operating cost were reduced approximately 40 percent and 32 percent, respectively, by increasing the wing loading from 156 to 303 kg/m^2 (32 lb to 62 lb per square foot).

- The parametric synthesis analyses completed on the five candidate engines showed that engine characteristics such as weight, cost, and performance have a major influence on airplane size and resultant cost.

- The airplane synthesis calculations with the five candidate turbofan engines showed a substantial spread in resultant airplane first cost and total operating cost. The airplane using Engine IIC/9BPR had the highest purchase price, and Engine IA the lowest.

- In terms of total operating cost, the airplane equipped with Engine IIA was the most economical to operate. The airplane matched with Engine IIC/9BPR was the most expensive to operate.

- On the basis of airplane cost-effectiveness and performance, Engine IIA was selected as the best engine among the five candidates for the specified mission.

- The cost-sensitivity analysis was completed with the use of Engine IIA. The results of this study showed that the airplane basic price changed $864 per kg ($392 per pound) of engine weight and $1228 per point of specific fuel consumption. The total operating cost changed $0.29 per kg ($0.13 per pound) of engine weight and $0.98 per point of specific fuel consumption.

- A cycle temperature-sensitivity study was completed on Engine IIA. The results of this study showed that reducing the cycle temperature 84°K (150°R) from the initial design point resulted in a 2-percent increase in specific fuel consumption and a 12.5-percent increase in engine weight. The effects on the basic airplane price and total operating cost calculated for the synthesis-designed IIA-engined airplane are an increase of 6.1 percent in purchase price and an increase of 4.5 percent in total operating cost.

- Cost effects of additional engine weight for acoustic material required to meet the 95-PNdB noise constraint were determined for the IIA-engined airplane. The effects were an increase of 1.5 percent in basic price and 1 percent in total operating cost.

- The effects of engine mounting location (wing-mounted versus fuselage-mounted) were investigated in terms of airplane cost. The results of this analysis showed that a wing-mounted engine reduced the airplane purchase price 4.5 percent for the reference IIA-engined airplane. The reduction in total operating cost on the referenced airplane was 3.1 percent.

- Substantial engine price reduction opportunities that were identified in earlier manufacturing investigations were found in tradeoff analysis to lack cost-effectiveness. Substitution of a lower-cost, but heavier steel fan rotors for the titanium rotor of Engine IIA resulted in an airplane basic price increase of about $3000, or approximately one percent.

Final engine selection and assessment.- Candidate Engine IIA was identified in aircraft synthesis results as the "best" of the candidate engines. Airplane total operating cost (including amortization of price) was established as the basis for determining the "best" candidate engine. The airplane using Engine IIA had the lowest total operating cost when utilized at a rate of approximately 300 hours per year.

The performance and cost specifics of the other candidates bracketed those of Engine IIA. The substantial configuration differences between candidates was reflected in their performance, cost, and installation effects on airplane performance. By assessing the factors that made Engine IIA superior to the other candidates, it can be shown that Engine IIA is not only better than the other candidates, but near optimum for the airplane performance and mission characteristics postulated for this investigation.

Synthesis results showed that Engines IA and IIA resulted in smaller airplanes that were less costly to operate than those engines with centrifugal compressors. Although the engines with centrifugal compressors have comparable cycles and TSFC's, the axial-flow engines were lighter, smaller in diameter, and less expensive. Even though Engine IA was less expensive and lighter, the substantial TSFC advantage of Engine IIA made it more cost-effective. The resulting operating cost difference between the engines was slight, which indicates that both engines were near optimum with respect to TSFC versus weight and TSFC versus engine cost.

While Engine IIA was the best of the candidates evaluated, sensitivity analysis showed that the cost-effectiveness of the engine could be improved. It was determined that weight could be removed, and TSFC improved, with an accompanying engine price increase, but with a net decrease in airplane price and operating cost.

CONCLUSIONS

This report describes the methods and results of the NASA/AMES-AiResearch investigation into the applicability of turbofan propulsion to smaller general-aviation airplanes. The investigation identified relevant engine and engine/airplane size, weight, performance, and cost interrelationships. An evaluation was made of pertinent noise constraints. A conceptual, six-seat, light-twin airplane was defined, and a "best" turbofan engine cycle and configuration was identified for this airplane.

The conclusions, drawn from the results of this investigation are as follows:

1. Turbofan engine cycle variables affecting propulsive efficiency, and internal or thermodynamic efficiency may be separately analyzed and optimized. This reduces the amount of parametric cycle analysis and engine preliminary design that is required to make cost-versus-efficiency evaluations for any performance envelope desired in new airplane investigations.

2. When a larger production base is predicated for small turbofans, there are existing engine design approaches and manufacturing methods that will significantly lower the specific cost (dollars per unit thrust). Adoption of simplified engine configurations, minimization of non-aerodynamic machinery, the maximum use of integral-wheel investment castings, and the continued development of high-production techniques for integral-wheel castings are examples that were identified as cost-effective means of reducing engine specific cost. This should in turn permit general-aviation manufacturers to design and sell smaller and less expensive turbofan-powered airplanes.

3. At the airplane performance level specified for this investigation, the engine performance quality has a major effect on airplane size and resultant costs. Therefore, over the range of values that are concluded to be achievable, more emphasis should be placed on attaining low specific weight and specific fuel consumption rather than on low engine specific cost.

4. Turbofan engines can be designed for future general-aviation airplanes that will meet reasonable requirements of future government regulation of their social qualities, i.e., noise, emissions, and safety, while retaining a high degree of overall propulsion system efficiency.

5. The size, price, and operating costs of fast, light airplanes will be very sensitive to wing size, wing loading, flap quality, and stall speed. There is an obvious need for the wing technology featured in the NASA/University of Kansas/Robertson Aircraft 177 Cardinal demonstrator airplane, if smaller turbofan-powered airplanes are to be efficient and economical.

6. The NASA-developed aircraft synthesis computer program that was used in this investigation can be a valuable and economic aid in the definition of future small, turbofan-powered airplanes. As a preliminary design tool, it will ease the tedium of a multitude of design, configuration, and performance evaluations. As a management tool it will quickly test these evaluations that are vital in defining new products. In general use, it will provide an industry-wide baseline of communication.

Due to the imminence of additional government regulation, there is strong incentive now to provide general-aviation airplanes with more socially acceptable, as well as efficient, propulsion systems. We are encouraged by the results of this investigation, and recommend that NASA continue this work to establish pertinent engine/airplane interrelationships. Sound methods have been developed for use in further evaluation of engine and airplane concepts. Further conceptual work and evaluations are necessary if the advantages of turbofan propulsion are to be made available for smaller and less expensive general-aviation airplanes.

APPENDIX A

Discussion of New Turbofan Optimization Method

The efficiency of aircraft propulsion systems is conventionally addressed in a manner that makes the definition of an optimum or "best" new engine a time consuming and expensive process. The overall propulsion system efficiency consists of four elements that are identifiable in all engine types:

- Thermal efficiency (converting fuel to gas or shaft power)
- Propulsive efficiency (converting power to propulsive thrust)
- Installed-to-uninstalled thrust ratio (drag penalty charged to engine installation)
- Thrust to weight ratio (weight penalty charged to engine installation)

In defining turbofan engines, thermodynamic and propulsive efficiency are normally not addressed separately. Cycle analysis computer programs are used to directly determine the product of these efficiencies, thrust specific fuel consumption (TSFC). To define an optimum design-point cycle, i.e., the cycle having lowest TSFC at a specified flight speed and altitude, it is necessary to perform parametric cycle analysis. This consists of calculating many cycles, using many variables affecting the TSFC, plotting the results, examining the plots, and making countless judgements about the mechanical characteristics of the many low-TSFC candidates that have been found to exist. The procedure is cumbersome and indecisive because the best of the low-TSFC candidates cannot be identified without recourse to a great amount of additional analysis and comparison of engine layout drawings. This is often avoided by "eye-balling" the candidate cycles, making an arbitrary selection, and proceding with the design of an engine that has less than the best overall propulsion system efficiency.

The basic shortcoming of the conventional turbofan cycle definition procedure is that the fundamental operators on overall efficiency are not visible in parametric cycle analysis results. When turbofan cycle computer programs originated, bypass ratio was unexplainably assigned a prominence that it does not deserve. Bypass ratio has little to do with the specific fuel consumption and specific thrust of a turbofan engine. In an optimized engine cycle, the fan pressure ratio is the determinant of specific thrust, and the specific fuel consumption is a function almost entirely of cycle pressure ratio, turbine inlet temperature, and fan propulsive

efficiency, which is in turn a function of fan pressure ratio. Engines of greatly different bypass ratio can have the same design-point values of TSFC and specific thrust. Yet, nearly all parametric cycle analyses, and all references to engine performance qualities are referenced to the bypass ratio parameter. The effect is to obscure the consideration of fundamentals that would make the definition of a "best" engine a simpler procedure.

The following outline for a simpler engine definition procedure is based on the fact that turbofan propulsive and thermodynamic efficiencies are directly calculable; therefore, the cycle and component characteristics that determine the highest possible value of these efficiencies can also be determined directly.

The propulsive efficiency of the fan flow of a turbofan engine may be defined as follows:

$$\eta_p = \frac{\text{Work done in flight}}{\text{Work supplied to fan}}$$

To make the calculation of this expression simple, it has been put in the following form:

$$\eta_p = \frac{\left(\frac{V_o}{\sqrt{T_o}}\right)^2 \times \left(\frac{V_j}{V_o} - 1\right)}{g\, J\, c_p\, \frac{\Delta T_F}{T_o}}$$

where:
- V_o = flight speed (ft/sec)
- T_o = ambient total temperature (°R)
- V_j = jet velocity (ft/sec)
- g = gravitational constant (32.17 ft/sec^2)
- J = conversion constant 778 ft-lb/Btu
- c_p = specific heat at constant pressure of fan inlet air
- ΔT_F = fan temperature rise (°R)

NOTE: Fan and nozzle efficiencies and duct pressure loss assumptions must be made to calculate ΔT_F and V_j for a specified for pressure ratio.

APPENDIX A

A plot of this propulsive efficiency expression with fan pressure ratio and flight speed and altitude as parameters is presented in Figure 76. The peak efficiency values for the separate curves were plotted in the adjacent figure. The best fan pressure ratio for a given flight speed can be determined from these curves, for the following values of the component efficiencies and losses that were assumed:

Fan polytropic efficiency index - 3.20

Jet velocity coefficient - 0.98

Fan duct pressure loss ($\Delta P/P$) - 0.02

In a manner similar to this, it can be shown that there is a best core jet velocity for a previously determined fan pressure ratio and resultant fan propulsive efficiency. Then with this much of the optimum cycle directly calculated, attention can be turned to the cycle thermal efficiency.

Over the ranges of values normally considered, the cycle pressure ratio is a greater determinant of thermal efficiency than is the cycle temperature (turbine inlet temperature). Generally, the greater the two values are, the higher the thermal efficiency will be.

In a new engine design effort, a range of practical, desirable cycle pressure ratios is known before cycle analysis is begun. The size or power class, the previous definitive engine in the class, and the general performance quality desired of the new engine are considerations that make the range of candidate cycle pressure ratios obvious. If the new engine is to have low TSFC, the highest practical pressure ratio must be determined. This is usually done by examining the limitations of candidate compressor designs. To this point in the optimization method no parametric cycle analysis has been required.

Turbine inlet temperature is the only significant cycle parameter remaining to be examined. Again, the highest practical value will provide the lowest TSFC. In an optimized turbofan cycle, (that is; one in which the fan pressure ratio and core jet velocity have been calculated to maximize propulsive efficiency), the turbine inlet temperature has no effect on engine specific thrust. It only affects the thermal efficiency of the cycle, and is the major determinant of the specific power output of the core. Consequently, the core airflow required to drive a fan of predetermined airflow and pressure ratio (while supplying the correct pressure to the core jet, to obtain the predetermined core jet velocity) is primarily determined by the turbine inlet temperature. Thus, bypass ratio, (fan duct flow divided by core flow), is mainly

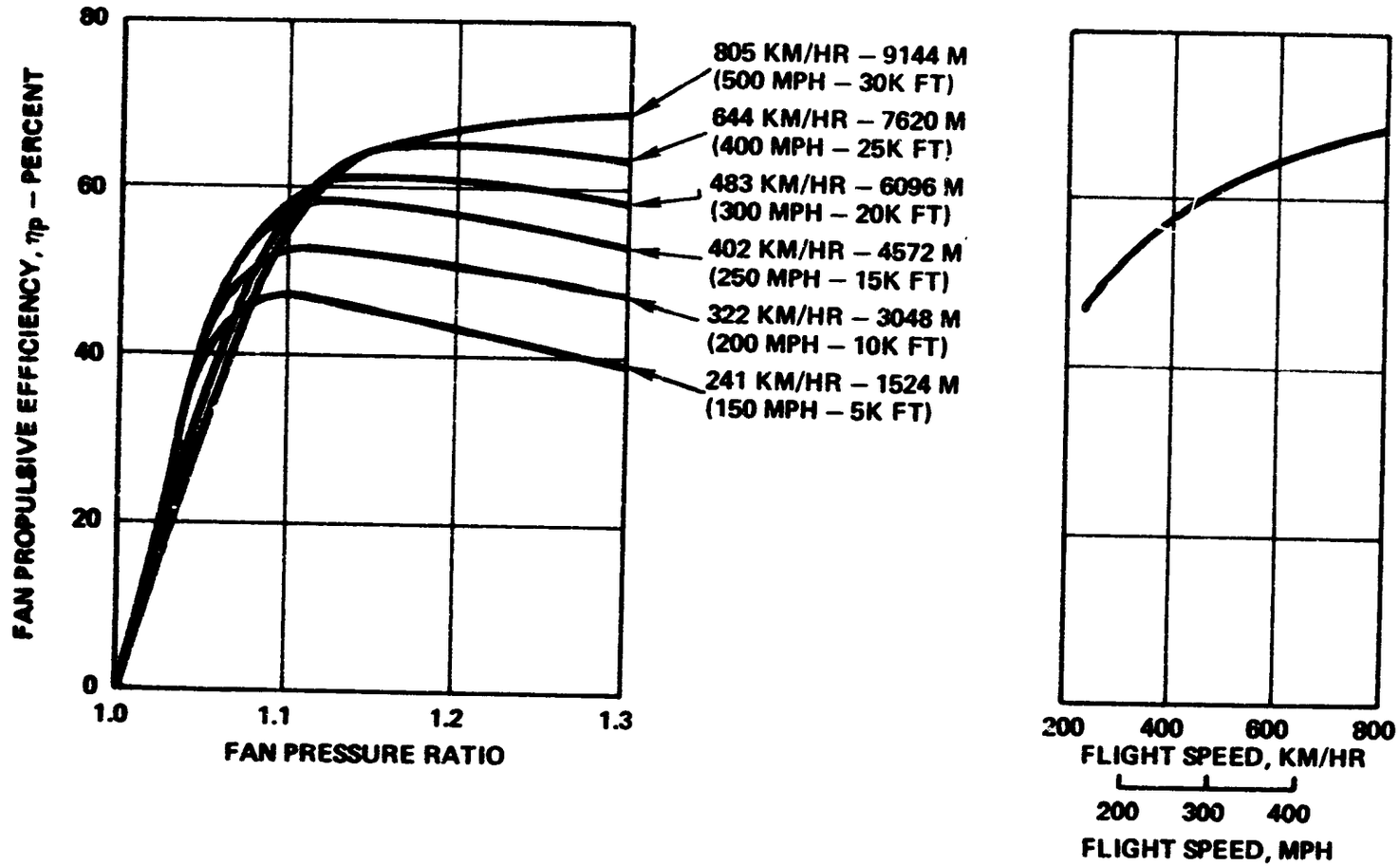

Figure 76. Fan Propulsive Efficiency Versus Fan Pressure Ratio and Flight Speed.

a function of turbine inlet temperature. Considerations similar to those given the compressor usually determine a range of candidate values. The most important consideration in the design of contemporary engines is that of turbine cooling. The decision to have a temperature so high that turbine blade cooling is required does not usually demand recourse to parametric cycle analysis. In either case, whether the decision is to cool or not to cool, the highest possible temperature permitted by candidate turbine design limitations is best, and is usually the one chosen.

Having selected a fan pressure for best propulsive efficiency, a core jet velocity that is best for the fan pressure ratio, and the highest practical values for the cycle pressure ratio and cycle temperature, the best engine cycle has been determined. Now, cycle analysis must be performed. The TSFC that is subsequently calculated cannot be improved upon if the limitations put on cycle pressure ratio and temperature cannot be exceeded. The bypass ratio that is calculated is only a derived value, and not an operator on TSFC or specific thrust.

At this point the "best" cycle has been determined, but not the "best" engine. The "best" engine can only be determined from extensive tradeoff studies which will finally alter the best cycle. Fan propulsive efficiency will be traded down by increasing fan pressure ratio, which provides lighter fan weight, smaller size, lower nacelle drag and less cost. The same will be true of the remaining determinants of cycle quality. These tradeoffs must be accomplished in conjunction with aircraft synthesis and sensitivity analyses, as well as mission analyses consistent with the intended application of the engine. The most cost-effective engine can only be defined by tradeoff and sensitivity analyses, or by accident.

The methods of turbofan optimization outlined here are particularly applicable to the definition of engines for smaller general-aviation airplanes. There are many airplane performance envelopes and mission definitions represented in the general-aviation spectrum of airplanes. Each of the many performance and mission increments will require a near-optimum engine, if the turbofans are to be sufficiently cost-effective that they can be afforded. What cannot be afforded is an expensive hit-and-miss approach to engine definition and development, in which lessons of engine cost-effectiveness are learned during an expensive engine development and certification program. The rational engine optimization methods described here could provide the assurance that smaller turbofan-powered airplanes can be made available. The following is an example of the application of these methods.

Mid-way in this small turbofan program a preliminary design study was undertaken to define some characteristics of a turbofan-powered, 150-mph cruise, two-seat utility/training airplane. This

exercise, while not entirely relevant to the contract work statement, was carried out in order to gain insight into eventual investigative opportunities, made possible by the present contract. Because the engine was defined by the methods outlined in this appendix, the work was completed quickly and economically. The result was a technically viable engine/airplane concept that merits further definition work.

The following engine cycle was defined at a cruise design point of 241 km/hr (150 mph) at 1524 m (5000 ft) altitude:

Fan Pressure Ratio	1.15
Core Pressure Ratio	4.0
Turbine Inlet Temperature	788°C (1450°F)
Bypass Ratio	11.0
TSFC	0.054 kg/N·hr (0.526 lb/hr/lb)
Specific Thrust	90.9 N·s/kg (9.27 lb/lb/sec)

The component efficiency assumptions and cycle pressure losses were based on assessments of cursory component designs and a flow path layout. The engine was initially sized for 1779.3 N (400 lb) thrust, and was estimated to have an installed weight of 45.4 kg (100 lb).

The airplane analysis was based on a cursory preliminary design procedure, using the known weight and drag characteristics of an existing light airplane having the same general performance. A three-view configuration sketch was prepared for the study, provided additional bases for the weight and drag analysis. The physical and performance characteristics determined for the airplane are presented in Table A-I.

The data derived for this conceptual design compares favorably with contemporary utility/training airplanes. It appears from these results that a turbofan engine having an appropriate cycle, rationally defined, could be an attractive propulsion system candidate for future small airplanes.

APPENDIX A

TABLE A-1. UTILITY/TRAINING AIRPLANE PHYSICAL AND PERFORMANCE CHARACTERISTICS

Design Point - Max Cruise	241 km/hr/1524 m	(150 mph/5000 ft)
V_{stall}	97 km/hr	(60 mph)
V_{max}	> 241 km/hr	(150 mph)
Ceiling	> 3048 m	(10,000 ft)
Landing	< 457 m	(1500 ft)
Drag Polar	$0.29 + 0.05\ C_L$	
Range (max $c\gamma$)	850 km	(528 mi)
Endurance (max $c\gamma$)	3.5 hr	
W_{gross}	632 kg	(1393 lb)
W_{empty}	328 kg	(723 lb)
W_{fuel}	113 kg/146 l	(250 lb)/(38.5 gal)
$W_{payload}$	191 kg	(420 lb)
W/S_{max}	98 kg/m^2	(20 lb/ft^2)
S_{wing}	6.5 m^2	(70 ft^2)
AR_{wing}	8	
S_{tail}	2.6 m^2	(28 ft^2)
AR_{tail}	6	
Length	635 cm	(250 in.)
Span	721 cm	(284 in.)
Height	191 cm	(75 in.)
Cabin	112 x 112 x 152 cm	(44 x 44 x 60 in.)

APPENDIX B

EVALUATION REPORT - APPLICABILITY OF FUEL-CONTROL CONCEPT DESCRIBED IN NASA TN D-5871 TO CANDIDATE TURBOFAN ENGINES

The fuel-control concept described in NASA Report TN D-5871 (Reference 12) was demonstrated on a turbojet engine. The control was simplified in order to effect a reduction in the cost of manufacture. However, because of its simplicity, engine operation was compromised. The concept is comparable in simplicity to the manual-mode backup for the electronic control installed on the AiResearch Model TFE731 Turbofan Engine. Aspects of this control concept pertaining to mechanization, a comparison with the manual mode of the TFE731 control, the requirement for engine design margins, and operational limitations are discussed below. This review describes the compromises in engine design and performance that would be required if the control concept were adopted.

Mechanization.- The metering valves illustrated in the NASA report are positioned by either the compressor inlet pressure or the compressor pressure rise. No seal is shown between the fuel and compressor inlet or discharge pressure. Current design practice prohibits a source of fuel-path leakage such as this. In addition, it is anticipated that clean air regulations will also prohibit it. If bellows seals or torque tube seals are used, the cost of utilizing both inlet pressure and compressor pressure rise to position the metering valve could be excessive.

Comparison with TFE731.- The manual-mode backup control for the TFE731 utilizes a fixed W_f/P_3 acceleration schedule. The speed is set by a flyball governor bleeding the P_3 pressure to reduce the fuel flow. The P_3 pressure reduction is limited to a fixed ratio. Therefore, the minimum schedule is also a fixed W_f/P_3 ratio. In the specific case, the governor reduces the ratio from 9.5 to 5.

Both controls meter the flow by bypassing the fuel pump to maintain a differential pressure. The TFE731 maintains a fixed differential pressure across the metering valve. In the NASA concept, the pressure drop across the control pump is maintained at zero.

The TFE731 has a single metering valve, which is positioned in response to a P_3 absolute pressure signal. This requires an evacuated bellows and a high-pressure bellows. The NASA concept requires one evacuated bellows, two low-pressure bellows, and one high-pressure bellows. Two sets of two valves must be positioned. One set is proportional to P_2 absolute, and the other set is proportional to (P_3-P_2).

APPENDIX B

The TFE731 requires a flyball governor that is more expensive than the control pump and orifice of the NASA concept. However, the accuracy is probably superior in that fuel specific gravity does not influence the measurement. The control pump requires a zero pressure drop to avoid leakage and measures volume flow rather than weight flow proportional to speed.

The TFE731 start flow is satisfactory because the fixed W_f/P_3 schedule provides more flow than that required to accelerate the engine. However, the W_f/NP_2 schedule of the NASA control will provide less than is required to accelerate the engine unless the starter provides for cranking to high engine speeds. The NASA concept could be augmented with a minimum fuel nozzle pressure regulator in parallel with the control to provide for starting.

Engine design margin.- A bleed valve was incorporated in the TFE731 to avoid compressor surge during acceleration. For the manual mode, the bleed valve is set at 1/3 bleed position. The engine acceleration and deceleration rates in the manual mode are 1/2 to 1/3 as great as they are in the normal mode.

In order to permit the use of a simple schedule for acceleration and deceleration, engine margins for surge and combustor blowout must be increased over those margins provided in current practice. Also, required schedule shifts with Reynolds-number effect on aerodynamic components at higher altitude become a concern at altitudes above 35,000 feet.

Operational limits.- To avoid excessive thrust and engine case pressure, the TFE731 must be flat-rated on cold days at sea level. This requires a corrected engine speed limit as a function of inlet total pressure. In its absence, the pilot would be required to monitor these limits.

The thrust of a turbofan engine is very sensitive to high spool speed. The relationship is of the order of 7 percent thrust increment for 1 percent speed increment. The thrust tolerance range is generally narrow because of takeoff distance requirements and single-engine asymmetric thrust limitations. The allowable engine thrust tolerance would have to be increased over the present practice to permit a reduced-accuracy droop governor.

Turbofan turbine inlet temperature is normally controlled by an accurate speed control biased with compressor inlet temperature and pressure, or a temperature limiting control. In order to eliminate the automatic temperature-control feature, engine temperature margins would have to be increased substantially.

APPENDIX B

The relatively simple acceleration and deceleration schedule in this control concept will result in slow acceleration and deceleration of the engine.

Redundant overspeed protection may also be required, for safety considerations.

Summary.- The control concept described in NASA Report TN D-5871 is very similar to the manual-mode backup control. There are limitations in this mode that make it unacceptable as a primary engine control. For example, the pilot must monitor and set all engine limits. Full throttle bursts could not be permitted unless large margins were provided in the engine design. It is considered impractical to design turbofan engines with sufficient margins to permit the elimination of automatic control of all engine limits.

Starting fuel schedules and overspeed protection would have to be added to the control concept described in TN D-5871. The control features addressed above, and additional refinements such as automatic compensation for fuel specific gravity and inlet temperature and pressure inputs for adequate engine control, would substantially increase the cost of the control concept.

The control described in TN D-5871 would merit re-evaluation when a specific engine is defined and operational characteristics are specified that are more suited to the capabilities of the control unit as it is described.

REFERENCES

1. Anon., "Business Aviation 1972", Business and Commercial Aviation, April 1972.

2. Anon., "1972 Aircraft Directory," Flying Annual & Pilots Guide, 1972 Edition.

3. Anon., "Jet Noise Prediction," Soc. Auto. Eng. AIR 876, N.Y., 1965.

4. Grande, E., "Jet Noise Generation," AiResearch Report SD-8005, Phoenix, Arizona, 1972.

5. Franken, P.A., "Jet Noise," Chapter 25 in Noise Reduction, ed. by L. L. Beranek, McGraw Hill, N.Y., 1960.

6. Anon., "Standard Values of Atmospheric Absorption as a Function of Temperature and Humidity for Use in Evaluating Aircraft Flyover Noise," Soc. Auto. Eng. ARP 866, N.Y., 1964.

7. Galloway, T. L., and M. H. Waters, "Computer Aided Parametric Analysis for General Aviation Aircraft," presented at the SAE National Business Aircraft Meeting, Wichita, Kansas, April 1973.

8. "Technology Assessment of Advanced General Aviation Aircraft," Lockheed-Georgia Company, NASA CR-114339, June 1971.

9. Sanders, K. L., "High Lift Devices; A Weight and Performance Tradeoff Methodology," SAWE Technical Paper 761, May 1969.

10. Schoen, A. H., "The V/STOL Aircraft Sizing and Performance Computer Program-VASCOMP II," Volume VI, Boeing Company, Vertol Division, Boeing Document D8-0375, March 1968 (revised October 1971).

11. Raisbeck, J. D., "Considerations of Application of Currently Available Transport-Category Aerodynamic Technology in the Optimization of General Aviation Propeller-Driven Twin Design," Robertson Aircraft Corp, SAE 720337, March 1972.

12. Seldner, Kurt, and Harold Gold, "Computer and Engine Performance Study of a Generalized Parameter Fuel Control for Jet Engines," NASA-Lewis Research Center, NASA Technical Note TN D-5871, June 1970.